



**Universidade do Minho**  
Escola de Engenharia

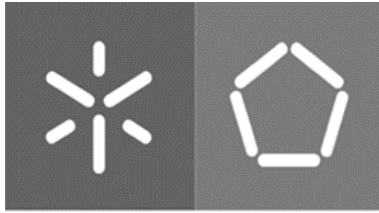
Inês da Silva Tavares **Study on the Kinetic Behaviour of Photochromic Systems**

Inês da Silva Tavares

**Study on the Kinetic Behaviour of  
Photochromic Systems**

Julho de 2021





**Universidade do Minho**  
Escola de Engenharia

Inês da Silva Tavares

## **Study on the Kinetic Behaviour of Photochromic Systems**

Dissertação de Mestrado  
Mestrado Integrado em Engenharia Têxtil

Trabalho realizado sob a orientação de:  
**Professor António Pedro Souto**  
**Doutora Isabel Dias Cabral**

Julho de 2021

## **DIREITOS DE AUTOR E CONDIÇÕES DE UTILIZAÇÃO DO TRABALHO POR TERCEIROS**

Este é um trabalho académico que pode ser utilizado por terceiros desde que respeitadas as regras e boas práticas internacionalmente aceites, no que concerne aos direitos de autor e direitos conexos.

Assim, o presente trabalho pode ser utilizado nos termos previstos na licença abaixo indicada.

Caso o utilizador necessite de permissão para poder fazer um uso do trabalho em condições não previstas no licenciamento indicado, deverá contactar o autor, através do RepositóriUM da Universidade do Minho.



**Atribuição-NãoComercial-SemDerivações**  
**CC BY-NC-ND**

<https://creativecommons.org/licenses/by-nc-nd/4.0/>

## Acknowledgements

I would like to pay homage and express my deepest gratitude to my co-supervisor, Professor Pedro Souto, for all that he has taught me inside and outside of university. He was a truly remarkable person who made a difference in my life and in the lives of so many others. I can only hope that he would be proud of this work.

Additionally, I would like to thank my co-supervisor, Doctor Isabel Dias Cabral – an intelligent, humble, and caring person – for the availability and understanding always displayed throughout this process.

I am grateful to my co-supervisor Professor Martina Viková for granting me the opportunity to work at TUL and for the continuous availability and good mood throughout the laboratorial stage of this research and to Professor Michal Vik for all that he has taught me about colourimetry and photochromics and for always clarifying my doubts.

I would like to thank Marcela and Utkarsh for their kindness and availability to help me in the laboratory whenever needed and for helping me get acquainted with the TUL facilities.

Moreover, I am grateful to my family for always encouraging and believing in me and, especially, to my mom, who has always been there for me no matter what; who is an example of strength and perseverance; and to whom I owe everything.

I would like to thank my Portuguese friends for the wonderful memories I will take with me and for making Guimarães feel like home for the past six years, in particular to Bernardo, who has been the greatest friend I could ever ask for. Additionally, I ought to express my gratitude towards the friends I made in the Czech Republic, especially to Göksu and Seval, for making me feel safe and loved while going through a pandemic in a foreign country.

I want to finish by paying homage to my dear friend Mariann, who is my greatest inspiration; who has shown me how to live and love fearlessly; and who has taught me to believe in myself. She was a ray of sunshine in the lives of everyone around her and has surely left this world too soon.

“The people in your life are like the pillars on your porch. Sometimes they hold you up, and sometimes they lean on you. Sometimes it's enough to know they are standing by.”

## **DECLARAÇÃO DE INTEGRIDADE**

Declaro ter atuado com integridade na elaboração do presente trabalho académico e confirmo que não recorri à prática de plágio nem a qualquer forma de utilização indevida ou falsificação de informações ou resultados em nenhuma das etapas conducente à sua elaboração.

Mais declaro que conheço e que respeitei o Código de Conduta Ética da Universidade do Minho.

## Resumo: Estudo do Comportamento Cinético de Sistemas Fotocrômicos

Os corantes fotocrômicos têm algumas aplicações, exemplos incluem lentes fotocrômicas, *designs* têxteis e interruptores moleculares. No entanto, o seu custo elevado, a falta de *standards* laboratoriais e certas limitações tecnológicas impedem-nos de entrar no mercado e na indústria *mainstream*. Para superar esse problema, um protótipo (o *Photochrom-2*) foi desenvolvido na Universidade Técnica de Liberec (TUL) para realizar medições dinâmicas com precisão em materiais fotocrômicos e termocrômicos. Este dispositivo permite que o usuário controle a temperatura da amostra, o tempo de exposição à fonte de luz excitante e o tempo de decaimento. O *Photochrom-2* foi usado para estudar amostras têxteis estampadas com o pigmento *Matsui Photopia Purple* (MPP). O objetivo principal foi analisar o comportamento cinético do composto ao longo de cinco ciclos consecutivos enquanto se variava a concentração do pigmento, a temperatura e o tempo de exposição à fonte de luz excitante. Seis concentrações de pigmento distintas, cinco temperaturas e dois tempos de exposição foram testados. Depois de definir o comprimento de onda de absorção máximo e o tempo de decaimento apropriado, os ensaios de cinco ciclos começaram. Pela aplicação direta da transformada de Kubelka-Munk, gráficos dos valores  $K/S$  em função do tempo foram obtidos. A partir daí, foi possível avaliar a influência da concentração, temperatura e tempo de exposição na intensidade da cor resultante. Em seguida, os valores de  $K/S$  foram tratados com o modelo matemático de decaimento exponencial com o *software GraphPad Prism* para avaliar como a resposta fotocrômica é perdida ao longo de ciclos consecutivos de ativação e decaimento. Durante a primeira etapa de análise dos dados, concluiu-se que maiores concentrações e menores temperaturas produzem maior intensidade de cor. Na segunda etapa, foi analisado o comportamento cinético do pigmento. Concluiu-se que o tempo de meia vida varia com a temperatura e concentração de pigmento. Durante o decaimento, as amostras adquiriram cada vez mais cor residual em ciclos consecutivos, independentemente dos parâmetros. Em geral, concluiu-se que o pigmento resiste a cinco ciclos consecutivos de exposição e decaimento sem perda significativa da resposta fotocrômica. Para além disso, os parâmetros seleccionados foram adequados ao objetivo proposto; estes são uma valiosa contribuição para a investigação de corantes fotocrômicos e futuramente podem ser utilizados como modelo para outros trabalhos.

## Palavras-chave

Colorimetria, comportamento cinético; espectrofotometria; fotocromismo; Kubelka-Munk.

## Abstract: Study on the Kinetic Behaviour of Photochromic Systems

Photochromic colourants have found some applications, such as spectacle lenses, textile designs, and molecular switches. However, their somewhat high cost, lack of standardized laboratory procedures, and technological limitations are preventing them from entering the mainstream market and industry. To overcome this problem, a prototype (the *Photochrom-2*), consisting of a modified spectrophotometer, was developed at the Technical University of Liberec (TUL) to accurately perform dynamic measurements on photochromic and thermochromic materials. This device allows the user to control the sample's temperature, the time of exposure to the exciting light source, and the time of decay. Using the *Photochrom-2*, textile samples screen-printed with the *Matsui Photopia Purple* (MPP) pigment were studied. The main goal was to analyse the kinetic behaviour of the compound over five consecutive cycles while varying the pigment concentration, the temperature, and the time of exposure to the exciting light source. Six distinct pigment concentrations, five temperatures, and two exposure times were tested. After defining the maximum absorption wavelength and the appropriate decay time, the five cycle assays began. By direct application of the Kubelka-Munk transform, graphics of  $K/S$  values as a function of time were obtained. From there, it was possible to evaluate the influence of concentration, temperature, and exposure time on the resulting colour strength. Then, the  $K/S$  values were run through the one-phase decay mathematical model with the aid of the *GraphPad Prism* software to evaluate how the photochromic response is lost throughout consecutive cycles of activation and decay. During the first stage of data analysis, it was concluded that higher concentrations and lower temperatures were able to produce greater colour strength. In the second stage, the kinetic behaviour of the pigment was analysed. It was concluded that the half-life strongly correlates to pigment concentration and temperature. During decay, the pigment increasingly acquired residual colour over consecutive cycles, regardless of the parameters. Overall, it was concluded that the pigment does withstand five consecutive cycles of exposure and decay without a significant loss of photochromic response. Moreover, the parameters selected were suitable for the proposed objective, and, thus, are a valuable contribution to research on photochromic colourants and can be used as a model for further research.

## Keywords

Colour change behaviour; colourimetry; Kubelka-Munk; photochromism; spectrophotometry.



# Contents

Acknowledgements.....	iii
Resumo: Estudo do Comportamento Cinético de Sistemas Fotocrômicos.....	v
Abstract: Study on the Kinetic Behaviour of Photochromic Systems .....	vi
Abbreviations & Acronyms List.....	x
Units .....	xii
Figure List .....	xiii
Table List .....	xiv
Equation List .....	xv
1. Chapter I – Introduction.....	1
1.1 Research Background .....	1
1.2 Motivation .....	2
1.3 Aim of the Research .....	4
1.4 Research Methodology .....	4
1.5 Dissertation Structure.....	5
2. Chapter II – Theoretical Framework & State of the Art .....	7
2.1. Chromic Materials.....	7
2.2 Photochromic Colorants .....	8
2.2.1 Classification of Photochromic Colorants.....	10
2.2.1.1 Spiroanthoxazines.....	11
2.2.2 Applications of Photochromic Colourants .....	12
2.2.3 Advantages of Textile Based Sensors .....	14
2.2.4 Production of Photochromic Materials.....	14
2.3 Electromagnetic Radiation & Colour .....	16
2.4 The Human Perception of Colour.....	18
2.5 Colour Measurement & Reproduction .....	19

2.5.1	Colour Spaces .....	20
2.5.2	Traditional Colour Measurement Devices .....	20
2.5.3	Spectrophotometer for Dynamic Measurements – <i>Photochrom-2</i> .....	22
2.5.4	Light Sources .....	24
2.5.5	Reflection Conditions .....	24
2.5.6	Kubelka-Munk Equation .....	25
2.6	State of the Art .....	26
3.	Chapter III – Experimental Work.....	29
3.1.	Materials & Equipment .....	29
3.1.1.	Samples.....	29
3.1.2	Laboratory Devices & Setup .....	30
3.2	Methods.....	31
3.2.1	Parameters of the Experiment.....	31
3.2.2	Experimental Procedure.....	32
3.2.3	Data Analysis Methodology .....	34
3.2.3.1	Software: <i>OceanView</i> .....	36
3.2.3.2	Software: <i>GraphPad Prism</i> .....	36
3.2.3.3	Kinetic Model for Photochromism: One Phase Decay.....	36
4	Chapter IV – Results & Discussion .....	38
4.1	Stage I – Average Range of <b><i>K/S</i></b> Values Over Five Cycles .....	38
4.1.1	Influence of Exposure Time.....	40
4.1.2	Influence of Pigment Concentration.....	41
4.1.3	Influence of Temperature.....	41
4.2	Stage II – Pigment Kinetic Behaviour Over Five Cycles .....	42
4.2.1	Consecutive Cycles of Exposure .....	42
4.2.2	Consecutive Cycles of Decay.....	45

5	Chapter V – Conclusion .....	49
5.1	Future Perspectives .....	52
	Bibliography .....	53
	Annex I – Graphics: $K/S$ as a Function of Time.....	58

## Abbreviations & Acronyms List

AATCC – *American Association of Textile Chemists and Colorists*

B – Blue

C – Cyan blue

$c$  – Pigment concentration

CCD – Charge-coupled device

CCT – Correlated colour temperature

CIE – *Commission Internationale de l'Eclairage*

CIELAB (or CIE  $L^*a^*b^*$ ) – CIE 1976 colour space where  $L^*$  is lightness,  $a^*$  represents the red-green axis, and  $b^*$  represents the blue-yellow axis

CIELUV (or CIE  $L^*u^*v^*$ ) – CIE 1976 colour space where  $L^*$  is lightness,  $u^*$  represents the green-red axis, and  $v^*$  represents the blue-yellow axis

CIEUVW (or CIE  $U^*V^*W^*$ ) – CIE 1964 colour space where  $U^*$  represents the green-red axis,  $V^*$  represents the blue-yellow axis, and  $W^*$  is lightness

CIEXYZ (or CIE  $X^*Y^*Z^*$ ) – CIE 1931 colour space where  $X^*$  represents the green-red axis,  $Y^*$  is luminance, and  $Z^*$  represents the blue-yellow axis

CMYK – Cyan, magenta, yellow, black colour space

G – Green

IR – Infrared

ISO – *International Organization for Standardization*

$k$  – Light absorption coefficient

K-M – Kubelka-Munk

$K/S$  – Kubelka-Munk transform

M – Magenta

MPP – *Matsui Photopia Purple*

LED – Light-emitting diode

PBT – Poly(butylene terephthalate)

PET – Poly(ethyleneterephthalate)

R – Red

RGB – Red, green, blue colour space

$R_\infty$  – Decimal reflectance of an infinite thickness of a coloured fabric

$s$  – Light scattering coefficient

SEM – Scanning electron microscope  
SPD – Spectral power distribution  
T – Temperature  
 $t$  – Time  
 $t(\text{exp})$  – Time of exposure to the exciting light source  
TUL – Technical University of Liberec  
UV – Ultraviolet  
VIS – Visible light  
Y – Yellow  
 $Y_0$  – Colour response when  $X = t = 0$   
2D – Two dimensional  
3D – Three dimensional  
 $\alpha$  – Total absorption of a single layer  
 $\sigma$  – Total scattering of a single layer  
 $\lambda$  – Wavelength  
 $\lambda_{\text{max}}$  – Absorption maximum wavelength

## Units

*A* – Amperes

*g* – Grams

*h* – Hours

*K* – Kelvin

*Kg* – Kilograms

*klx* – Kilolux

*mA* – Milliamperes

*mm* – Millimetres

*mW* – Milliwatts

*nm* – Nanometres

*s* – Seconds

*V* – Volts

*W* – Watts

$^{\circ}\text{C}$  – Celsius degrees

## Figure List

Figure 1 Hydrochromic umbrella in the "off" and "on" state, left and right, respectively (Design Futures - Immortality, 2021). .....	8
Figure 2 Photochromism. ....	9
Figure 3 Spiro naphthoxazine derivative in the colourless (left) and coloured (right) states (Barnfield, 2001). ....	11
Figure 4 Photochromic sunglasses (TJUTR Vision, 2018). ....	12
Figure 5 "Rainforest" dress indoors (Winters, 2020). ....	13
Figure 6 "Rainforest" dress after exposure to sunlight (Winters, 2020). ....	13
Figure 7 Electromagnetic radiation chart (AIS LED, 2021). ....	17
Figure 8 Comparison between the RGB and CMYK colour spaces (Shacklett, 2021). ....	20
Figure 9 Representation of how a spectrophotometer works (CRAIC Technologies, 2020). ....	21
Figure 10 Timer device connected to the computer, spectrophotometer, and ammeter. ....	23
Figure 11 Modified spectrophotometer with thermostat pipes connected to the sample holder. ....	23
Figure 12 Inferred chemical structure of the <i>Matsui Photopia Purple</i> (MPP) pigment (Periyasamy, 2018). ....	29
Figure 13 Laboratory setup scheme. ....	30
Figure 14 Samples A, B, C, D, E, and F. ....	31
Figure 15 Laboratory setup. ....	33
Figure 16 Light trap and barium sulphate (BaSO <sub>4</sub> ) plaque. ....	34
Figure 17 One phase decay kinetic model graphic (GraphPad Software, 1995-2020). ....	37
Figure 18 Activated/coloured sample D. ....	38
Figure 19 Semi-activated/coloured sample F. ....	38
Figure 20 Samples A, B, D, E, and F in the coloured state after 20 seconds of UV exposure. ....	41

## Table List

Table 1 Pigment's chemical nomenclature, commercial name, and class. ....	29
Table 2 Parameters of the experiment.....	32
Table 3 Data analysis methodology.....	36
Table 4 Samples' concentration in $g/Kg$ .....	39
Table 5 Average range of $K/S$ values for 150 s of exposure.....	39
Table 6 Average range of $K/S$ values for 300 s of exposure.....	40
Table 7 <i>Plateau</i> and half-life values for sample A with 300 s of exposure at 10 °C.....	43
Table 8 <i>Plateau</i> and half-life values for sample A with 150 s of exposure at 10 °C.....	43
Table 9 <i>Plateau</i> and half-life values for sample F with 150 s of exposure at 10 °C.....	44
Table 10 <i>Plateau</i> and half-life values for sample F with 150 s of exposure at 30 °C.....	44
Table 11 <i>Plateau</i> and half-life values for decay for sample A with 300 s of exposure at 10 °C.....	46
Table 12 <i>Plateau</i> and half-life values for decay for sample A with 150 s of exposure at 10 °C.....	47
Table 13 <i>Plateau</i> and half-life values for decay for sample F with 150 s of exposure at 10 °C.....	47
Table 14 <i>Plateau</i> and half-life values for decay for sample F with 150 s of exposure at 30 °C.....	48



## Equation List

Equation 1 K-M diffuse reflectance.....	25
Equation 2 Absorption coefficient.....	25
Equation 3 Scattering coefficient.....	25
Equation 4 K-M transform.....	26
Equation 5 K-M transform.....	35
Equation 6 One phase decay kinetic model.....	37

# 1. Chapter I – Introduction

In this introductory chapter, the research background is presented. In addition, the motivation and aim of the research are described, as well as its structure and research methodology.

## 1.1 Research Background

Photochromic materials change colour when irradiated with a particular wavelength through various mechanisms. The simplest ones work like a switch, defining only two states: in the “off” state, it should be colourless or weakly coloured. After irradiation with a specific wavelength, the molecule turns to the “on” state, becoming coloured (Vik & Periyasamy, 2019). The reversion to its initial state may be triggered either by another wavelength (P-type photochromics) or by thermal means (T-type photochromics) (Viková & Vik, 2006). Moreover, the colour shift should be quick and easily detected by the naked eye. The pigment should be free of residual colour when coming back to the original state and should respond the same way over several colouring cycles (Bamfield, 2001). These compounds can be applied in several substrates, including glass, plastics, metals, and textiles (Ferrara & Bengisu, 2014). Thus, photochromic compounds have found a wide array of applications, including the well-known spectacle lenses, innovative textile designs, molecular switches, and data storage, among others (Bamfield, 2001; Tian & Zhang, 2016). Creating textile photochromic systems comes with a set of advantages, including its easiness to be maintained, to be sown or bonded to other surfaces, and to integrate into protective clothing; its low weight and good strength, tensibility, and flexibility; and the possibility of producing them through conventional means (Viková & Vik, 2006).

However, the lack of standardized laboratory procedures and relatively high cost is preventing them from entering mainstream industrial usage. In particular, studying the kinetic behaviour of photochromic compounds and how they respond over consecutive cycles of activation and decay has been a technical challenge.

Conventional colour measuring devices include colourimeters and spectrophotometers. Spectrophotometers measure the transmittance and reflectance of a sample as a function of wavelength and are useful in measuring surface colour (Régula, 2004). The three components essential in a spectrophotometer are a light source, a monochromator – a wavelength selection device –, and a photodetector (Vik & Periyasamy, 2019). The light reflected from a sample is measured for each wavelength in the visible spectrum, relating the light intensity on a surface and the resulting

spectral curve of that light reflected on the surface back to the device's sensor (Bertolini, 2010). Notwithstanding, these are unable to perform dynamic measurements necessary when working with chromic materials. To overcome this issue, a prototype, the *Photochrom-2*, was developed at the Technical University of Liberec (TUL) laboratories. This prototype consists of a traditional spectrophotometer but its integrating sphere has another slit to include a second light source and light filters that limit the range of incident wavelengths and exclude infrared (IR) and ultraviolet (UV) radiation. This way, the sample can be continuously irradiated during both the activation and decay cycles allowing continuous reflectance measurement. Additionally, the spectrophotometer sample holder was modified by being linked to a thermostat that regulates the sample's temperature (Viková, Vik & Christie, 2014; Periyasamy, 2018). Further, the system is connected to a timer to control the exposure and decay times. This way it is possible to perform dynamic measurements in photochromic and thermochromic samples while simultaneously controlling the light, time of exposure, and temperature (Viková, 2010).

With the aid of this innovative colour measurement device, the chemical kinetic behaviour of the *Matsui Photopia Purple* (MPP) pigment was studied, which belongs to the spironaphthoxazines family. This class of colourants is known for its fatigue resistance (i.e. resistance to photodegradation) and thermal stability (Bamfield, 2001; Ferrara & Bengisu, 2014). Chemical kinetic behaviour is an area of physical chemistry that studies the speed of chemical reactions and the factors that influence them. It includes the study of how different experimental conditions may influence the speed of a chemical reaction and informs about the reaction mechanism yield and transition states. It also assists in the construction of mathematical models that describe a reaction. The reaction rate may be influenced by many factors such as reagents' concentration, presence of catalysers, or pressure. In the present research, the influence of time of exposure, pigment concentration, and temperature in the pigment's kinetic behaviour during both the exposure and decay cycles was studied in screen printed textile samples.

## 1.2 Motivation

Chromic materials and photochromics, in particular, are rising in popularity and have found plenty of applications. Besides the well-established use of photochromics in plastic lenses (Periyasamy, Viková, & Vik, 2017), there is a growing list of other outlets, including actinometry, optical memories for data storage, photo-optical switches, filters, displays, self-developing photography (Bamfield, 2001), security

inks used to print invisible images and text (Ferrara & Bengisu, 2014), and novel designs for clothing items and accessories. Moreover, there is a growing interest in using photochromics in the development of camouflage patterns for military protective clothing that can mimic the surrounding environment colours when exposed to sunlight and for smart garments that can block UV radiation (Ramlow, Andrade, & Immich, 2020).

In consequence, there is a pressing need for uniformity in experimental procedures and conditions for chromic materials – only through standardization can these truly be embraced by the industry. In this research work, testing parameters were established and used. Aside from discussing the results, the effectiveness of the established parameters was evaluated so that future research on the topic can be conducted using the same parameters or change them accordingly, in case they were not effective. The influence of three parameters on the kinetic behaviour of both the exposure and decay cycles was studied.

In addition to the lack of standardized procedures, technological limitations have restricted the use of photochromics in the mainstream industry. At the Faculty of Textile Engineering of the Technical University of Liberec, a prototype – the *Photochrom-2* – was developed to solve this issue by Professors Martina Viková and Michal Vik from TUL and Robert M. Christie from Heriot-Watt University in Edinburgh, Scotland (Viková, Vik, & Christie, 2014). This prototype is capable of performing dynamic measurements in photochromic and thermochromic materials by controlling the time of exposure to an exciting light source and the time of decay, while continuously irradiating the sample with a secondary light source. Moreover, the prototype can reliably control the sample's temperature. For this reason, this partnership between Minho University and the Technical University of Liberec is of considerable interest.

The photochromic textile samples used in these experiments were previously produced through screen printing, which is one of the most common methods for the production of said samples. The three parameters studied were the time of exposure to an exciting light source, the pigment concentration, and the sample's temperature. The time of exposure and temperature are preponderant to understand both how the pigment would behave in real-life situations and how these parameters can affect its fatigue resistance. Evaluating the influence of pigment concentration is of particular interest for industrial applications given that the costs should always be reduced as much as possible and if a lower concentration can produce satisfactory results, it is wasteful to apply a higher concentration.

### 1.3 Aim of the Research

The main aim of this research was to study the kinetic behaviour of the *Matsui Photopia Purple* pigment and its fatigue resistance in screen printed textile samples. Thus, three parameters were selected and varied in the assays conducted: the temperature, concentration, and time of exposure to an exciting light source. For this purpose, the colour response and half-life of the pigment during irradiation, over consecutive cycles, were analysed to understand how the mentioned parameters influenced the chemical kinetic behaviour and fatigue resistance of the pigment. Moreover, the residual colour and half-life of consecutive cycles of decay were also studied with the same aim. Additionally, it was intended to study the influence of the mentioned parameters in the colour strength of the samples.

Given that there is a pressing need for standardization of laboratory procedures for photochromic textiles, another important aim of this research was to establish effective parameters for the experiment that could potentially be used in future research.

### 1.4 Research Methodology

Regarding the investigation methodology, it was divided into five parts: firstly, the motivation and aim of the research were clearly defined. Following, bibliographic research was conducted to establish the theoretical framework necessary for the work and to aid in selecting the parameters for the experiments. Then, the experiment was designed. During the first experiments, the absorption maximum wavelength was determined in order to be used in all assays and the decay time was adjusted to make sure the whole cycle is encompassed. Taking into consideration that it was unknown whether or not the MPP was a T-type photochromic, it was necessary to study the influence of temperature in the pigment's kinetic behaviour. Additionally, the influence of exposure time to the exciting light source and pigment concentration were evaluated. For this purpose, five temperatures, six concentrations, and two exposure times were tested over five consecutive cycles of exposure and decay. To understand the influence of each individual parameter, only one variable was changed between assays and at least three assays for each were required. Considering there are always possible errors of measurement and system malfunctions, some assays had to be repeated up to eight times for the results to be statistically relevant.

It is important to note that the present work mainly consisted of quantitative analysis. After obtaining the experimental results, the data analysis was carried out in two stages. Firstly, the  $K/S$  values were calculated from the reflectance values obtained using the Kubelka-Munk (K-M) transform and the influence of individual parameters on colour strength was evaluated. By direct interpretation of the graphics of  $K/S$  as a function of time, assessing which temperature, concentration, and time produced the most strongly coloured response was possible.

In the second stage of data analysis, how the photochromic function is lost throughout consecutive cycles was studied. The previously obtained  $K/S$  values were added to the *GraphPad Prism* software. Aided by this software, the mathematical model utilized for the analysis was the one-phase decay, resulting in a graphic with time as  $X$  and photochromic response as  $Y$ . Other relevant values for study obtained with this model were  $Y_0$ , which represents the initial  $K/S$  value, *Plateau*, which represents the maximum or minimum value  $K/S$  is tending to, *Span*, which represents the difference between  $Y_0$  and *Plateau*, and the half-life, which translates the time it took for the pigment to reach or lose half of its photochromic response. After running all the data through this mathematical model, the results were analysed and discussed. Finally, conclusions were drawn and future perspectives were presented.

## 1.5 Dissertation Structure

This dissertation is divided into the following five chapters:

**Chapter I – Introduction:** the study was contextualized by defining the background and motivation behind the research. Further, the aim of the research was clearly stated, followed by the research methodology and structure of the report.

**Chapter II – Theoretical Framework & State of the Art:** the knowledge foundation necessary to fully understand the scope of the research was laid out in this chapter. It consisted of extensive bibliographic research, privileging but not exclusively featuring recent sources and research. Firstly, chromic materials and, in particular, photochromics were described along with their classification, applications, advantages, and production methods. Following is the necessary foundation to understand colour and colour measurement, including what is electromagnetic radiation and colour, how humans perceive it, the traditional colour measuring devices and how the novel *Photochrom-2* distinguishes

from them, as well as light sources, reflection conditions, and the Kubelka-Munk transform. Finally, the state of the art is presented.

**Chapter III – Experimental Work:** the experimental procedures were described, starting with the materials and equipment, followed by the parameters of the experiment, and the experimental procedures carried out. Moreover, the methodology for data analysis was described, including the software and kinetic model used.

**Chapter IV – Results & Discussion:** the resulting values were presented and discussed in this section in two parts. Firstly, the influence of the established parameters in the colour strength was analysed. Then, the kinetic behaviour of the pigment was studied during both its exposure and decay cycles.

**Chapter V – Conclusion & Future Perspectives:** in this final chapter, conclusions were drawn regarding the influence of the selected parameters in the kinetic behaviour, fatigue resistance, and maximum colour strength of the samples and about the effectiveness of the parameters set based on the quantitative data analysis that was previously performed, and future perspectives were presented.

Finally, the bibliographic references used were listed according to the 6th Edition of APA by the American Psychological Association. In *Annex I*, the  $K/S$  graphics as a function of time can be consulted.

## 2. Chapter II – Theoretical Framework & State of the Art

### 2.1. Chromic Materials

Chromic materials change colour when exposed to a particular stimulus, such as light, temperature, a given chemical concentration, electricity, mechanical impact, among others. Thus, these may be classified according to the stimulus that activates them as photochromic, thermochromic, electrochromic, piezochromic, etc. (Viková, 2010). The shift between the two states may be due to several properties of the molecules such as electron transfer, isomerism, differences in the complexation behaviour, and photocyclization (Vik & Periyasamy, 2019). The change between the two states is activated, for example, by light, heat, magnetic or electric fields or chemical reactions – therefore, these are active intelligent textiles (also known as “smart textiles”), in opposition to passive intelligent textiles, such as optic fibre which is sensitive to different stimuli but does not respond to it (Viková & Vik, 2006). Considering colours convey different visual signals that can carry information to the user (e.g. road signs) its application and importance become clear – some everyday life applications include thermochromic temperature indicators, mirrors, and visual displays. It is noteworthy that this class of pigments and dyes has found applications far beyond the textile industry (Bamfield, 2001).

Regarding their structure, chromic materials are molecular devices, meaning they are constructed to perform a given function at a molecular scale. The simplest ones work like a switch, defining only two states: “on” or “off”. In the “on” state, the switch must perform its function or allow another device to do so; in the “off” state it should completely prevent given action (Vik & Periyasamy, 2019), as exemplified in Figure 1. A chromic compound will turn to its “on” state upon contact with the stimulus that activates it, be it a specific wavelength in the case of photochromics, a given temperature in the case of thermochromics, water in the case of hydrochromics, and so on. Further, they are called “systems” since the chromic compound is incorporated into another structure such as a polymer or enzyme, to regulate its activity.





Figure 1 Hydrochromic umbrella in the "off" and "on" state, left and right, respectively (Design Futures - Immortality, 2021).

One essential characteristic of all chromic materials is that the colour shift, whether it is from colourless to coloured or from one colour to another, must be easily detected by the human eye (Bamfield, 2001). They have also been referred to as “chameleon textiles” (Viková & Vik, 2006). In the specific case of photochromics, when radiation at a certain wavelength is absorbed, the way atoms are linked within the molecules changes, transitioning to an excited state and changing or starting to reflect a given visible wavelength (Bamfield, 2001).

Most chromic materials are pigments. The major difference between pigments and dyes is that the first ones are insoluble in water and have no affinity to textile substrates, whereas dyestuff is at least partly soluble and possesses substantivity. Moreover, usually, dyes produce stronger and brighter colours (Ferrara & Bengisu, 2014). Since pigments have little to no affinity to textile substrates, they ought to be applied through other means, such as included in microcapsules or in pastes or dispersions with a binding agent in its composition.

The current goal is to understand this technology’s limitations and set specifications so that manufacturers and designers can use these colourants industrially (Ferrara & Bengisu, 2014).

## 2.2 Photochromic Colorants

The term photochromism was originally suggested by Hirshberg in the 1950s and had been first observed by Fritsche with the photobleaching of tetracene in 1867 (Vik & Periyasamy, 2019). The study of excited states resulting from the photochromic response and the transient species involved in the photoreactivity of photochromic molecules was facilitated by the development of techniques such as flash spectroscopy and laser photophysical methods in the 1950s and 60s (Tian & Zhang, 2016). Interest in the application of these systems increased in the 1980s after stable organic photochromic

compounds such as spirooxazine, naphthopyran, and diarylethenes were synthesized, which overcame the big issue of low fatigue resistance. Since then, its commercial applications have increased (Bamfield, 2001; Vik & Periyasamy, 2019). However, these molecules have no substantivity to textile substrates. Still, a few have minor solubility which allows them to be applied as dyes. It is noteworthy that inorganic photochromic colourants are more suitable for coatings on glass, ceramic, or metal whereas organic ones are more fitting for textiles (Ferrara & Bengisu, 2014). The most well-known example is the photochromic spectacle lenses, but there are an increasing number of potential application areas: since the 1990s, applications for data storage and molecular switches have started to emerge (Tian & Zhang, 2016). Currently, the most relevant families of photochromic compounds used in textiles are spiropyrans, spirooxazines, and naphthopyrans (Chowdhury, Joshi, & Butola, 2014).

Photochromism happens thanks to a reversible transformation of chemical species, induced by light, between two forms with different absorption spectra. The reverse reaction may occur either by exposure to another set of wavelengths (P-type photochromics) or by thermal means (T-type photochromics) (Viková & Vik, 2006). In most cases, they go from colourless or weakly coloured to coloured and are activated by UV radiation. Furthermore, usually, the change is bathochromic – to a longer wavelength. Nevertheless, a reversible colour change is not the only alteration in physical properties experienced during photochemical transformations of photochromic materials. There are also changes in refractive index, relative permittivity (dielectric constant), oxidation/reduction potentials, and geometrical structure (Bamfield, 2001). There are also a few factors that can influence the colour, such as temperature, moisture, electricity, and gases (Hwu, Bai, Tao, Luo, & Hu, 1995). It is important to distinguish between photochromism (Figure 2), which is a reversible process, and photo-induced chemical reactions, which are irreversible (Vik & Periyasamy, 2019).

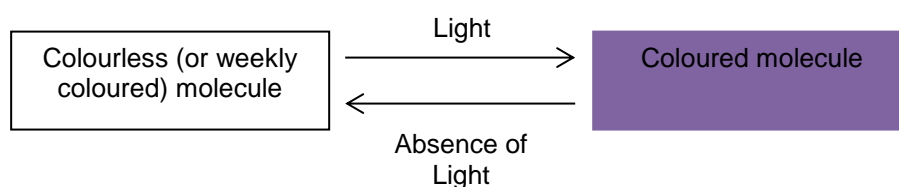


Figure 2 Photochromism.

Requirements in organic photochromic compounds include colour development – the transition ought to be rapid and easily visible upon irradiation; the rate of colour return to the initial state – which must be controllable; a wide range of colours; weak or no residual colour in the original state, and durability

– it should respond the same way over several colouring cycles (Bamfield, 2001). Additionally, thermal stability is very important for any type of application and designers should bear in mind both the process and application temperature. These colourants are unstable when exposed to UV light. Due to their low light stability, they start to lose photochromic response through photodegradation, photobleaching, photooxidation, and other secondary reactions. The low photostability of photochromic colourants happens because photochromic reactions cause the rearrangement of chemical bonds and undesired side reactions may occur during that rearrangement (Periyasamy, Viková, & Vik, 2017). Its fatigue resistance is related to both the total time of exposure and the number of cycles completed. An array of compounds may be added in order to improve the colourant's performance, such as light or thermal stabilizers, antioxidants, and UV absorbers, among others. Regarding the photochromic inks' shelf life, these can last years when properly stabilized (Ferrara & Bengisu, 2014).

### 2.2.1 Classification of Photochromic Colorants

Inside the photochromic realm, most authors divide photochromic compounds into categories according to the mechanism behind the chemical reaction involved in the photochromic process (Tian & Zhang, 2016; Vik & Periyasamy, 2019). Five main classes satisfy the requirements stated above: spiropyrans (spiroindolinobenzopyrans specifically), spironaphthoxazines, naphthopyrans, fulgides, and diarylethenes (Bamfield, 2001). Naturally, as research progresses some compounds become obsolete, whereas newer ones take their place – currently, the most researched compounds belong to the diarylethenes' family, followed by the azobenzene derivatives. Others still relevant but not as intensely researched include spiropyrans, spirooxazines, naphthopyrans, fulgides, and anils (Tian & Zhang, 2016).

Alternatively, these colourants may be classified according to its reversion mechanism as T-type or P-type photochromics. On one hand, T-type regards those whose reversion is thermally influenced – they are the most commonly used ones (Chowdhury, Joshi, & Butola, 2014). In other words, if it is a T-type photochromic compound, when exposure to the activation wavelength ceases the system returns to its initial, colourless (or weakly coloured) state spontaneously; examples of thermally reversible photochromic molecules include anils, perimidine spirocyclohexadienones, spirodihydroindolizines, etc. (Vik & Periyasamy, 2019). Further, the T-type photochromics' function is weakened or fully inhibited at some temperatures, depending on the compound. On the other hand, P-type photochromics need to be irradiated with another wavelength to return to the initial state and its reversion is photochemically

induced (Chowdhury, Joshi, & Butola, 2014). In this case, a chemical species shifts between isomers A and B depending on the wavelength that irradiates it – the irradiation of the isomer A with a given wavelength leads to a photoisomerization reaction resulting in isomer B; when it is irradiated by a different wavelength, the reaction is reversed returning to the initial isomer (Viková, 2010).

### 2.2.1.1 Spiroanthoxazines

The photochromic pigment studied belongs to the spiroanthoxazines' class, which are organic photochromic molecules. Its colour change is caused by a molecular conversion that happens when radiation with a certain wavelength irradiates the molecule. To go from colourless to coloured, ring-opening occurs either by heterolytic cleavage of the C<sub>(spiro)</sub>-O bond (Figure 3) or by electrocyclization. The return to its uncoloured initial state happens when irradiation ceases and, thus, they belong to the T-type photochromics family (Xiong, et al., 2018).

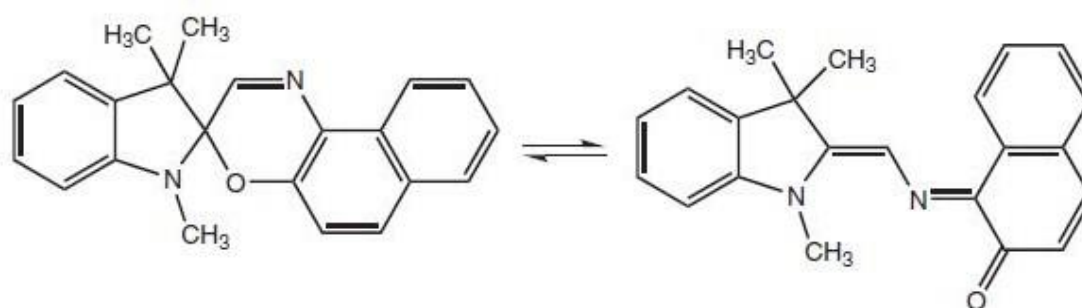


Figure 3 Spiroanthoxazine derivative in the colourless (left) and coloured (right) states (Bamfield, 2001).

Spiroanthoxazines, when compared to other photochromics, are known for its exceptional resistance to photodegradation, also known as fatigue resistance, which makes them suitable for many applications, including solar protective uses (Bamfield, 2001). Particularly, when compared to spiropyrans, the structural variation of spiroanthoxazines is what grants them higher fatigue resistance (Pargaonkar, Sanjay, Patil, & Vajekar, 2020). Aside from its excellent fatigue resistance, spiroanthoxazines exhibit high photoconversion (85–95%), broad absorption in the visible (Xiong, et al., 2018), and great pH stability (Pargaonkar, Sanjay, Patil, & Vajekar, 2020). It is believed that the photodegradation of spirooxazines and their derivatives depends only on the excited state of the oxygen in their structure (Vik & Periyasamy, 2019). Spiroanthoxazine powders also offer great thermal stability. They can withstand temperatures between -40 and 250 °C (Ferrara & Bengisu, 2014).

### 2.2.2 Applications of Photochromic Colourants

Besides the well-established use of photochromic materials in ophthalmics, especially in plastic lenses for sunglasses (Figure 4) to reduce the light transferred through them (Periyasamy, Viková, & Vik, 2017), there is a growing list of other outlets, including actinometry, optical memories for data storage (mostly used in military applications) (both 3D and near-field), filters, photo-optical switches, self-developing photography, image displays (Bamfield, 2001), security inks used to print invisible images and text (Ferrara & Bengisu, 2014), and many others.



Figure 4 Photochromic sunglasses (TJUTR Vision, 2018).

Specifically in the textile industry, these colourants' popularity has grown since the first photochromic t-shirts were marketed in 1989 (Ferrara & Bengisu, 2014). Photochromic printed or embroidered t-shirts are still one of the strongest commercial outlets and there is a wide range of colours to choose from (Bamfield, 2001; Periyasamy, Viková, & Vik, 2017). "Smart textiles" differ from their conventional counterparts since they can sense and react to external environmental stimuli or conditions, such as mechanical, thermal, or magnetic stimuli (Syduzzaman, Patwary, Farhana, & Ahmed, 2015). Some examples include shape memory, thermoregulating, and chromic materials. They can also be incorporated into interactive textile – examples of these include a keyboard made of a single layer of capacitive sensing fabric and a pair of gloves that allow users to control their phone with them.

In the case of photochromics, light is the external stimuli that activates them (Syduzzaman, Patwary, Farhana, & Ahmed, 2015). The pigment used in this research, for example, can work as sensor for its activation wavelength. Currently, photochromic textiles are being used to sense environmental changes and to protect users by blocking UV radiation. Additionally, they offer great opportunities for brand protection, sports clothing, security bar codes, solar heat, light management, special clothing for the police and fire brigades, for example, and for the military, namely to develop camouflage patterns that change when exposed to sunlight to mimic the surrounding environment (Ramlow, Andrade, & Immich, 2020). Aside from technical applications, photochromic textiles can be used to make

innovative decorations and offer consumers the opportunity to express themselves depending on their style and mood and to be creative in an unprecedented way. Hence, they are receiving great interest from artists and designers (Chowdhury, Joshi, & Butola, 2014). The brand *Rainbow Winters* is pioneering the use of chromic materials in fashion, entertainment, and marketing (Ferrara & Bengisu, 2014). Figure 5 and Figure 6 show the *Rainbow Winters* "Rainforest" dress indoors and after exposure to sunlight, respectively. The *Swedish Interactive Institute* has developed UV-sensitive curtains to create computer-controlled dynamic textile patterns (Chowdhury, Joshi, & Butola, 2014). Another quite renowned example is the photochromic sculpture by Tomoko Hashida, Yasuaki Kakehi, and Takeshi Naemura (Ferrara & Bengisu, 2014). In both of these examples, a UV light projector is directed at the photochromic objects to create computer-controlled dynamic prints.



Figure 5 "Rainforest" dress indoors (Winters, 2020).

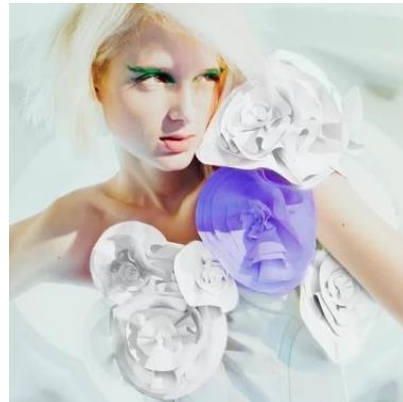


Figure 6 "Rainforest" dress after exposure to sunlight (Winters, 2020).

Besides clothing items and innovative designs, smart textiles have found several technical applications, including in protective, medical, sports, and geo-textiles (Periyasamy, Viková, & Vik, 2017). An example of protective clothing is photochromic swimsuits which change colour, alerting and protecting against the nefarious health effects of UV radiation. These are considered "added value products" since their functionality is increased compared to their conventional equivalents (Ferrara & Bengisu, 2014). Moreover, photochromics are being used in military protective clothing to produce camouflage patterns that mimic the surrounding environment (Chowdhury, Joshi, & Butola, 2014). In this case, a photochromic coating is applied over the traditional camouflage print; it can then change according to the ambient light and mimic shadows, natural elements, like leaves and stems, or simply change the shade of the patterns underneath it to fit better with the surrounding environment (Conner, 1998). Innovative technologies, such as chromic materials, will lead to the development of totally new products and services, even some that are not conceptualized yet (Ferrara & Bengisu, 2014).

### 2.2.3 Advantages of Textile Based Sensors

Advantages of textile-based sensors include its easiness to be sown, thermally bonded or glued to other surfaces; easy maintenance; low specific weight with good strength, tensibility, and flexibility; production and application through the common means; extremely large specific surface; low price and easy integration into protective clothing systems (Viková & Vik, 2006). Additionally, when used as sensors, for example, they don't require electronics or electricity like most sensors do.

### 2.2.4 Production of Photochromic Materials

Photochromic colourants can be acquired in powder, paste, or dispersion to then be applied to textile materials. A challenge that photochromic colourants present is that, apart from a minority which is partly soluble, these have no affinity to textile substrates (Chowdhury, Joshi, & Butola, 2014; Ferrara & Bengisu, 2014), nonetheless, there are several techniques for incorporating photochromic compounds in textile materials. Regardless of the process, most commercial photochromics are known to degrade at temperatures higher than 240 °C (Ferrara & Bengisu, 2014).

The most well-established means to produce photochromic textiles is by integrating these molecules, or microcapsules containing them, in polymeric chains, as long as the compound is unaffected by the temperature required in the process (Hwu, Bai, Tao, Luo, & Hu, 1995; Ferrara & Bengisu, 2014); it is also possible to add other compounds to the polymeric chain to lower its melting point. Examples of polymers capable of taking photochromic molecules in their chain include polypropylene, polyethylene, polyolefins copolymers and terpolymers thereof (e.g.: ethylene-propylene copolymers and ethylene-propylene-diene terpolymers); polyamides (e.g.: nylon 6, nylon 66, nylon 8, nylon 11, nylon 12 and thence blends); and polyesters (e.g.: poly(ethyleneterephthalate) (PET) and poly(butylene terephthalate) (PBT) and copolymers or blends thereof) (Hwu, Bai, Tao, Luo, & Hu, 1995). The biggest advantage of this technique over the remaining is increased durability since the colourant is dispersed through the whole fibre, not just at its surface, not allowing it to be removed by external attacks, such as washing and other abrasive actions (Chowdhury, Joshi, & Butola, 2014; Ferrara & Bengisu, 2014). This process may also be referred to as "mass colouring" (Vik & Periyasamy, 2019).

Another popular technique is coating substrates with these pigments, although at times these offer unsatisfactory colourfastness. The compound is encapsulated in a compatible low melting

thermoplastic polymer before being immobilized on the textile's surface; through this technique, more durable and brightly coloured photochromic textiles are produced (Hwu, Bai, Tao, Luo, & Hu, 1995). Microencapsulation techniques include coacervation, spray-drying, *in situ* polymerization, and interfacial polymerization. These structures protect the colourant only to a certain extent, external attacks such as light, pressure, or heat are able to degrade its wall's quality. Hydrogels are comparable to coatings – a macromolecular network made of hydrophilic polymers swollen with water or other aqueous liquid contains photochromic molecules in its structure. These are usually cross-linked on surfaces (Ferrara & Bengisu, 2014).

Other possibilities include being comprised in silica nanoparticles and added to textiles through printing with a binding agent (e.g.: polyurethane) (Pinto, et al., 2016); epoxy groups can be added to silica nanoparticles, to create bonds with wool fibres (Cheng, Lin, Brady, & Wang, 2008) or with cotton, once its surface is modified to possess thiol groups (Yu, Xu, Hu, Li, & Wang, 2017); a silica sol-gel coating can also be formed on a wool fabric's surface using a solution in which the photochromic molecules are contained (Liu, Cheng, Parhizkar, Wang, & Lin, 2010; Parhizkar, Zhao, Wang, & Lin, 2014).

Various compounds may be added as UV stabilizers to increase the products' durability. In 1999, Mennig et al developed a new photochromic organic/inorganic nanocomposite coating system based on an epoxysilane network, and organic bisepoxide, and organic amine as a thermal cross linker, and surface modifier silicium dioxide nanoparticles. It was concluded that the long term stability of the photochromic dyes in the matrix is considerably improved by adding Tinuvin 327, a UV absorber. The half-life of the spirooxazine dye increased tenfold (from 20h to 200h) (Mennig, Fries, Lindenstruth, & Schmidt, 1999). In 2012, Liu et al produced a hybrid photochromic silica coating on wool fabrics with a spirooxazine dye and a silane with a long alkyl chain. Four stabilizers were added separately to the coatings and their influence on photostability and photochromic behaviour was studied. It was concluded that despite slightly hindering the photochromic response speed and photochromic absorption, UV stabilizers improve the photochromic lifetime considerably (Liu, Cheng, Parhizkar, Wang, & Lin, 2010). Later, in 2014, Parhizkar et al applied a photochromic pigment from the spironaphthoxazine family with two UV stabilizers (HMBP and Tinuvin-329) to merino wool. Adding UV stabilizers improved photostability without significantly affecting other photochromic properties (Parhizkar, Zhao, Wang, & Lin, 2014).



Regarding printing techniques, both traditional (e.g.: rotary stencil printing, screen printing, roller printing, etc.) and novel (e.g.: digital printing, etc.) processes may be chosen as long as it does not damage the photochromic compound. Digital inkjet printing is one of the most used processes, due to its flexibility; it is also more economical, considering it is a niche application that usually does not require mass production (Seipel, et al., 2018). Printing processes may be used to apply coatings. In both, printing and coating, microencapsulated colourants are preferred, since these offer, on one hand, the possibility to include other compounds, such as UV stabilizers, and, on the other hand, higher protection against external attacks. In recent years, research has focused on developing specific processes for chromogenic colourants that suited their particularities (Ferrara & Bengisu, 2014). It is noteworthy that printing is economically and ecologically more advantageous than dyeing, since no wastewater outcomes.

### 2.3 Electromagnetic Radiation & Colour

Before getting into the colourimetry apparatus, one must understand what colour is and how it can be measured. Electromagnetic radiation is a phase oscillation of both the electric and magnetic fields, which is organized in sections according to wave frequency. The visible light, or visible spectrum, is only a small part of the entire spectrum of possible electromagnetic radiation (Dartora, n.d.). Figure 7 shows the different wavelengths of electromagnetic radiation and its inversely proportional relation with frequency. The wavelengths visible to the human eye are approximately between 380 and 780 *nm* (Vik & Periyasamy, 2019). Ultraviolet, X-rays, and gamma rays are shorter waves and, hence, with a higher frequency. Longer waves – with lower frequencies – include infrared, heat, microwaves, and radio and television waves.

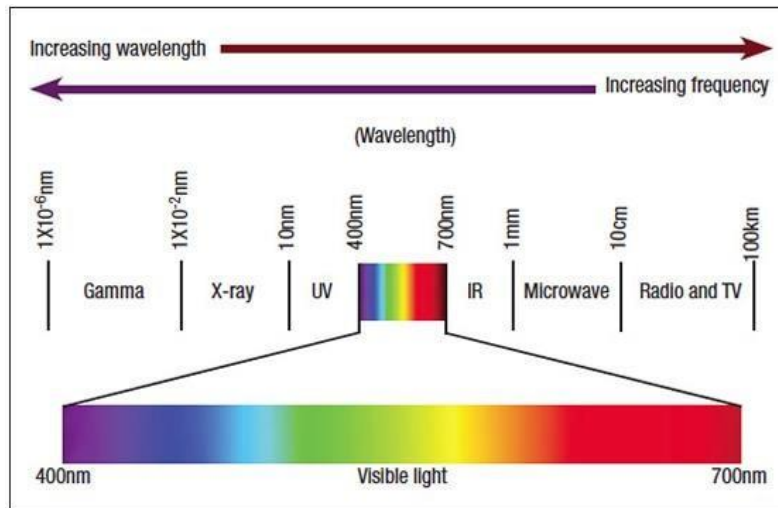


Figure 7 Electromagnetic radiation chart (AIS LED, 2021).

The first known colour theory was by the Greek philosopher Aristotle. He concluded that colour was a property of objects, like weight or texture. However, the study of colour has always been influenced by psychological and cultural aspects, so, throughout the Middle Ages and the Renaissance, colour was studied mostly by writers and artists. In the 17th century, Isaac Newton developed the corpuscular theory of light; simultaneously Christiaan Huygens defended the wave theory (Bassalo, 2002). It was Albert Einstein, using the idea of Max Planck, who theorized about the dual wave-particle nature of light, managing to demonstrate that a beam of light corresponds to small packs of energy called photons. When light spreads it behaves like a wave, but once it hits a surface, it behaves like a particle (Vik, 2017). Currently, the study of colour theory is divided into three categories: physical, physiological, and chemical colour.

Colour is correlated to different wavelengths of the electromagnetic spectrum. The colour of an object corresponds to the visible radiation that is reflected the most by it – with white being the combination of all colours reflected and black none at all. An object will have a certain colour if it does not absorb the wavelengths that correspond to that colour (Bertolini, 2010; Vik, 2017). Colour perception is a physical and physiological phenomenon governed by the reflectance characteristics of the sample, the spectral composition of the incident light, and the personal physiological characteristics of the observer (Vik & Periyasamy, 2019). Any colour can be defined according to three parameters: the hue, which is defined by wavelength; lightness, which is related to the proximity to white or black; and saturation, which corresponds to the degree of colour purity (Guimarães, 2004; Vik, 2017). Coloured lights can be defined by three parameters: the hue, which is defined by wavelength or frequency; brightness, which is related to the amount of light emitted by the colour; and chroma, which corresponds to the degree

of colour purity or, in other words, the measure of the presence of achromatic colours. When colour is produced with colourants, the process is called subtractive colour mixture and its primaries are magenta (M), yellow (Y) and cyan blue (C); whereas in the case of lights, the process is named additive colour mixing and uses red (R), green (G), and blue (B) as primaries. Curiously, the primary colours of these processes correspond to each other's secondary colours (Vik, 2017). Colours also convey useful meanings, for instance, traffic signs or others related to psychology or cultural traditions and are preponderant in textile and garment design.

The light reaching the eye from an image may be described by its spectral power distribution, which generally specifies the radiant power density at each wavelength in the visible spectrum ( $\approx 380$  to  $780$  nm) (Brainard & Stockman, 2009). The perception of colour is a human experience, only possible thanks to the human vision being trichromatic.

## 2.4 The Human Perception of Colour

The human eyes are made of several components. Similarly to a camera's aperture, the pupil controls how much light is admitted to the eye. Also similarly to a camera, the cornea and the retina work like two lenses. The cornea works like a focus lens, allowing it to control the distance adaptation. The retina is located in the back of the eye and has five layers of cells responsible for the first instance of image processing in the eye system. The first layer of the retina contains two types of photoreceptors – the cones and rods. Rods have a low spatial acuity and they do not mediate colour vision; they are responsible for vision at low light levels (at night, for example). There are approximately 120 million rods in the human eye. Cones work at higher light levels, are responsible for spatial acuity, and colour vision (Vik, 2017). There are around eight million cone cell photoreceptors and they are sub-divided in three classes:

- Short-wavelength (S-cones) – these peak at 440 nm and are referred to as B (blue) despite sensing violet.
- Middle-wavelength (M-cones) – these peak at 550 nm and are referred to as G (green) despite sensing yellowish-green.
- Long-wavelength (L-cones) – these peak at 570 nm and are referred to as R (red) despite sensing yellow.

Each type responds univariantly to the rate of photon absorption of each light colour making the human vision trichromatic. By overlapping them, other colours are produced and by varying the

relative intensities of each light, intermediate colours are obtained. It is also noteworthy that rods are concentrated in the periphery of the retina while cones take a more central spot. Furthermore, photoreceptors individually are colour blind; it is by comparison of the three individual outputs that colour is seen. In the optic disk there is an optical nerve that connects the photoreceptors in the retina to the ganglion cells in the brain to transfer the signals received for further processing (Vik, 2017). This is known as the trichromatic theory of vision and it was developed by Hermann von Helmholtz. However, this theory is not enough to fully describe the human colour vision. It explains how the “hardware” (the three types of cones) works but not how the “software” (brain) processes these signals (Baumann, 1992).

In the late 1800s, Ewald Hering proposed the opponent process theory since he did not agree with the previous explanation. However, this theory does not oppose the previous one, it complements it. The opponent process theory suggests that the human perception of colour is controlled by three opposing systems that need four unique colours to perceive colour: blue, yellow, red, and green. Those opposing systems are blue and yellow, red and green, and black and white. The hue is perceived using two colours simultaneously but only one opposing colour can be detected at a time since one of the colours in the pair suppresses the other – this is why humans can see reddish-yellows and yellowish-greens but never reddish-green or yellowish-blue (Baumann, 1992).

## 2.5 Colour Measurement & Reproduction

The science of colour measurement is colourimetry. Colourimetry allows expressing colour numerically, given that standardized light sources and observation geometries are used and the average sensitivity of the human eye is considered (Fernandes, 2002; Brainard & Stockman, 2009). For this reason, the *Commission Internationale de l'Eclairage* (CIE), born in 1913, developed standardized light sources, observation geometries, and methods to express colour numerically. CIE is currently recognized as the greatest authority on colour measurement and as an international standardization body by the *International Organization for Standardization* (ISO) (Bertolini, 2010). Colour measurement is fundamental to create, compare, and reproduce colour with precision.

### 2.5.1 Colour Spaces

To organize and facilitate the reproduction of colours, several colour models or spaces were created. These may be absolute or arbitrary, like the *Pantone* system that attributed names and numbers to a collection of physical samples. Absolute colour systems include the RGB that uses three coordinates to express colour – red, green, and blue; the CMYK that uses four coordinates – cyan, magenta, yellow, and black; or the ones created by CIE (Leite, 2006). Moreover, it is possible to convert colours from one colour system to another. Figure 8 shows the difference in colour appearance between a computer monitor (RGB) and those same colours reproduced by a printing device (CMYK).

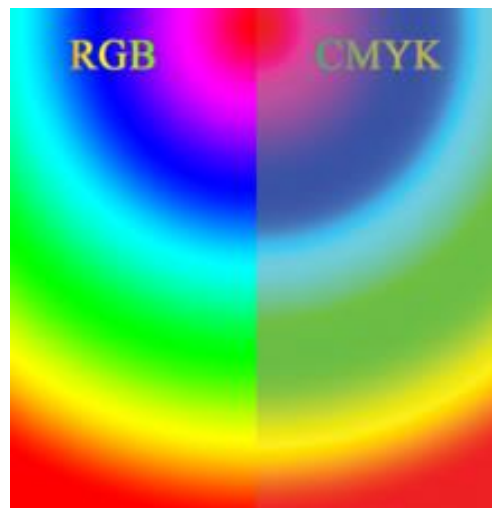


Figure 8 Comparison between the RGB and CMYK colour spaces (Shacklett, 2021).

In 1931, CIE developed the first colour system based on measurements of the human perception of colour – the CIEXYZ. This system was an incredibly important step forward in the science of colour measurement. Later, other systems were derived from this one, including the CIELUV, CIEUWV, and CIELAB (or CIE  $L^*a^*b^*$ ). The latter was created in 1976 to provide an accurate representation of the colour differences and the corresponding differences in human perception (Bertolini, 2010) and is based on standardized light sources and observation geometries – it is one of the most widely used colour spaces in the textile industry. This system also relates to the opponent process theory since each colour is defined by the coordinates  $L^*$  (lightness),  $a^*$  (the red-green axis), and  $b^*$  (the blue-yellow axis) (Yuan, Brewer, Monaco, & Davis, 2007).

### 2.5.2 Traditional Colour Measurement Devices

There are several methods for measuring colours, such as colourimeters, spectrophotometers, spectroradiometers, image analysers, or a combination of these. The most used ones are

colourimeters and spectrophotometers, which define colour through the spectral composition of light reflected by the surface (Lagouvardos, Fougia, Diamantopoulou, & Polyzois, 2009). Spectrophotometry studies the quantitative analysis of radiation in relation to its spectral composition (Bertolini, 2010). With commercial spectrophotometers, the light emitted from a light source irradiates the sample. Then, depending on the experiment, the light reflected by or transmitted through the sample enters a slit that directs it to a monochromator. This component aims to divide the light by wavelength using a dispersing element, like an optical grating. After separation, the light reaches a charge-coupled device (CCD), which consists of thousands of light detectors that can measure the intensity of light for each wavelength. The information from the CCD can then be analysed by a computer software in the form of the intensity of light per wavelength (CRAIC Technologies, 2020). Figure 9 represents the how the different components of a spectrophotometer work.

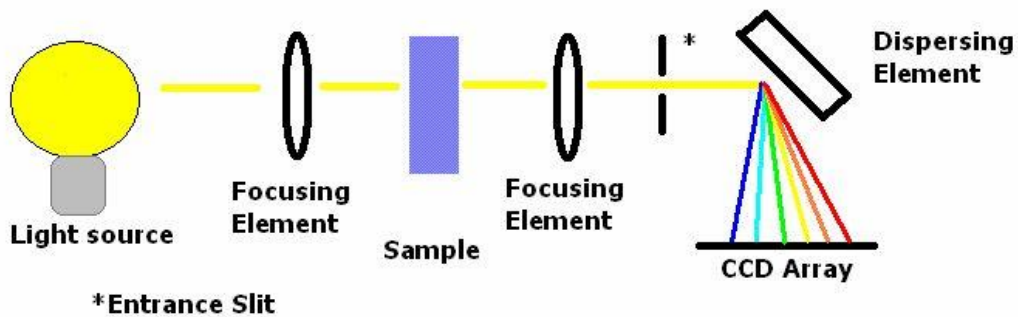


Figure 9 Representation of how a spectrophotometer works (CRAIC Technologies, 2020).

*VITA Easyshade* and *Spectroshade Micro* are examples of spectrophotometers (Dias, 2016). Spectrophotometers have longer durability than colourimeters and are not affected by metamerism (Berns, 2019). Illuminant metamerism happens when two samples appear to be the same colour under one illuminant and viewing conditions but different when exposed to other conditions; geometric metamerism happens when the same sample appears to have different colours when the viewing angle changes; field-size metamerism happens when the same sample appears to have a different colour when seen in a small, centrally fixed area and in a large colour area; observer metamerism happens when the same sample seems to have a different colour for different users; and, finally, device metamerism – which happens in colorimeters – happens when the device was built by a different manufacturer or has aged and registers a different colour in the same sample (Brady, 2006).

Colourimeters measure the three-dimensional values of light reflection of a sample, according to the standardized CIE lighting and observation geometry, after the light source passes through a series of filters (Dias, 2016; Berns, 2019). These filters are composed of a photodiode in order to control the

light that reaches the sample. The light reflected from the sample is then measured by a sensor. These instruments are easier to use and cheaper than spectrophotometers, however, reproducibility may be low due to the ageing of filters and the phenomenon of metamerism (Dias, 2016). The biggest advantage of using a spectrophotometer for colour determination, compared to a colourimeter, is accuracy. Spectrophotometric data is unaffected by ambient light, and the amount of light reflected from objects is measured over the complete spectral wavelength (Ishikawa-Nagai, Yoshida, Da Silva, & Miller, 2010).

However, the traditional colour measuring devices cannot perform the dynamic measurements needed when working with chromic samples. A commercial spectrophotometer is unable to continuously measure colour change without interrupting UV exposure. When using a separate UV source, the problem intensifies as the time between irradiation and measurement allows fading – a photochromic reaction happens in the order of attoseconds to nanoseconds (Periyasamy, 2018). To fulfil this necessity, a prototype was developed at TUL, which can perform dynamic measurements on chromic materials, eliminating certain problems such as the difficulty in controlling the intensity and spectral distribution of the source, the temperature, and the frequency of exposure (Viková, 2010).

### 2.5.3 Spectrophotometer for Dynamic Measurements – *Photochrom-2*

Given the pressing need for a device able to perform dynamic colour measurements in chromogenic materials – namely in photo and thermochromic surfaces – a prototype was developed at the Technical University of Liberec by Professor Martina Viková and Professor Michal Vik in partnership with Professor Robert M. Christie from Heriot-Watt University in Edinburgh, Scotland (Viková, Vik, & Christie, 2014). The prototype, named *Photochrom-2*, consists of a modified spectrophotometer as depicted in Figure 10 and Figure 11. It allows continuous measurement of colour while keeping the sample's temperature under control. Firstly, there are two apertures instead of one. In one aperture there is an excitation light source with a shutter – the light is blocked by the shutter during the decay cycle to allow the photochromic molecules to return to their colourless state. However, to evaluate the colour fading during the decay cycle there ought to be light – otherwise, there is no radiation being reflected by the sample for the sensors to register. To solve this issue, an additional aperture was added. In this second aperture, there is a light source with an IR and UV filter in order to illuminate the sample without activating the photochromic molecules. In addition, there is a thermostat connected to the sample holder of the spectrophotometer that ensures the sample remains at the desired

temperature. Aside from these features, it works like a commercial spectrophotometer using a monochromator and diaphragm to separate and select wavelength bands that irradiate the sample during excitation and light sensors that continuously measure the radiation reflected by the sample (Periyasamy, 2018).



Figure 10 Timer device connected to the computer, spectrophotometer, and ammeter.

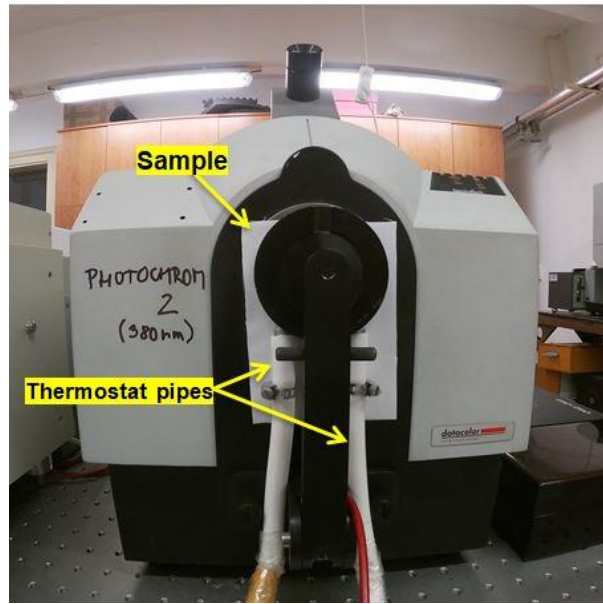


Figure 11 Modified spectrophotometer with thermostat pipes connected to the sample holder.

This way, it is possible to measure continuously over multiple cycles and accurately study photochromic kinetics. Since it is possible to assess the sample's sensitivity to exposure time, temperature, and spectral composition of the light source, this device can test fatigue resistance. Moreover, just like with traditional spectrophotometers, measurements are carried out at the sample's absorption maximum wavelength since higher absorption provides greater sensitivity, meaning that the maximum response from the sample is attained. Another advantage of using the sample's absorption maximum wavelength is that, at its maximum, the curve is relatively flat and even if the monochromator drifts slightly there is little variation in absorbance, which guarantees the accuracy of measurement (Harris, 2015). This prototype (Figure 10 and Figure 11) can perform dynamic measurements by overcoming the problems of commercial spectrophotometers, such as the difficulty in controlling the intensity and spectral distribution of the source, the temperature, and the time of exposure (Viková, 2010).



#### 2.5.4 Light Sources

The main difference between a blue body (illuminated by white light) and a blue-emitting light source is that the blue pigment is absorbing all colour frequencies but blue, while the blue light-emitting source effectively emits only blue. If the object was illuminated by this light it would remain blue, but if it was illuminated by a red light, for example, it would be black (Bertolini, 2010). Hence, choosing an adequate light source for colour measurement is paramount. The perceived colour of an object depends on the spectral power distribution (SPD) of the light source illuminating it, aside from its intrinsic reflectivity properties (Vik & Periyasamy, 2019). To measure colour accurately, the SPD of the light source ought to be well defined and known. An SPD value defines the power per unit area per unit wavelength of a light source. In other words, it describes the concentration of any radiometric or photometric quantity as a function of wavelength (McCluney, 1994). Colour measurement requires standard illumination and geometries of observation. The light source is essential for accurate colour measurement, thus, CIE defined spectral values for each wavelength for different illuminants such as daylight and incandescent, among others (Shevell, 2003).

Generally, there are two ways of specifying illuminants, either in terms of relative energy tabulated for each wavelength or wavelength band or based on colour temperature. Colour temperature is a simple way of describing the colour characteristics of light, measured in Kelvin ( $K$ ). A 'warm' light is yellowish whereas a 'cool' light is blueish (Vik & Periyasamy, 2019). For example, an incandescent lamp ( $T \approx 2700 K$ ) has a yellowish light, while fluorescent lamps or daylight ( $4000 K < T < 20000 K$ ) are more bluish or white (Bertolini, 2010). CIE together with ISO standardized illuminants that are used in colourimetry. Examples include illuminant A and illuminant D65. Illuminant A represents a domestic tungsten lamp, with a temperature close to  $2856 K$ , while illuminant D65 represents daylight, with a temperature of approximately  $6500 K$  (CIE, 2020).

#### 2.5.5 Reflection Conditions

When measuring colour, the surface topography of the sample will have a great influence on the reflected light. A smooth surface reflects most of the light in a well-defined direction – specular reflectance. Whereas an irregular surface spreads the light in all directions creating diffuse reflectance (Vik & Periyasamy, 2019). Most surfaces belong to this last category. An integrating sphere is required to perform measurements with a spectrophotometer in textured samples, such as textiles.

### 2.5.6 Kubelka-Munk Equation

Reflectance and absorbance are the most commonly used parameters to measure colour. Reflectance (also known as reflectivity) corresponds to the fraction of incident light on a surface that is reflected back – each material has unique reflectance and emission properties depending on the incident radiation. Absorbance (also known as optical density) represents the fraction of incident light that is absorbed by the sample. Transmittance is another important parameter that describes the fraction of incident light that is neither absorbed nor reflected by the sample but transmitted through it. If an object is perfectly opaque, its transmittance is null; a mirror, for example, perfectly reflects incident light, so its reflectance is close to 100%; and a hypothetical perfect black body would have 100% absorbance.

As previously mentioned, most materials, including textiles, have internal inhomogeneities that cause light to scatter off of its surfaces – this is known as diffuse reflectance. The most commonly used model to describe diffuse reflectance is the Kubelka-Munk (K-M) equation (Harrick Scientific Products, Inc., 2014). For semi-infinite samples, all inhomogeneities are translated into a single parameter, the scattering coefficient ( $S$ ). This coefficient accounts for internal scattering processes and is dominated by the particle size and refractive index of the sample. The scattering coefficient is not dependant on the absorption coefficient ( $K$ ) and only varies slightly with wavelength ( $\lambda$ ), it is, therefore, considered a constant. So, the decimal reflectance of an infinite thickness of a coloured fabric ( $R_\infty$ ) can be found with the following equation:

$$R_\infty = 1 + \frac{K}{S} - \sqrt{\frac{K}{S} \left(2 + \frac{K}{S}\right)}$$

Equation 1 K-M diffuse reflectance.

Where the absorption coefficient ( $K$ ) and the scattering coefficient ( $S$ ) is given by the following equations, where  $\sigma$  represents the total scattering of a single layer and  $\alpha$  represents the total absorption of a single layer (Hecht, 1976).

$$K = \frac{2\alpha}{\sigma + \alpha}$$

Equation 2 Absorption coefficient.

$$S = \frac{\sigma}{\sigma + \alpha}$$

Equation 3 Scattering coefficient.

For practical applications, the equation is transformed to obtain the  $K/S$  value:

$$\frac{K}{S} = \frac{(1 - R_{\infty})^2}{2R_{\infty}}$$

Equation 4 K-M transform.

The K-M transform is approximately proportional to the absorption coefficient ( $K$ ), which is proportional to pigment concentration ( $c$ ). This equation is widely used in spectrophotometry for its simplicity.

## 2.6 State of the Art

In 2010, Little and Christie established a methodology to evaluate the performance of photochromic textiles using traditional colour measurement instrumentation. Aside from optimizing this process, they carefully controlled the laboratory temperature and time interval between irradiation and measurement. Additionally, they described a semi-quantitative methodology for consistent and reproducible statistical analysis. For measurement, a *Datacolor Spectraflash SF600* spectrophotometer, *Datamatch 3.1* software, and D65 illuminant were used. The laboratory temperature was controlled and localized air heating was used to ensure the air temperature around the sample was uniformly stabilized. A strip thermometer was attached to the sample. The statistical results revealed that this method was much more rigorous and appropriate for photochromic textile sample testing than previous methods (Little & Christie, 2010). In that same year, Liu et al. used a *SUB4000* optical fibre UV-VIS spectrometer with a *DH2000-BAL* UV-light source. The photochromic effect was evaluated by analysing the difference in absorbance between a sample's inactivated and activated states. To measure photostability (or durability), two methods were used. Method I dictated that the samples were irradiated continuously with a strong UV light source and changes in absorption were recorded as a function of UV exposure time. The time taken to lose half of its photochromic response was also recorded. With method II, samples were repeatedly covered and uncovered while exposed to direct sunlight in 2.5 minute intervals. The number of cycles the sample could withstand until fully losing its photochromic effect was recorded (Liu, Cheng, Parhizkar, Wang, & Lin, 2010). In 2014, this experiment was repeated by Parhizkar et al. but using different samples (Parhizkar, Zhao, Wang, & Lin, 2014). In that same year, Chowdhury et al. used the colour measurement methodology developed by Little and Christie to study the photostability of photochromic textiles. It was concluded that less than 10 hours of exposure were enough for the samples to lose 90% of their photochromic effect. The half-life of photochromic

colourants was also studied (Chowdhury, Joshi, & Butola, 2014). In 2016, Brixland used a different method to test photochromic fatigue in textile samples printed with three different formulations. Measurements were made before activation and one minute after irradiation with a UV light source, then, the sample was stored for 23 hours. This process was repeated over five days and then the sample was stored in a dry place for ten days (240 h) before being repeated for five days more completing a total of ten cycles of activation and decay. To assess whether or not the pigment lost photochromic effect over ten cycles, colour measurements were performed before and after the ten cycles using a *Datacolor CHECKPRO™* spectrophotometer. To avoid decolouration between irradiation and placing the sample in the spectrophotometer, the temperature was controlled at 0 °C (Brixland, 2016).

Professor Martina Viková and Professor Michal Vik have been working on developing the prototype used in this research work since 2006 to eliminate several problems other methodologies have, such as the difficulty in controlling the sample's temperature, the time of exposure, and decolouration between irradiation and measurement (Periyasamy, Viková, & Vik, 2017). In 2014, they patented this revolutionary device and co-authored an article describing its components and how it works (Viková, Vik, & Christie, 2014). On that same year they used the *Photochrom-2* to study the influence of temperature in the kinetic behaviour of photochromic pigments in textile substrates (Viková & Vik, 2014). Two years later, they assessed the influence of two different light sources, a Xenon 450 W and an LED 395-410, on the photochromic response of pigments and whether or not it was viable to use such lights (Viková & Vik, 2016). In 2017, Periyasamy et al. authored a review of photochromic textiles and their measurement, where they extensively described this new prototype and methodology to measure photochromic textiles (Periyasamy, Viková, & Vik, 2017). In 2018, Periyasamy used this prototype to study mass coloured polypropylene filaments and polypropylene filaments coated with photochromic pigments that can be used as flexible UV sensors. He studied the influence of pigment concentration and filament cross-section in optical properties, such as  $K/S$  value, optical density, colour difference, half-life of both the exposure and decay cycles, rate constant, and colour intensity in the beginning, half of the cycle, and when tending to infinite. Additionally, he used SEM analysis to study surface change of both the filaments and fabrics (Periyasamy, 2018). Later, in 2019, Viková and Vik studied the influence of photochromic pigment concentration in polypropylene and polypropylene multifilaments produced through the mass coloration technique over five cycles of exposure and decay (Viková & Vik, 2019).

Since the experimental work of this dissertation took place, some similar research has been carried out. Abate et al. used a different version of the same prototype, the *Photochrom-3*, to study supercritical carbon dioxide dyeing of polyester fabric with two different photochromic dyes. A *LED Engine LZ1-00UV00* LED was used as the activation light source, 60 *klx* were used to illuminate the sample during decay, and the temperature was kept constant at 21 °C. Reflectance values were recorded every 2 s during both activation and decay. The main parameters analysed in the experiment were the colour strength (*K/S* value), photoswitching rates, and washing fastness. This last parameter was evaluated according to the ISO 6330:2012 for one and ten washing cycles. It was concluded that this colouration method produced uniformly coloured photochromic textiles with excellent photochromic performance while providing a more economical and environmentally friendly alternative (Abate, et al., 2020). Qi et al. developed a novel type of smart photochromic fabric for image information storage based on the thiol-ene click chemistry principle and tested its fatigue resistance and fading rate by irradiating the samples with UV light for 30 s and letting them fade back to their original state in the dark. This process was repeated 30 times. Immediately after each irradiation, the maximum absorption was measured using a *Datacolor 650* spectrophotometer and compared to the original colour of the fabric. The *K/S* value was used to make these comparisons and the CIELAB colour space was used to graphically illustrate them. It was concluded that the photochromic effect hardly changes after 10 cycles and just decreases slightly after 20 cycles. Additionally, the washing fastness was evaluated according to the AATCC 61–2007 standard and the staining percentage was measured (Qi, et al., 2021). A study that simultaneously evaluates the influence of pigment concentration, temperature, and time of exposure in the kinetic behaviour of screen printed photochromic textile samples over consecutive cycles has not been previously carried out.

### 3. Chapter III – Experimental Work

#### 3.1. Materials & Equipment

##### 3.1.1. Samples

The samples used were previously prepared through screen printing with two layers and mesh 50. A solution of binder and microcapsules containing both the photochromic pigment and a UV stabilizer was applied to the substrate – plain weave made out of 35/65% cotton/PES. The samples were dried for three minutes at 120 °C and cured at 150 °C. Six different concentrations (50, 100, 150, 200, 250, and 300 *g/Kg*) were used. Below is the chemical and commercial name of the colourant, as well as its class.

Table 1 Pigment's chemical nomenclature, commercial name, and class.

<b>Chemical Nomenclature</b>
5-chloro-1,3,3-trimethylspiro[indoline-2,3'-(3H) naphtho(2,1-b) (1,4)-oxazine] (Kamada & Suefuku, 1991) (Kamata, Suno, Maeda, & Hosikawa, 1994)
<b>Commercial Name</b>
<i>Matsui Photopia Purple</i> (MPP) (Matsui International)
<b>Class of Colourant</b>
Spironaphthoxazines

Figure 12 shows the inferred chemical formula of the pigment used, considering the brand did not make it available.

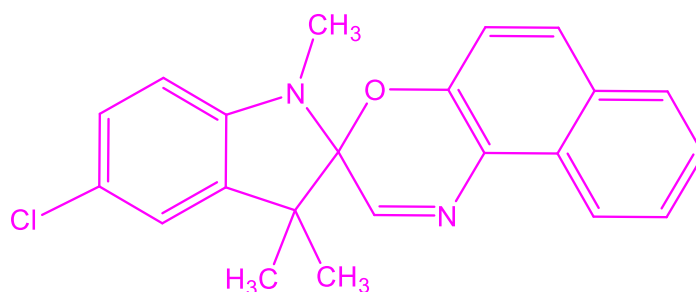


Figure 12 Inferred chemical structure of the *Matsui Photopia Purple* (MPP) pigment (Periyasamy, 2018).

### 3.1.2 Laboratory Devices & Setup

The laboratory setup depicted in **Erro! Auto-referência de marcador inválida.** included a timer, an ammeter, a *Julabo F25* thermostat, a *VOLTCRAFT VLP 2403 pro* voltmeter, a computer, and a modified *Datacolor Spectraflash SF600* spectrophotometer (*Photocrom-2*) with a *Thorlabs M385LP1* Mounted LED (385 nm, minimum 1650 mW, 1700 mA) and a LAV aperture of 30 mm; the secondary light source was a *Yuji* violet-chip based white LED with 5600 K correlated colour temperature (CCT) and a 420 to 680 nm wavelength filter in the secondary aperture. This light filter is required because the pigment is greatly affected by ambient light and in previous tests, in which this filter was not used, the sample could never return to its initial colour, showing even lower reflectance values after finishing the decay cycle. The diffuse geometry used was d:8°.

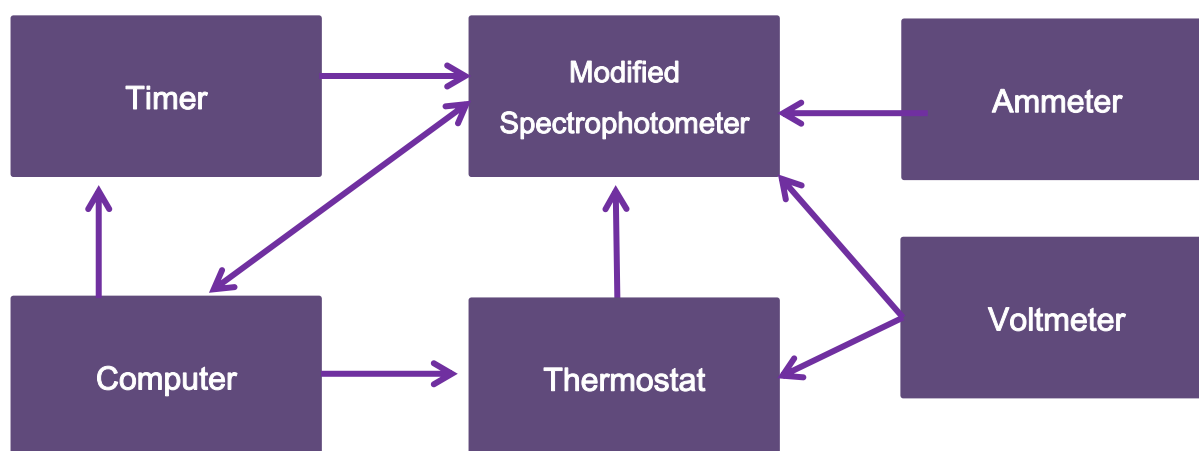


Figure 13 Laboratory setup scheme.

The voltmeter's role was to make sure the light source was being supplied with 21 V and the thermostat with 12 V. The ammeter made sure the light source was being supplied with 0,001 or 0,002 A during thermostabilization and decay, and 0,400 A during exposure. In the computer, one could, firstly, control the thermostat's temperature with the *Julabo* software and, secondly, control the timer and the modified spectrophotometer with the *OceanView* software. Additionally, all data from the spectrophotometric measurements was displayed on the computer. The sample was kept at a relatively constant temperature thanks to the thermostat and its robustness. The timer controlled the exposure and decay cycles time during spectrophotometric measurements. After the sample was placed in the spectrophotometer holder and the parameters were set in the computer, another device, the *Diametral*, would be turned on. Its job was to link all components of the setup for them to work together.

## 3.2 Methods

### 3.2.1 Parameters of the Experiment

A solution of binder and microcapsules containing both the *Matsui Photopia Purple* (MPP) pigment and a UV stabilizer was applied at six different concentrations – 50, 100, 150, 200, 250, 300 *g/Kg* (Figure 14). Testing the influence of concentration on colour intensity, both in one cycle and over five cycles, is especially interesting from an industrial perspective – to maximize profits, cost should be as low as possible so, knowing whether or not it is possible to produce satisfactory results by using less amount of pigment is very important.

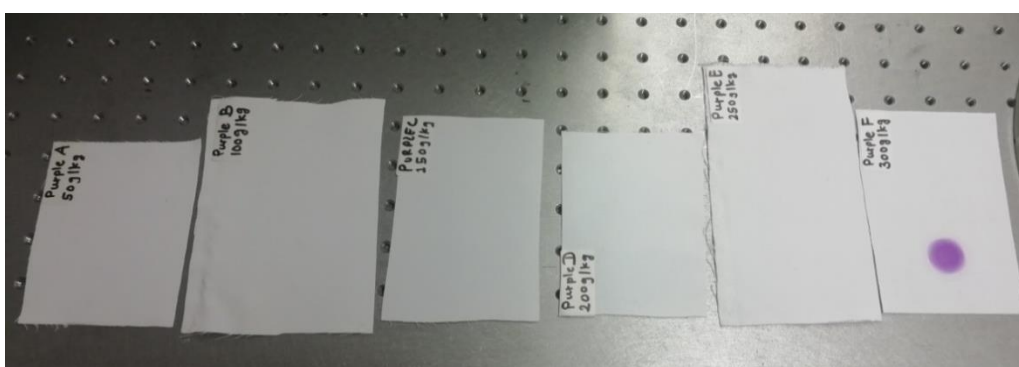


Figure 14 Samples A, B, C, D, E, and F.

If the *Matsui Photopia Purple* (MPP) pigment is, indeed, a T-type photochromic, it wouldn't need to be irradiated with another wavelength to trigger its return to the colourless state and its activation and decay rate would be intimately related with temperature. Thus, five different temperatures were tested – 10, 15, 20, 25, and 30 °C. Further, knowing how the pigment behaves at different temperatures is of uppermost importance if it is to be used in any real-world applications.

To study how the time of exposure to the UV light influences the colour intensity over the growth and decay cycles, the samples were submitted to 150 and 300 *s* of exposure and 900 *s* of decay after each exposure cycle. Previously to the first exposure cycle, the sample remained in the holder for 900 *s* to ensure it is thermally stabilized and in its totally colourless state. Initially, only 600 *s* were intended for decay but it was observed that it was not enough time for the sample to fully return to its colourless state.

Each five-cycle assay was repeated at least three times to be statistically representative. Some assays were repeated up to eight times since the values deviated greatly. Additionally, all assays were carried out using the absorption maximum wavelength ( $\lambda_{max}$ ), which was 570 *nm*. The  $\lambda_{max}$  is used because



the sample has greater sensitivity with a higher absorption, which means that the maximum response from the sample will be attained. Another reason for using this wavelength is that, at the maximum, the curve is relatively flat – even if the monochromator drifts slightly, there is little variation in absorbance, which guarantees greater accuracy during measurement (Harris, 2015).

Table 2 Parameters of the experiment.

<b>Parameters of the experiment</b>	
<b>Pigment</b>	<i>Matsui Photopia Purple</i> (MPP) (Matsui International)
<b>Concentration (g/ Kg)</b>	50; 100; 150; 200; 250; 300
<b>Time (s) for 1 cycle</b>	900/150/900 (total = 1950)
	900/300/900 (total = 2100)
<b>Time (s) for 5 cycles</b>	900/(150/900)*5 (total = 6150)
	900/(300/900)*5 (total = 6900)
<b>Temperature (°C)</b>	10; 15; 20; 25; 30

### 3.2.2 Experimental Procedure

The laboratory setup is depicted in Figure 15. In this section, the experimental procedure carried out in each assay is described as follows. Before systematically following this procedure, the absorption maximum wavelength was determined as well as the appropriate time for the exposure and decay cycles.

1. Turn on the thermostat – *Julabo F25*;
2. Turn on *VOLTCRAFT VLP 2403 pro* and guarantee it measures 21 V for the light source and 12 V for the thermostat;
3. Run *Julabo*, the thermostat software;  
Remark: If *Julabo* beeps it is necessary to add distilled water.
4. On the computer, run software *Julabo* and select the configuration “Icam”, then, run this configuration and select the target sample temperature;  
Remark: In this software, it is possible to follow both the device's internal and external temperatures, which corresponds to the sample's temperature and is the one to consider. The device's robustness ensures temperature control.

5. Once both temperatures are close to the target, run software *OceanView* and run project “PHOTOREFL” (to measure the photoreflectance of the sample);
6. Calibrate spectrophotometer:
  - 6.1 Begin with dark calibration, with a black cylinder (the resulting graph should be a straight line  $y \approx 0$ );
  - 6.2 Afterwards, do the white calibration with barium sulphate plaque (the resulting graph should be a straight line  $y \approx 100$ );

Remark: If both values do not match the expected values, repeat the calibration.
7. Place the sample in the spectrophotometer;
8. On the software *OceanView*, configure the graph data and select how long should the test go for;
9. Run the software and turn on the *Diametral* device to start testing;
10. Start recording the graph;
11. Once the assay is finished, turn off the *Diametral* device;
12. To start a new measurement, it is not necessary to recalibrate the spectrophotometer – simply remove the sample and repeat steps 7 to 11.

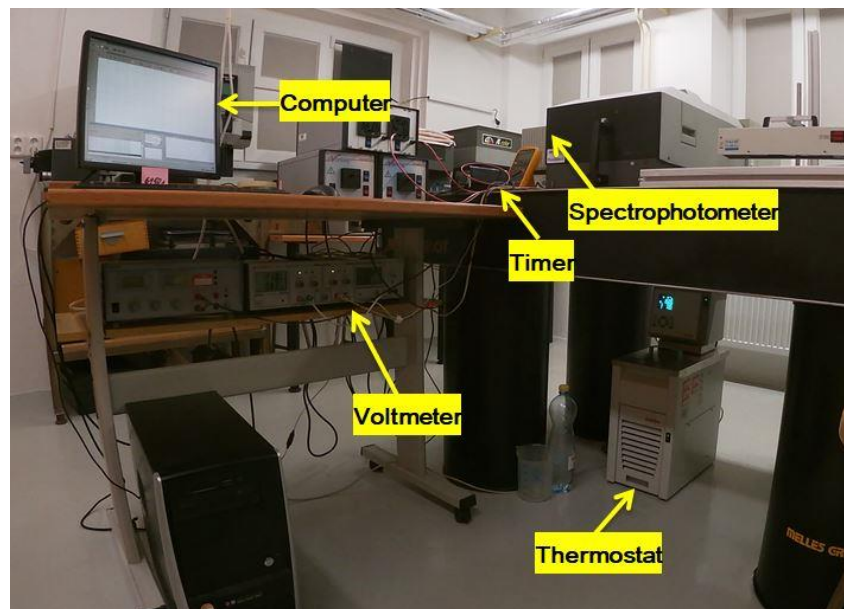


Figure 15 Laboratory setup.

To calibrate the spectrophotometer certified reference materials are used, in this case, a light trap and barium sulphate ( $\text{BaSO}_4$ ) plaque (as depicted in Figure 16), which is a  $\approx 99\%$  reflective material; the first should have a reflectance value of  $\approx 0$  counts and the second  $\approx 100$  counts for all incident wavelengths

(calibration curves correspond to straight lines in the graphic). The validity of the results obtained in the measurements depends entirely on the proper functioning of the device determined by its calibration.

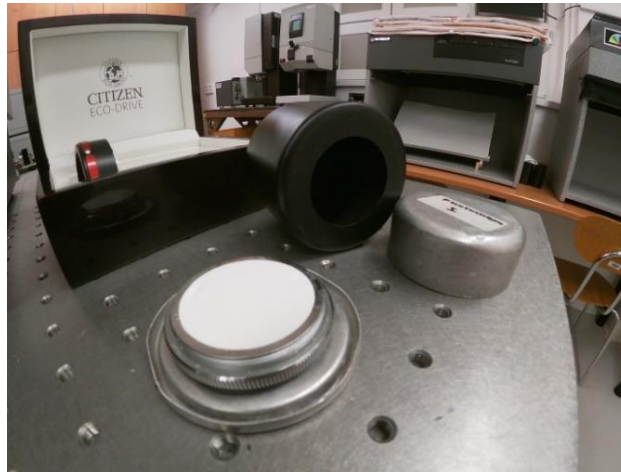


Figure 16 Light trap and barium sulphate (BaSO<sub>4</sub>) plaque.

The samples ought to be kept in a black box so that the measurements are not influenced by ambient light. The sample being tested should be removed from the box and placed immediately on the spectrophotometer, checking only if it is stained or contaminated.

Since it is relatively time-consuming to stabilize the device at a given temperature, all samples should be tested with the same temperature before moving on to the next. Further, different assays on the same sample should evaluate different areas of the sample since the distribution of pigment during screen printing could be uneven. Therefore, the same sample should not be tested continuously since it is also sensitive to ambient light and the results would be compromised – as previously mentioned, the sample should remain in the black box right until the moment it is placed in the spectrophotometer holder.

### 3.2.3 Data Analysis Methodology

The methodology of data analysis is divided into two stages as follows:

**Stage I** – The first measurement obtained had  $X$  as wavelength and  $Y$  as *counts*, from 0 (black) to 100 (white). Its purpose was to determine the absorption maximum wavelength ( $\lambda_{max}$ ), which is around 570 *nm* and which was used in all measurements. The direct data provided by the spectrophotometer was a graphic with time as  $X$  and reflectance as  $Y$ . From those values, it

was possible to attain a graphic with time as  $X$ , and the  $K/S$  value as  $Y$ . The  $K/S$  value was obtained by substituting the reflectance value in the Kubelka-Munk transform and it represents colour strength or intensity.

$$\frac{K}{S} = \frac{(1 - R_{\infty})^2}{2R_{\infty}}$$

Equation 5 K-M transform.

From these values one could assess which temperature, concentration, and time produce the most strongly coloured response – the lower the reflectance, the greater is the colour strength (or  $K/S$  value).

**Stage II** – The goal of the second stage of data analysis was to understand how the photochromic function was lost throughout consecutive cycles, both how the colour intensity decreased with consecutive cycles, and how the degree of white in the deactivated form was reduced. So, the consecutive activation stages were analysed separately from the consecutive deactivation stages. The  $K/S$  value as a function of time was added to the *GraphPad Prism* software. Aided by this software, the mathematical model utilized for this analysis was the one phase decay (Figure 17). The graphics obtained have time as  $X$ , and photochromic response as  $Y$ . In the case of exposure,  $Y_0$  was set to zero and the values that are important to analyse are *Plateau* (limit in  $Y$ , to infinite), and half-life. In the case of decay, *Plateau* was set to zero and the values that are important to analyse are the *Plateau* (limit in  $Y$ , to infinite) and half-life.

The data analysis methodology is summarized in the following Table 3:

Table 3 Data analysis methodology.

	<b>Source</b>	<b>Data</b>
<b>Stage I</b>	<i>OceanView</i>	Counts as a function of wavelength
		Reflectance as a function of time
	<i>Microsoft Excel</i>	$K/S$ value as a function of time
<b>Stage II</b>	<i>GraphPad Prism</i>	$K/S$ value as a function of time
		$Y_0$
		<i>Plateau</i>
		Half-life

#### 3.2.3.1 Software: *OceanView*

*OceanView* is a spectroscopy software that provides stable data acquisition and processing through a smooth graphical interface. Moreover, it allows users to design their own measurement procedures by dragging-and-dropping spectrometers, transform functions, and display nodes to automate the user's workflow – this feature allowed the creation of the "PHOTOREFL" pre-set mentioned earlier. Users can also edit and export data and diagrams easily.

#### 3.2.3.2 Software: *GraphPad Prism*

*GraphPad Prism* is a commercial, scientific software used to obtain 2D graphics and perform statistical analysis. Aside from featuring a wide array of possible operations and mathematical models, it provides guidance on each of its features so that even newcomers can easily work with it.

#### 3.2.3.3 Kinetic Model for Photochromism: One Phase Decay

Exponential decay equation models are used to describe several chemical and biological processes in which the rate of something happening is proportional to what is left. The most famous application is for radioactive isotopes decay. In the specific case of a photochromic exposure cycle, the one phase decay mathematical model (Figure 17) evaluates the rate at which photochromic molecules become coloured, while some remain uncoloured. When evaluating the decay cycle, it assesses the opposite –

the rate at which photochromic molecules return to their initial colourless state, while some remain coloured.  $X$  represents time and  $Y$  represents the response, in this case, it relates to the  $K/S$  value.

$$Y = \text{Span} \cdot e^{-K \cdot X} + \text{Plateau}$$

Equation 6 One phase decay kinetic model.

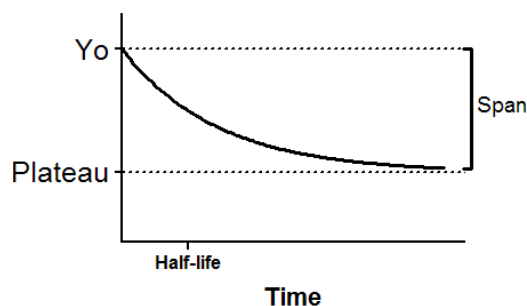


Figure 17 One phase decay kinetic model graphic (GraphPad Software, 1995-2020).

After the values were processed by the model, a wide array of values was provided. The values of interest are:

- $Y_0$  represents the value of  $Y$  when the assay began ( $t = X = 0$ ). As previously mentioned, when studying the exposure cycle,  $Y_0$  was set to zero since there's no interest in studying the initial colour of the sample.
- *Plateau* represents the  $Y$  value at an infinite time;
- Half-life represents the time it takes to reach half of the *Span* (GraphPad Software, 1995-2020).

In practice, when evaluating the exposure cycle,  $Y_0$  represents the  $K/S$  value in the colourless state and *Plateau* represents the  $K/S$  value that the sample progressively tends to. In the decay cycle,  $Y_0$  represents the  $K/S$  value of the coloured sample in the first second of non-exposure to the light source. The remaining values translate into the same values. In the exposure cycle,  $Y_0$  will, undoubtedly, be lower than *Plateau* – the opposite happens with the decay cycle. The half-life translates the time the sample needs to reach half of its maximum colour strength. It is an important parameter, especially, when considering that one of the requirements for photochromic compounds is that the transition must be quick upon irradiation.

## 4 Chapter IV – Results & Discussion

In this section, the results will be presented and discussed. The influence of exposure time, pigment concentration, and temperature on colour intensity is individually analysed. Moreover, the influence of these parameters on  $Y_0$ , half-life, and *Plateau*, over consecutive cycles, is discussed. Figure 18 and Figure 19 show samples D and F in their coloured and semi-coloured states, respectively.

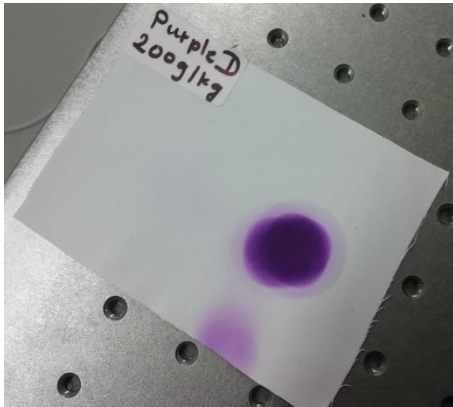


Figure 18 Activated/coloured sample D.



Figure 19 Semi-activated/coloured sample F.

Subsequently to the first test (at 10 °C for 1350 s (600/150/600 s)) the stabilization and decay times were changed from 600 s to 900 s after concluding that it was not enough time to record all the relevant information about the sample's decay cycle. Moreover, initially, it was clearly observed that the sample's absorption maximum wavelength ( $\lambda_{max}$ ) was 570 nm and, thus, all assays were conducted with this wavelength since higher absorption provides greater sensitivity, meaning that one will get the maximum response from the sample. Another advantage of using the  $\lambda_{max}$  for measurements is that, at the maximum, the curve is relatively flat – even if the monochromator drifts slightly, there is little variation in absorbance, which guarantees the accuracy of measurement (Harris, 2015).

### 4.1 Stage I – Average Range of $K/S$ Values Over Five Cycles

Following is Table 4 detailing the concentration of pigment in each sample. Additionally, Table 5 shows the value gaps of the maximum  $K/S$  values obtained in the assays carried out for 150 s for different samples and temperatures.

Table 6 presents the  $K/S$  value ranges for 300 s of exposure for different samples and temperatures. These results were obtained through the graphics in Annex I.

Table 4 Samples' concentration in  $g/Kg$ .

<b>Sample</b>						
	A	B	C	D	E	F
<b>Concentration (<math>g/Kg</math>)</b>	50	100	150	200	250	300

Table 5 Average range of  $K/S$  values for 150 s of exposure.

<b>150 s of Exposure</b>					
<b>Temperature (<math>^{\circ}C</math>)</b>					
<b>Sample</b>	10	15	20	25	30
A	[4.30; 4.60]	[3.70; 3.90]	[4.20; 4.40]	[3.45; 3.65]	[3.40; 3.70]
B	[9.00; 10.9]	[8.10; 9.20]	[8.40; 9.50]	[7.00; 7.60]	[7.15; 7.45]
C	[13.3; 16.6]	[12.0; 13.9]	[11.9; 13.7]	[10.8; 12.2]	[9.40; 11.4]
D	[18.2; 20.1]	[15.4; 18.0]	[16.2; 18.2]	[13.3; 14.8]	[13.9; 15.3]
E	[18.3; 20.0]	[15.6; 19.5]	[15.8; 18.8]	[14.8; 17.3]	[13.7; 16.3]
F	[18.8; 21.8]	[16.9; 20.1]	[17.5; 20.1]	[17.0; 19.1]	[15.3; 18.0]



Table 6 Average range of  $K/S$  values for 300 s of exposure.

<b>300 s of Exposure</b>					
<b>Temperature (°C)</b>					
<b>Sample</b>	10	15	20	25	30
A	[4.25; 4.80]	[3.95; 4.40]	[3.85; 4.30]	[3.30; 3.65]	[3.05; 3.40]
B	[8.20; 10.4]	[8.30; 9.20]	[8.10; 8.85]	[6.60; 7.70]	[5.85; 6.75]
C	[13.1; 16.5]	[14.4; 15.4]	[11.1; 13.2]	[11.3; 12.0]	[9.60; 11.3]
D	[17.3; 19.3]	[15.7; 19.1]	[16.0; 18.4]	[14.8; 15.9]	[12.6; 14.6]
E	[16.8; 20.8]	[17.1; 18.7]	[15.2; 19.6]	[16.6; 17.6]	[14.4; 16.3]
F	[20.0; 23.0]	[18.2; 22.0]	[17.3; 19.9]	[16.6; 17.6]	[14.9; 16.3]

#### 4.1.1 Influence of Exposure Time

In this study, two distinct exposure times were tested – firstly, 150 s ( $t_1$ ) and then 300 s ( $t_2$ ). It was hypothesized that a longer exposure time would produce a stronger colour response in the samples. In some cases,  $t_2$  led to less strongly coloured samples. To maintain the pigment concentration constant, sample A was chosen for this comparison. It was not clearly observed that a longer exposure time leads to stronger colour as expected. When comparing the colour strength produced by sample A at 10 °C, with  $t_1$  the  $K/S$  value range was [4.30; 4.60], while with  $t_2$  it was [4.25; 4.80]. At 20 °C, the  $K/S$  values for sample A ranged between [4.20; 4.40] for  $t_1$  and were generally lower for  $t_2$ , ranging between [3.85; 4.30]. At 30 °C the disparities were more pronounced, with the  $K/S$  value surpassing 3.40 with  $t_1$  and remaining below 3.40 for  $t_2$ . These results did not fulfil what was initially expected. The same tendency was followed in all other temperatures and concentrations, apart from sample C, whose values for  $t_2$  were either higher or very close to the  $t_1$  ranges.

In general, it was observed that the maximum  $K/S$  value for  $t_2$  was slightly lower than for  $t_1$  but with  $t_2$ , the sample was able to remain at its maximum  $K/S$  (strongly coloured) for longer than with  $t_1$ . There are two possible explanations for this phenomenon. The most probable cause is that 150 s of exposure are enough for the sample to reach its maximum colour intensity and, thus, 300 s do not lead

to stronger colour. Another possible explanation is the fact that the  $t_2$  assays were carried out after all  $t_1$  assays were finished and performed on the same samples. Hence, the pigment might have started to lose photochromic function by undergoing a high number of cycles. Still, given the small difference in values, it is not possible to draw definitive conclusions.

#### 4.1.2 Influence of Pigment Concentration

By analysing the obtained values, it was concluded that the higher the pigment concentration, the higher the colour response (or final colour strength), as expected – generally, sample A had the lowest  $K/S$  values for any given temperature and exposure time, while sample F attained the highest values. But it can also be observed that the  $K/S$  values are tending to a maximum limit as concentration increases – one example of this phenomenon is marked purple on Table 6. It is noteworthy that the colour produced by sample A was strong enough to be detected by the naked eye as illustrated by Figure 20. This means that for most applications a higher pigment concentration is unnecessary.

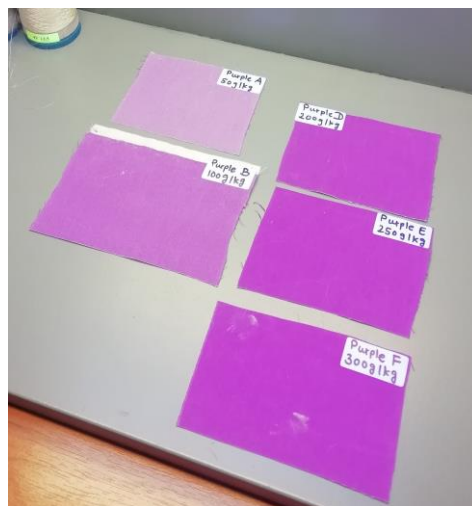


Figure 20 Samples A, B, D, E, and F in the coloured state after 20 seconds of UV exposure.

#### 4.1.3 Influence of Temperature

Generally, it was observed that the lower the temperature, the higher the  $K/S$  values attained. Still, there were instances where this did not happen – those are marked orange on Table 5 and

Table 6. This denotes the pigment's thermal dependence during activation. Moreover, greater  $K/S$  value differences were registered with higher concentrations of pigment. Since the samples are continuously irradiated to allow measurements during both its activation and decay cycles, the reversion might be driven by a specific wavelength instead of being thermally driven. Therefore, it is not possible to rule out photo-driven reversion and it cannot be undoubtedly concluded that the pigment is T-type – although it is very likely because the pigment belongs to the spironaphthoxazine's family. To know if the pigment is a T-type photochromic, more extreme temperatures should be tested, until a temperature that fully inhibits the process is reached. As an alternative, this dissertation's author proposes that the activated sample is placed in a black box and removed only after 900 s of decay. Since there is no light inside the box, if the sample still reverted to its initial state, it can be concluded that the pigment is T-type.

## 4.2 Stage II – Pigment Kinetic Behaviour Over Five Cycles

In this second stage of data analysis, the aim is to analyse how the pigment loses its photochromic response over five consecutive cycles. By photochromic response, it is meant not only to reach the same colour strength over repeated cycles but also not acquiring residual colour in the deactivated form. To make this evaluation, the data was organized by the concentration of pigment to assess the influence of exposure time and temperature on the fatigue resistance of the pigment. Further, the cycles and assays will be presented separately unlike in the previous stage where average values were considered and only three temperatures – 10, 20, and 30 °C were studied in this stage.

### 4.2.1 Consecutive Cycles of Exposure

For the exposure cycles,  $Y_0$  was set to zero on all assays, since what was intended to be studied was the value reached in each cycle of exposure. Following are the *Plateau* and half-life values relevant for comparisons and which are representative of the whole. It is noteworthy that the half-life is expressed in seconds and corresponds to the  $X$  axis while *Plateau* corresponds to the  $Y$  axis and translates into photochromic response. Further, the following tables were displayed as such to make comparisons easier – between the first and second the only variation is the exposure time; between the second and third the only variation is the pigment concentration (different samples); and between the third and fourth

the only variation is the temperature. This organization method was used to analyse the consecutive cycles of decay as well.

Table 7 *Plateau* and half-life values for sample A with 300 s of exposure at 10 °C.

<b>Sample A for 300 s of exposure at 10 °C</b>						
<b>Assay</b>		<b>Cycle 1</b>	<b>Cycle 2</b>	<b>Cycle 3</b>	<b>Cycle 4</b>	<b>Cycle 5</b>
<b>1</b>	<b>Plateau</b>	4.41	4.40	4.39	4.38	4.38
	<b>Half Life (s)</b>	4.41	3.99	4.45	4.04	4.43
<b>2</b>	<b>Plateau</b>	4.56	4.55	4.54	4.53	4.53
	<b>Half Life (s)</b>	4.08	4.60	4.21	4.05	4.49
<b>3</b>	<b>Plateau</b>	4.68	4.68	4.67	0.57	4.66
	<b>Half Life (s)</b>	4.60	4.13	4.64	Unstable	4.65
<b>4</b>	<b>Plateau</b>	4.33	4.33	4.32	4.32	4.32
	<b>Half Life (s)</b>	3.91	4.24	3.88	4.15	4.58

Table 8 *Plateau* and half-life values for sample A with 150 s of exposure at 10 °C.

<b>Sample A for 150 s of exposure at 10 °C</b>						
<b>Assay</b>		<b>Cycle 1</b>	<b>Cycle 2</b>	<b>Cycle 3</b>	<b>Cycle 4</b>	<b>Cycle 5</b>
<b>1</b>	<b>Plateau</b>	4.53	4.52	4.51	4.52	4.51
	<b>Half Life (s)</b>	4.10	3.89	3.81	4.44	4.34
<b>2</b>	<b>Plateau</b>	4.49	4.48	4.48	4.47	4.48
	<b>Half Life (s)</b>	4.06	3.10	3.94	3.84	4.58
<b>3</b>	<b>Plateau</b>	4.40	4.37	4.34	4.38	4.32
	<b>Half Life (s)</b>	4.25	4.12	4.02	4.04	3.65

Table 9 *Plateau* and half-life values for sample F with 150 s of exposure at 10 °C.

<b>Sample F for 150 s of exposure at 10 °C</b>						
<b>Assay</b>		<b>Cycle 1</b>	<b>Cycle 2</b>	<b>Cycle 3</b>	<b>Cycle 4</b>	<b>Cycle 5</b>
<b>1</b>	<b>Plateau</b>	19.04	19.04	19.04	19.04	19.03
	<b>Half Life (s)</b>	5.19	5.033	5.28	5.08	4.92
<b>2</b>	<b>Plateau</b>	20.04	20.06	20.04	20.09	20.10
	<b>Half Life (s)</b>	5.42	5.21	5.01	5.47	5.33
<b>3</b>	<b>Plateau</b>	21.02	20.91	20.80	20.75	20.72
	<b>Half Life (s)</b>	5.14	5.03	4.92	4.83	4.77
<b>4</b>	<b>Plateau</b>	19.84	19.84	19.90	19.89	19.89
	<b>Half Life (s)</b>	4.73	4.63	5.36	5.24	5.10

Table 10 *Plateau* and half-life values for sample F with 150 s of exposure at 30 °C.

<b>Sample F for 150 s of exposure at 30 °C</b>						
<b>Assay</b>		<b>Cycle 1</b>	<b>Cycle 2</b>	<b>Cycle 3</b>	<b>Cycle 4</b>	<b>Cycle 5</b>
<b>1</b>	<b>Plateau</b>	17.59	17.55	17.51	17.51	17.51
	<b>Half Life (s)</b>	4.28	4.03	3.83	4.21	4.71
<b>2</b>	<b>Plateau</b>	17.50	17.44	17.39	17.37	17.32
	<b>Half Life (s)</b>	3.86	3.73	4.27	4.11	3.93
<b>3</b>	<b>Plateau</b>	15.78	15.75	15.67	15.66	15.66
	<b>Half Life (s)</b>	5.03	4.72	3.68	3.49	4.01
<b>4</b>	<b>Plateau</b>	16.03	16.06	16.05	16.03	16.06
	<b>Half Life (s)</b>	3.28	3.88	3.63	3.54	4.17
<b>5</b>	<b>Plateau</b>	16.99	16.97	16.98	16.96	16.98
	<b>Half Life (s)</b>	4.20	4.10	3.10	3.90	3.77

Regardless of concentration or temperature, generally speaking, in the assays with 150 s of exposure, the *Plateau* values wavered, not showing a clear trend of reduction in photochromic response over the five consecutive cycles of exposure. However, this evaluation can only be done for the first assay performed on each sample since repeatedly testing on the same sample compromises these results. In

the assays where that trend was observed, the difference in values was very small and certainly less pronounced than in the assays with 300 s of exposure. In these longer assays, the variations in *Plateau* value, despite small, did suggest a loss in photochromic response over the five cycles. This fact may be due to the longer exposure time that lead the pigment to start exceeding its fatigue resistance or because, as previously mentioned, all 150 s assays were performed before the 300 s assays, on the same samples, which may have led the pigment to exceed its fatigue resistance. Moreover, regarding concentration, these values confirmed the analysis performed on the previous stage, with higher concentrations producing greater *Plateau* values. The assessment made about the effect of temperature was also corroborated – lower temperatures led to higher *Plateau* values – although, in lower concentrations, this trend was not as clear. When it came to the influence of exposure time, 300 s of exposure did not lead to higher *Plateau* values than those of 150 s of exposure, when keeping the concentration and temperature constant.

The half-life, however, varied much more depending on the conditions. When maintaining the time of exposure and temperature constant, it was observed that the half-life was greater for higher concentrations; meaning that the higher the concentration, the more time necessary to reach half the colour development. There was also a tendency for the half-life disparity between concentrations to be greater at higher temperatures. In fact, when comparing the half-life at different temperatures and keeping the concentration and exposure time constant, the higher the temperature, the lower the half-life. This is consistent with the previous conclusions drawn as higher temperatures are unable to produce the colour strength that lower temperatures can, hence, it takes less time to reach half of the total colour response at higher temperatures. When keeping the concentration and temperature constant and comparing the half-life for different times of exposure, no significant changes were registered – again, this is consistent with the previous conclusions as a longer exposure time did not produce stronger colour. Finally, when it comes to how the half-life evolved over consecutive cycles, the values oscillated not revealing a trend to grow or diminish as the cycles went on, regardless of the parameters.

#### 4.2.2 Consecutive Cycles of Decay

After some trial assays, it was concluded that 600 s was not enough for the pigment to return to its initial colourless state. Following, 900 s were used for the decay cycles and sample thermostabilization. In this case, the  $Y_0$  values represent the initial colour strength the sample displayed, the *Plateau*

corresponds to the final colour strength values after deactivation of the pigment, and half-life represents the time it took for the pigment to return to half of the colourless state. What is important to evaluate here is whether the pigment can fully return to its initial colourless state or if there is residual colour and if it increases over consecutive cycles. For this purpose, following are the *Plateau* and half-life values relevant for this comparison. Moreover, the individual influence of the experiment's parameters – concentrations, time of exposure, and temperature – are evaluated. The discussion below reflects the results obtained as a whole. Additionally, the following tables were displayed as such to make comparisons easier – between the first and second the concentration and temperature were kept constant; between the second and third the exposure time and temperature were kept constant; and between the third and fourth the concentration and time of exposure were kept constant.

Table 11 *Plateau* and half-life values for decay for sample A with 300 s of exposure at 10 °C.

<b>Sample A for 300 s of exposure at 10 °C</b>						
<b>Assay</b>		<b>Cycle 1</b>	<b>Cycle 2</b>	<b>Cycle 3</b>	<b>Cycle 4</b>	<b>Cycle 5</b>
<b>1</b>	<b>Plateau</b>	0.093	0.098	0.100	0.102	0.103
	<b>Half Life (s)</b>	58.940	58.440	58.120	57.660	57.660
<b>2</b>	<b>Plateau</b>	0.087	0.091	0.093	0.095	0.097
	<b>Half Life (s)</b>	58.490	57.910	57.760	57.450	57.250
<b>3</b>	<b>Plateau</b>	0.080	0.084	0.086	0.087	0.089
	<b>Half Life (s)</b>	61.570	61.800	61.610	62.030	61.940
<b>4</b>	<b>Plateau</b>	0.077	0.082	0.084	0.086	0.088
	<b>Half Life (s)</b>	62.070	61.220	60.990	60.570	60.180
<b>5</b>	<b>Plateau</b>	0.082	0.086	0.088	0.089	0.091
	<b>Half Life (s)</b>	58.180	58.160	57.990	57.980	57.850

Table 12 *Plateau* and half-life values for decay for sample A with 150 s of exposure at 10 °C.

<b>Sample A for 150 s of exposure at 10 °C</b>						
<b>Assay</b>		<b>Cycle 1</b>	<b>Cycle 2</b>	<b>Cycle 3</b>	<b>Cycle 4</b>	<b>Cycle 5</b>
<b>1</b>	<b>Plateau</b>	0.0831	0.086	0.088	0.089	0.090
	<b>Half Life (s)</b>	54.510	54.100	53.790	53.660	53.420
<b>2</b>	<b>Plateau</b>	0.069	0.072	0.074	0.075	0.076
	<b>Half Life (s)</b>	52.820	52.440	52.240	52.410	52.460
<b>3</b>	<b>Plateau</b>	0.060	0.063	0.070	0.047	0.065
	<b>Half Life (s)</b>	59.160	58.280	54.630	69.460	58.540

Table 13 *Plateau* and half-life values for decay for sample F with 150 s of exposure at 10 °C.

<b>Sample F for 150 s of exposure at 10 °C</b>						
<b>Assay</b>		<b>Cycle 1</b>	<b>Cycle 2</b>	<b>Cycle 3</b>	<b>Cycle 4</b>	<b>Cycle 5</b>
<b>1</b>	<b>Plateau</b>	-0.167	-0.139	-0.119	-0.115	-0.098
	<b>Half Life (s)</b>	91.280	90.490	89.840	90.200	89.380
<b>2</b>	<b>Plateau</b>	-0.114	-0.088	-0.081	-0.076	-0.067
	<b>Half Life (s)</b>	79.270	78.780	79.210	79.150	78.890
<b>3</b>	<b>Plateau</b>	-0.250	-0.199	-0.172	-0.178	-0.147
	<b>Half Life (s)</b>	93.400	90.700	89.070	89.530	87.600
<b>4</b>	<b>Plateau</b>	-0.336	-0.314	-0.307	-0.298	-0.289
	<b>Half Life (s)</b>	105.600	105.500	106.000	106.000	105.800



Table 14 *Plateau* and half-life values for decay for sample F with 150 s of exposure at 30 °C.

<b>Sample F for 150 s of exposure at 30 °C</b>						
<b>Assay</b>		<b>Cycle 1</b>	<b>Cycle 2</b>	<b>Cycle 3</b>	<b>Cycle 4</b>	<b>Cycle 5</b>
<b>1</b>	<b>Plateau</b>	0.156	0.160	0.162	0.163	0.164
	<b>Half Life (s)</b>	8.287	8.168	8.073	8.110	8.038
<b>2</b>	<b>Plateau</b>	0.159	0.163	0.163	0.165	0.166
	<b>Half Life (s)</b>	8.336	8.179	8.345	8.239	8.137
<b>3</b>	<b>Plateau</b>	0.163	0.165	0.167	0.168	0.168
	<b>Half Life (s)</b>	8.131	8.340	8.235	8.122	8.304
<b>4</b>	<b>Plateau</b>	0.156	0.162	0.163	0.165	0.164
	<b>Half Life (s)</b>	8.601	8.232	8.219	8.177	8.389
<b>5</b>	<b>Plateau</b>	0.164	0.167	0.169	0.171	0.173
	<b>Half Life (s)</b>	8.502	8.484	8.441	8.394	8.344

Firstly, it is important to note that a mathematical model is an approximation to reality and not actual reality. This is the reason why some of the *Plateau* values are negative in some of the assays.

It was observed that the *Plateau* values grow slightly over consecutive cycles, meaning that the pigment was unable to fully return to its initial colourless state in 900 s – it can, however, return to its initial degree of white afterwards, when placed in the black box. The half-life did not reveal an evident trend of increasing or decreasing as the cycles went on. Interestingly, the reversion was much slower at low temperatures than at high temperatures. Although lower temperatures reach greater colour strength, the difference in *Plateau* during the exposure cycle does not justify the massive increase in reversion time at lower temperatures – this denotes a strong correlation between the kinetic behaviour of the pigment during decay and the temperature. Still, at lower temperatures, the pigment was able to reach an inferior residual colour when compared to higher temperatures. It was previously observed that an increase in exposure time did not necessarily produce a stronger colour response, however, when the samples are in their active form for longer (300 s), the half-life for the decay is longer and they are not able to reach as low of a *Plateau* value as the samples irradiated for a shorter time (150 s). At 20 and 30 °C, the decay *Plateau* decreases as the concentration lowers, as expected. Curiously, at 10 °C, the reverse happens – the higher the concentration the lower the *Plateau* value, meaning that despite being much slower, the reversion is more efficient at 10 °C than at higher temperatures.

## 5 Chapter V – Conclusion

As previously mentioned, each grouping of pigment concentration, temperature, and exposure time to the exciting light source had to be tested at least three times for the values to be statistically relevant. However, in some cases, the assays had to be repeated up to eight times to find three similar graphic results – when the results come out similar in at least three assays, it can be assumed that those are the most correct values. Deviated results can have many causes, from human to machine error. Sample A was slightly stained while sample F was unevenly printed, in addition, at times, there were difficulties in controlling the temperature of the sample, thus, the rate of activation and decay might have been compromised. These were the two main sources of measurement errors.

Further, during the first rounds of testing, it was observed that 600 s was not enough time for the sample to fully return to its colourless state. That time was later changed to 900 s. In these first assays, it was also concluded that the absorption maximum wavelength ( $\lambda_{max}$ ) was 570 nm and, thus, all assays were conducted using that wavelength.

It was hypothesized that a longer exposure time would produce a stronger colour response, however, that was not observed – the values only varied slightly and definitive conclusions cannot be drawn. One possible explanation for this phenomenon is that the 300 s assays were conducted after all 150 s assays were completed and the pigment had lost some of its photochromic response by then. To curve this issue, bigger samples could be used in order to not continuously test over the same limited area and, thus, curving the potential fatigue problem. Another solution would be to test the same sample-temperature couple with the different times instead of testing all couples with 150 s and only then with 300 s – the fatigue problem would still prevail but the comparison of results would be more trustworthy than in the present case. Another explanation might be that 150 s are enough for the pigment to reach its maximum colour intensity and more time is unnecessary.

As expected, it was clearly observed that the higher the concentration, the stronger the colour response. Generally, sample A had the lowest  $K/S$  values for any given temperature and exposure time, while sample F attained the highest values. Still, in terms of direct observation of the samples, the lowest concentration produced a strong enough colour change for the naked eye to detect. Thus, using a concentration higher than 50 g/Kg is not necessary for most applications.

Regarding the influence of temperature in  $K/S$  values, it was generally observed that lower temperatures facilitate a stronger colour response, with 10 °C producing the best results. Although the

pigment denotes thermal dependence, it is not possible to conclude whether or not it is a T-type photochromic. Since the samples were continuously being irradiated by a range of wavelengths, photo-induced reversion cannot be ruled out. To determine if the pigment is T-type with certainty, more extreme temperatures should be tested to assess if they can fully prevent the reversion. An alternative way of determining whether or not the pigment is T-type was proposed in the present paper: placing the sample in its active form in a black box and remove it after 900 s – since there is no light irradiating the sample there, if it comes out back in its colourless state, it can be concluded that the reversion was thermally driven. Despite the fact that the parameters of the experiment were not effective at determining whether or not the pigment is T-type, it likely is – firstly, because it belongs to the spironaphthoxazines' family and, secondly, because the samples further returned to their initial colourless state when placed back in the black box.

When the kinetic behaviour of the pigment over five consecutive cycles was assessed, the previous conclusions were corroborated: a higher concentration leads to a higher colour response, higher exposure time does not necessarily lead to greater colour strength, and lower temperatures also produce a superior colour response. Regarding the response over consecutive cycles, the *Plateau* values oscillated with 150 s of exposure, not showing a clear trend of loss of photochromic response. Notwithstanding, with 300 s of exposure the pigment appeared to lose photochromic response cycle after cycle. This may be due to the explanation given above – the 300 s assays were conducted after the 150 s assays – or to the possibility of a longer exposure time being able to exceed the fatigue resistance of the pigment. However, no definitive conclusions can be drawn regarding fatigue resistance since the same samples were tested repeatedly, which can greatly influence the fatigue resistance. The half-life varied much more depending on the conditions. Firstly, it was observed that the higher the concentration, the longer the half-life, meaning that it takes more time to reach half of the total colour development. Additionally, the half-life disparity between concentrations was greater at higher temperatures. In general, the higher the temperature, the lower was the half-life – given that higher temperatures produce a weaker colour response, this result was expected. The half-life values did not suffer significant changes between different exposure times, as the *Plateau* values reached were similar.

Although the pigment did not lose photochromic response over consecutive cycles for 150 s of exposure, when analysing the kinetic behaviour of decay, in both exposure times the *Plateau* value showed a slight increasing trend cycle after cycle. This means that the pigment was not able to fully

return to its colourless state in 900 s. The half-life, contrarily, did not reveal any clear trend of changing as the cycles went on. The half-life increased tremendously with lower temperatures compared to the half-life at higher temperatures, this denotes great temperature dependence in the decay cycle. Another phenomenon that illustrates this high thermal dependence was the fact that at 20 and 30 °C, the *Plateau* decreases as the concentration increases, as expected; however, at 10 °C the opposite happens, the higher the concentration the lower the *Plateau* value, meaning that despite being much slower, the reversion is much more efficient at lower temperatures. Although no significant colour strength increases were registered with 300 s of exposure, with this longer exposure time the half-life is greater than with 150 s of exposure and they are not able to attain *Plateau* values as low as with the shorter exposure time – again, hinting to the loss of photochromic response with longer exposure times.

The experiment suggested that the pigment does withstand five consecutive cycles of exposure and decay without a significant decrease in colour response, which satisfies the requirement of durability. Still, when using the MPP pigment for commercial outlets, it is very important to understand under which conditions is the product meant to be used as its photochromic response is strongly linked to temperature. Further, when using it as a UV sensor, it is noteworthy that the reversion time is quite long for temperatures lower than 20 °C, so, it needs to be taken into account that consecutive UV detections in short periods are not possible. Regarding the remaining requirements for organic photochromic compounds, it is unknown if the return to the initial state is controllable, the colour is, indeed, none or very weak in the deactivated state, and *Matsui* offers only four colours to choose from, with two of them being similar.

All in all, the aim of this research was fulfilled. It was possible to analyse how the pigment's kinetic behaviour varied depending on the three parameters established – pigment concentration, temperature, and exposure time to the exciting light source. It was also concluded that the variants (*K/S* value, *Plateau*, and half-life), equations, and mathematical models used were suitable for this study. Therefore, this methodology and parameters are suitable to use in future research of photochromic textile nanosystems and represent a step towards standardization of photochromic testing. Moreover, a method to assess whether or not a photochromic colourant is T-type was proposed.

## 5.1 Future Perspectives

One of the requisites for photochromic materials is that the transition ought to be rapid upon irradiation. For this reason, in the future, it would be interesting to measure the colour strength dependence on temperature and concentration in short exposure times. Further, it was concluded that using a concentration higher than 50 *g/Kg* is not necessary for most applications, so, it would be of interest to assess what is the lowest concentration needed to be detected by the naked eye. Additionally, more research is needed to conclude whether or not the MPP pigment is a T-type photochromic or not – for this purpose, more extreme temperatures could be tested to assess if a certain temperature can fully prevent the photochromic response of the pigment. Alternatively, the method proposed in the present paper could be used – the samples could be placed in their active form in a black box, then, one can assess if the reversion still happens in the absence of any incising radiation to confirm whether or not the reversion is driven thermally. Additionally, in future research, a more thorough statistical analysis should be carried out and to accurately measure fatigue resistance, a new, untested sample should be used in each assay.

Bearing in mind that the price of producing chromogenic materials is much higher than that of conventional materials and the lack of standardized testing procedures, penetration into the mainstream market is not yet fully possible. One great step necessary to introduce photochromics in the industry is to standardize laboratory procedures. Due to the novelty of the prototype used to perform dynamic spectrophotometric measurements in this dissertation and the positive results obtained with the experiment parameters chosen, it would be of interest to adapt the present work for scientific publications or conferences.

## Bibliography

- Abate, M. T., Seipel, S., Yu, J., Viková, M., Vik, M., Ferri, A., . . . Nierstrasz, V. (2020). Supercritical CO<sub>2</sub> dyeing of polyester fabric with photochromic dyes to fabricate UV sensing smart textiles. *Dyes and Pigments*, 108671.
- AIS LED. (28 de September de 2021). *Smart tips to protect our eyes when using LED grow lights*.  
Obtido de AIS: <https://www.aisledlight.com/tips-protect-eyes-led-grow-lights/>
- Bamfield, P. (2001). *Chromic Phenomena - The Technological Applications of Colour Chemistry* (1st ed.). Cambridge, UK: The Royal Society of Chemistry.
- Bassalo, J. M. (2002). *Crônicas da Física* (6 ed.). Belém, Pará, Brasil: EDUFPA.
- Baumann, C. (1992). Ewald Hering's opponent colors. History of an idea. *Ophthalmologie*, 249-52.
- Berns, R. S. (2019). *Billmeyer and Saltzman's Principles of Color Technology* (4th ed.). Wiley.
- Bertolini, C. (2010). *Sistema para medição de cores usando espectrofotômetro*. Blumenau: Universidade Regional de Blumenau.
- Brady, R. (2006). Colour measurement in practice - Contemporary wool dyeing and finishing. *Australian Wool Textile Training Centre* (pp. 46-48). Victoria, Australia: Deakin University.
- Brainard, D. H., & Stockman, A. (2009). Colorimetry. In C. DeCusatis, G. Li, C. MacDonald, V. Lakshminarayanan, J. Enoch, V. Mahajan, E. Van Stryland, & M. Bass (Ed.), *The Optical Society of America - Handbook of Optics* (3rd ed., Vols. III - Vision and Vision Optics, pp. 10.1-10.46). New York, USA: McGraw Hill.
- Brixland, N. (2016). *Light Stabilisation of Photochromic Prints*. Boras, Sweden: The Swedish School of Textiles.
- Cheng, T., Lin, T., Brady, R., & Wang, X. (2008). Photochromic fabrics with improved durability and photochromic performance. *Fibers and Polymers*, 9, 521–526.
- Chowdhury, A.-A., Joshi, M., & Butola, B. (2014). Photochromic and thermochromic colorants in textile applications. *Journal of Engineered Fibers and Fabrics*, 9(1), 107-123.
- CIE. (2020). *Colorimetric Illuminants*. Obtido em 20th de April de 2020, de CIE Website:  
<http://cie.co.at/publications/colorimetric-illuminants>
- Conner, K. H. (1998). *Patente N.º US5985381A*. United States.
- CRAIC Technologies. (2020). *Technical Support: How a Spectrophotometer works and its design*, 1.  
Obtido em 23rd de December de 2020, de <http://www.microspectra.com/technical-support/248-spectrophotometer-design>

- Dartora, C. A. (n.d.). *Teoria do Campo Eletromagnético e Ondas* (1st ed.). Paraná, Brazil: Universidade Federal do Paraná.
- Design Futures - Immortality. (24th de January de 2021). *Design Futures - Immortality on WordPress.com*. Obtido de WordPress.com: [https://dfimmortality.files.wordpress.com/2014/04/hong-kong\\_skyline\\_squidlondon\\_gurus3-645x323.jpg](https://dfimmortality.files.wordpress.com/2014/04/hong-kong_skyline_squidlondon_gurus3-645x323.jpg)
- Dias, S. B. (2016). *Determinação da cor por dois métodos espectrofotométricos*. MSc dissertation, Universidade de Lisboa, Lisboa, Portugal.
- Fernandes, A. C. (2002). *Protótipo de visualização para modelos de cor para medição de objetos em espectrofotômetros por reflectância*. Bachelor's dissertation, Universidade Regional de Blumenau, Blumenau, Brazil.
- Ferrara, M., & Bengisu, M. (2014). *Materials that change color - Smart materials, intelligent design* (1st ed.). New York, USA: Springer International Publishing.
- GraphPad Software. (1995-2020). *GraphPad - Equation: One phase decay*. Obtido em 25 de May de 2020, de GraphPad Software Website: [https://www.graphpad.com/guides/prism/8/curve-fitting/reg\\_exponential\\_decay\\_1phase.htm?q=one+phase](https://www.graphpad.com/guides/prism/8/curve-fitting/reg_exponential_decay_1phase.htm?q=one+phase)
- Guimarães, L. (2004). *A cor como informação: a construção biofísica, linguística e cultural da simbologia das cores* (3rd ed.). São Paulo, Brazil: Annablume.
- Harrick Scientific Products, Inc. (2014). *FAQS/What is Kubelka-Munk?* Obtido em 24 de February de 2020, de [http://www.harricksci.com/sites/default/files/pdf/faqs/FAQ\\_Kubelka-Munk.pdf](http://www.harricksci.com/sites/default/files/pdf/faqs/FAQ_Kubelka-Munk.pdf)
- Harris, D. C. (2015). *Quantitative Chemical Analysis* (9th ed.). New York, USA: W. H. Freeman.
- Hecht, H. G. (1976). The Interpretation of Diffuse Reflectance Spectra. *Journal of Research of the National Bureau of Standards - Applied Physics and Chemistry*, 567-583.
- Hwu, Y.-R., Bai, C.-C., Tao, L.-C., Luo, D.-G., & Hu, A. (1995). *Patente N.º 5,422,181*. Taiwan, China.
- Ishikawa-Nagai, S., Yoshida, A., Da Silva, J. D., & Miller, L. (2010). Spectrophotometric Analysis of Tooth Color Reproduction on Anterior All-Ceramic Crowns: Part 1: Analysis and Interpretation of Tooth Color. *Journal of Esthetic and Restorative Dentistry*, 22(1), 42-52.
- Kamada, M., & Suefuku, S. (1991). *Patente N.º US5208132A*. United States.
- Kamata, M., Suno, H., Maeda, T., & Hosikawa, R. (1994). *Patente N.º US5431697A*. United States.
- Lagouvardos, P., Fougia, A., Diamantopoulou, S., & Polyzois, G. (2009). Repeatability and interdevice reliability of two portable color selection devices in matching and measuring tooth color. *The Journal of Prosthetic Dentistry*, 101 (1), 40-45.

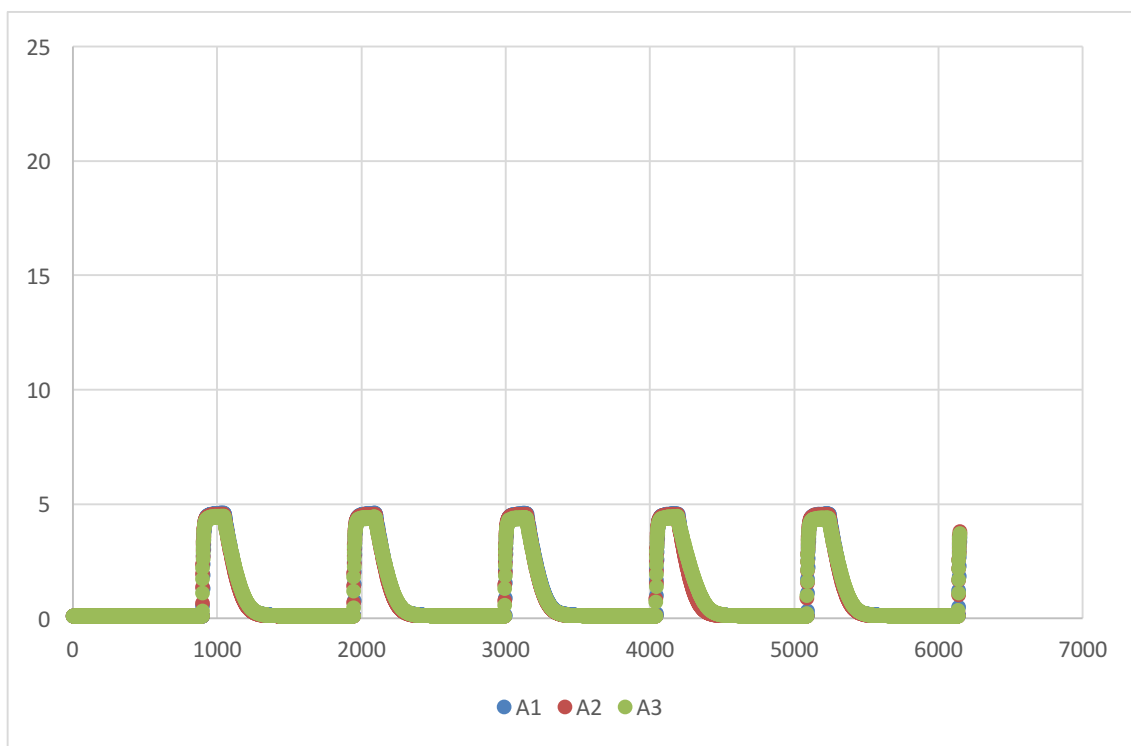
- Leite, F. N. (2006). *Calibração de dispositivos de cores utilizando uma câmera digital*. MSc dissertation, Universidade de Brasília, Brasília, Brazil.
- Little, A., & Christie, R. (2010). Textile applications of photochromic dyes. Part 1: establishment of a methodology for evaluation of photochromic textiles using traditional colour measurement instrumentation. *Coloration Technology*, 157-163.
- Liu, X., Cheng, T., Parhizkar, M., Wang, X., & Lin, T. (2010). Photochromic textiles from hybrid silica coating with improved photostability. *Research Journal of Textile and Apparel*, 14(2), 1-8.
- Matsui International. (s.d.). *Specialty Products: Photopia*. Obtido em 28th de December de 2020, de <https://www.matsui-color.com/ourproducts/specialty-product-separated/photopia>
- McCluney, W. R. (1994). *Introduction to Radiometry and Photometry* (1st ed.). Boston/London: Artech Print on Demand.
- Mennig, M., Fries, K., Lindenstruth, M., & Schmidt, M. (1999). Development of fast switching photochromic coatings on transparent plastics and glass. *Thin Solid Films*, 230-234.
- Pargaonkar, J. G., Sanjay, P., Patil, A., & Vajekar, S. (2020). Application of Fe<sub>3</sub>O<sub>4</sub> as a magnetic nanocatalyst in the synthesis of photochromic spironaphthoxazines. *Research Journal of Chemistry and Environment*, 61-69.
- Parhizkar, M., Zhao, Y., Wang, X., & Lin, T. (2014). Photostability and Durability Properties of Photochromic Organosilica Coating on Fabric. *Journal of Engineered Fibers and Fabrics*, 9(3), 65-73.
- Periyasamy, A. P. (2018). *Properties of Photochromic Textiles*. Liberec, Czech Republic: Technical University of Liberec - Faculty of Textile Engineering.
- Periyasamy, A. P., Viková, M., & Vik, M. (2017). A review of photochromism in textiles and its measurement. *Textile Progress*, 49(2), 53-136.
- Pinto, T., Costa, P., Sousa, C., Sousa, C., Pereira, C., Silva, C., . . . Freire, C. (2016). Screen-printed photochromic textiles through new inks based on SiO<sub>2</sub>@naphthopyran nanoparticles. *ACS Applied Materials & Interfaces*, 8(42), 28935-28945.
- Qi, Y., Fan, J., Chang, Y., Li, Y., Bao, B., Yan, B., . . . Cong, P. (2021). Smart photochromic fabric prepared via thiol-ene click chemistry for image information storage applications. *Dyes and Pigments*, 109507.
- Ramlow, H., Andrade, K. L., & Immich, A. P. (2020). Smart textiles: an overview of recent progress on chromic textiles. *The Journal of The Textile Institute*, 152-171.



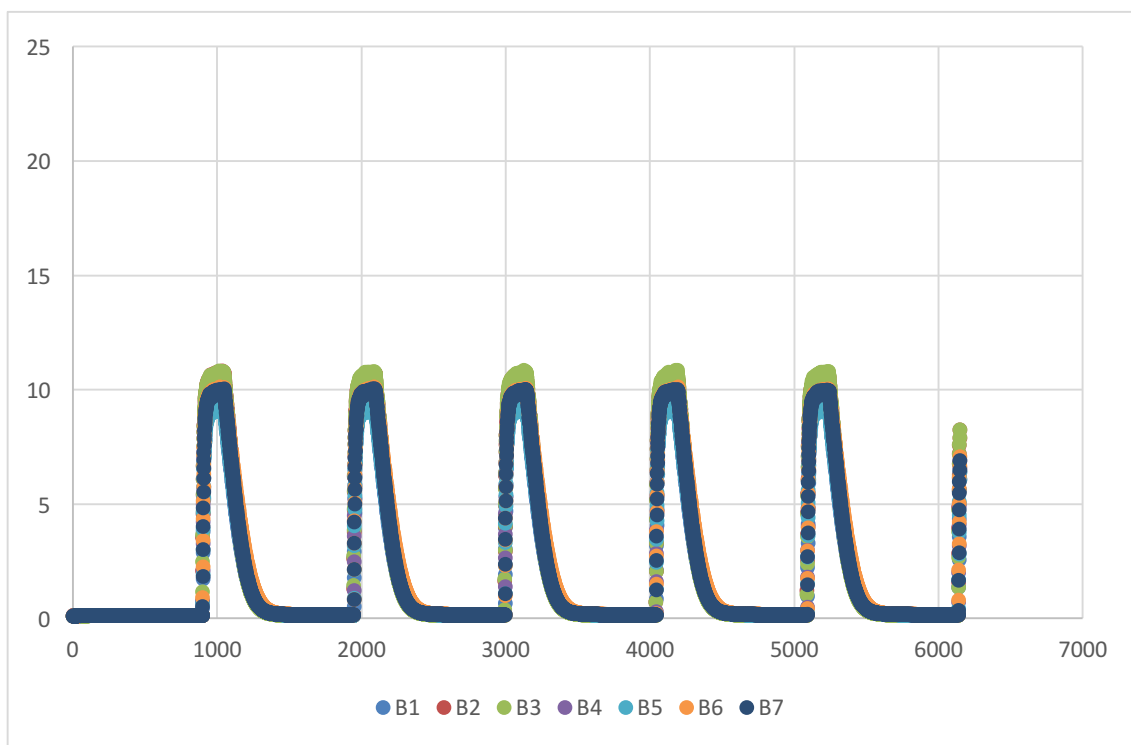
- Régula, L. M. (2004). *Padrões virtuais e tolerâncias colorimétricas no controlo instrumental de cores*. MSc dissertation, Pontifícia Universidade Católica do Rio de Janeiro, Rio de Janeiro, Brazil.
- Seipel, S., Yu, J., Periyasamy, A., Viková, M., Vik, M., & Nierstrasz, V. (2018). Resource-efficient production of a smart textile UV sensor using photochromic dyes: characterization and optimization. In Y. Kyosev, B. Mahltig, & A. Schwarz-Pfeiffer (Edits.), *Narrow and Smart Textiles* (1st ed., pp. 251-257). Cham, Switzerland: Springer International Publishing.
- Shacklett, A. (28 de September de 2021). *RGB vs CMYK Comparison*. Obtido de Scribe Graphics: <https://www.scribegraphics.ca/rgb-vs-cmyk-comparison/>
- Shevell, S. K. (2003). *The Science of Color* (2nd ed.). Chicago, USA: Elsevier.
- Syduzzaman, M., Patwary, S., Farhana, K., & Ahmed, S. (2015). Smart Textiles and Nano-Technology: A General Overview. *Journal of Textile Science & Engineering*, 1-7.
- Tian, H., & Zhang, J. (2016). *Photochromic Materials: Preparation, Properties and Applications* (1st ed.). John Wiley & Sons.
- TJUTR Vision. (2018). *Amazon - TJUTR Men's Photochromic Sunglasses with Polarized Lens for Outdoor 100% UV Protection, Anti Glare, Reduce Eye Fatigue*. Obtido em 27th de April de 2020, de <https://www.amazon.com/Photochromic-Sunglasses-Polarized-Outdoor-Protection/dp/B07K9KTC3Q?th=1>
- Vik, M. (2017). *Colorimetry in Textile Industry* (1st ed.). Liberec, Czech Republic: VÚTS.
- Vik, M., & Periyasamy, A. P. (2019). *Chromic Materials - Fundamentals, Measurements and Applications* (1st ed.). (M. Viková, Ed.) Oakville, Canada: Apple Academic Press.
- Viková, M. (2010). Methodology of measurement of photochromic materials. In P. R. Somani (Ed.), *Chromic Materials, Phenomena and their Technological Applications* (pp. 509-536). Liberec, Czech Republic: Applied Science Innovations.
- Viková, M., & Vik, M. (2006). SMART Textile Sensors for Indication of UV Radiation. Liberec, Czech Republic: Technical University of Liberec.
- Viková, M., & Vik, M. (2014). Photochromic Textiles and Measurement of Their Temperature Sensitivity. *RJTA*, 15-21.
- Viková, M., & Vik, M. (2016). Spectrophotometry of Dynamic Colorants. *PROCEEDINGS of the 4th CIE Expert Symposium on Colour and Visual Appearance*, (pp. 408-416). Prague, Czech Republic.
- Viková, M., & Vik, M. (2019). Photochromic Polypropylene Filaments: Impacts of Mechanical Properties on Kinetic Behaviour. *Fibres and Textiles in Eastern Europe*, 19-25.

- Viková, M., Vik, M., & Christie, R. (2014). A Unique Device for Measurement of Photochromic Textiles. *Research Journal of Textile and Apparel*, 6-14.
- Winters, A. (2020). *Rainbow Winters - Rainforest*. Obtido em 27th de April de 2020, de <http://www.rainbowwinters.com/>
- Xiong, Y., Jentzsch, A. V., Osterrieth, J. W., Sezgin, E., Sazanovich, I. V., Reglinski, K., . . . Anderson, H. L. (2018). Spiroanthoxazine Switchable Dyes for Biological Imaging. *Chemical Science*, 9(11), 3029-3040.
- Yu, D., Xu, L., Hu, Y., Li, Y., & Wang, W. (28 de Março de 2017). Durable antimicrobial finishing of cotton fabric based on thiol-epoxy click chemistry. *RSC Advances*, pp. 18838-18843.
- Yuan, J., Brewer, J., Monaco, E., & Davis, E. (2007). Defining a natural tooth color space based on a 3-dimensional shade system. *Journal of Prosthetic Dentistry*, 98 (2), 110-119.

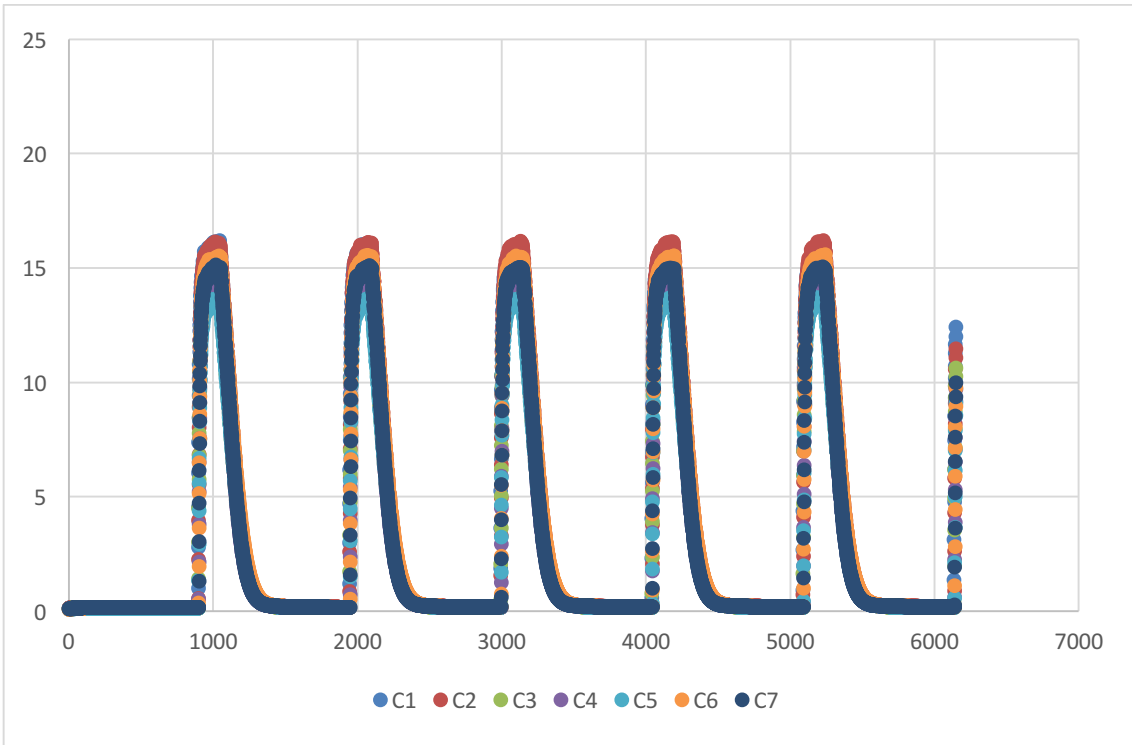
Annex I – Graphics:  $K/S$  as a Function of Time



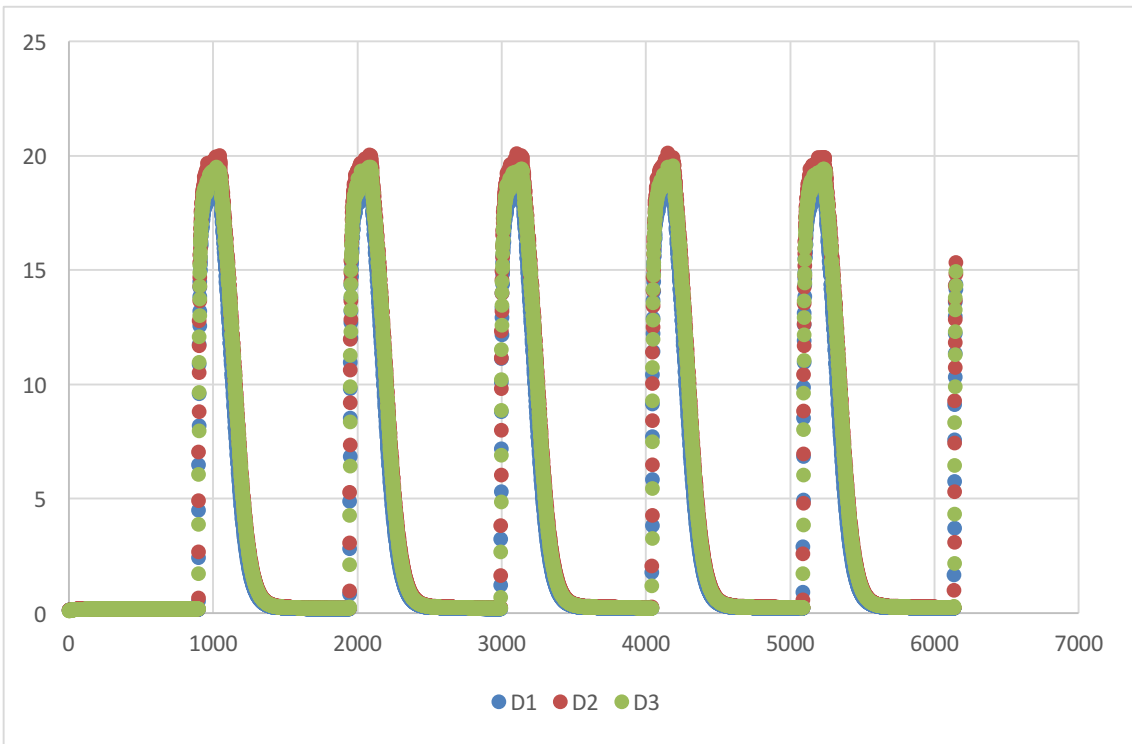
Sample A,  $t(\text{exp})=150$  s,  $T=10$  °C.



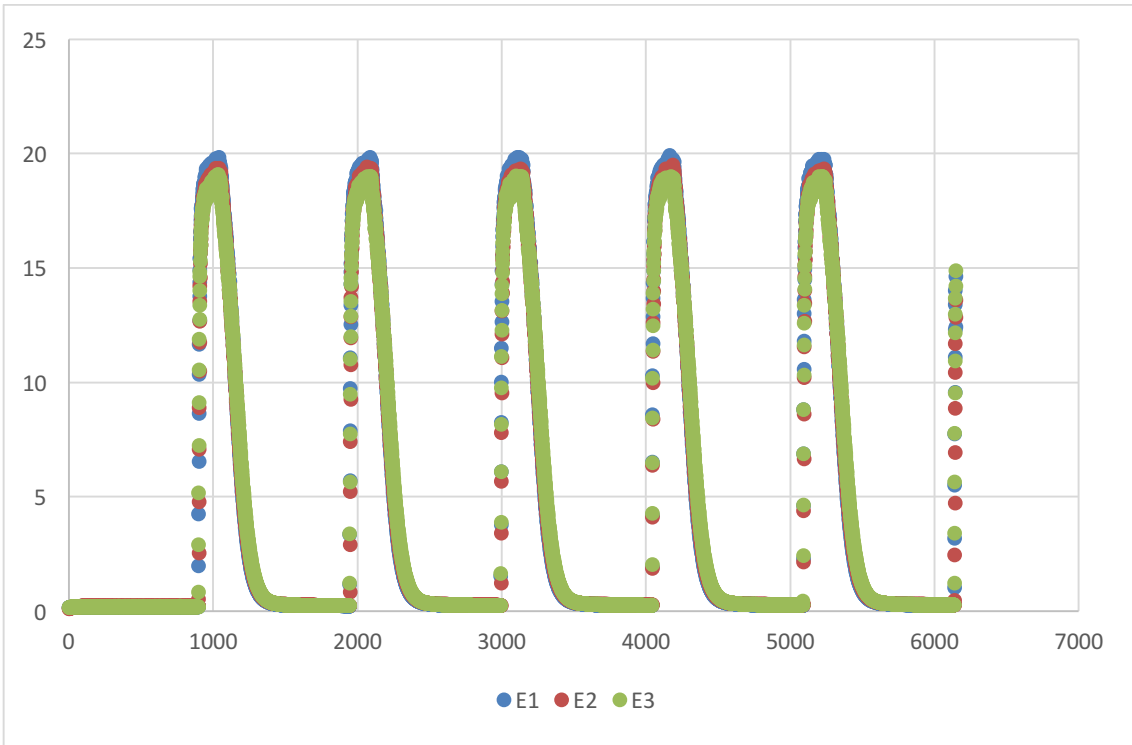
Sample B,  $t(\text{exp})=150$  s,  $T=10$  °C.



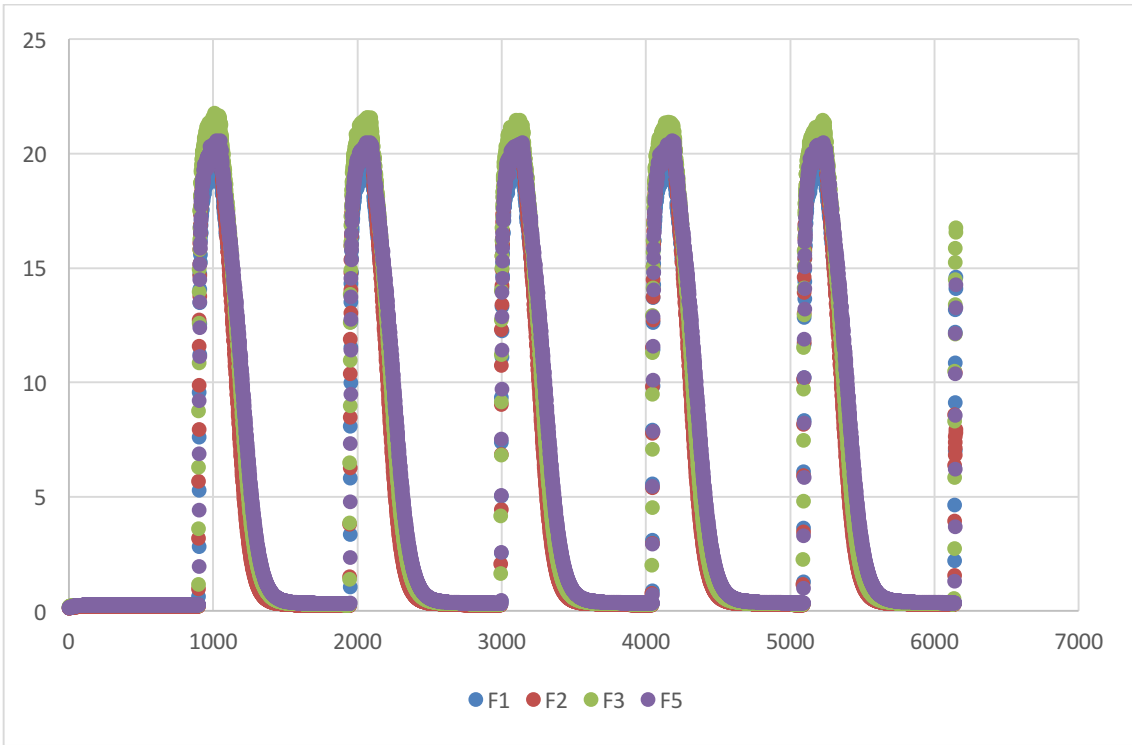
Sample C,  $t(\text{exp})=150 \text{ s}$ ,  $T=10 \text{ }^\circ\text{C}$ .



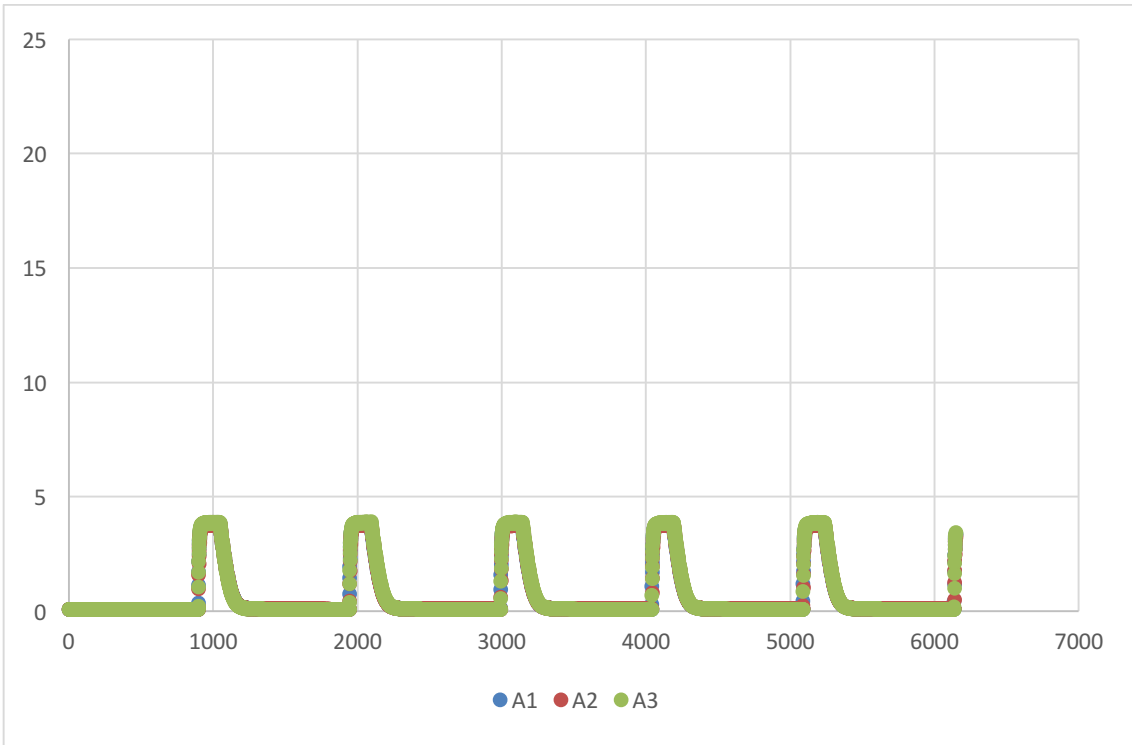
Sample D,  $t(\text{exp})=150 \text{ s}$ ,  $T=10 \text{ }^\circ\text{C}$ .



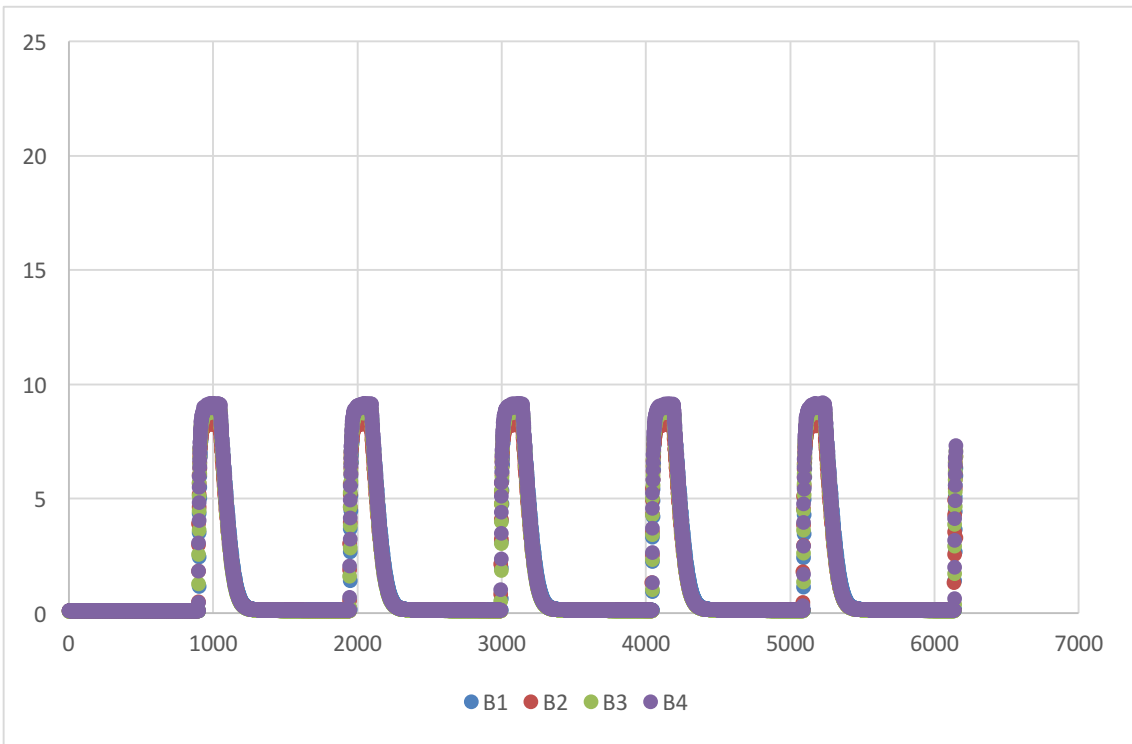
Sample E,  $t(\text{exp})=150 \text{ s}$ ,  $T=10 \text{ }^\circ\text{C}$ .



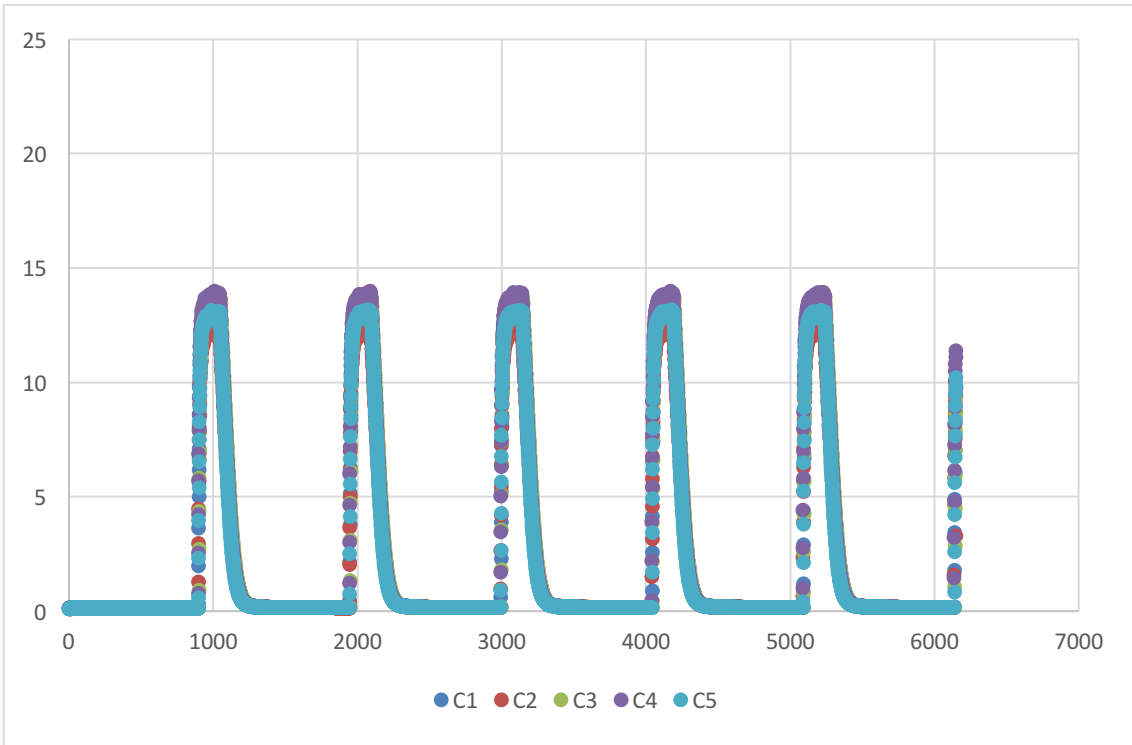
Sample F,  $t(\text{exp})=150 \text{ s}$ ,  $T=10 \text{ }^\circ\text{C}$ .



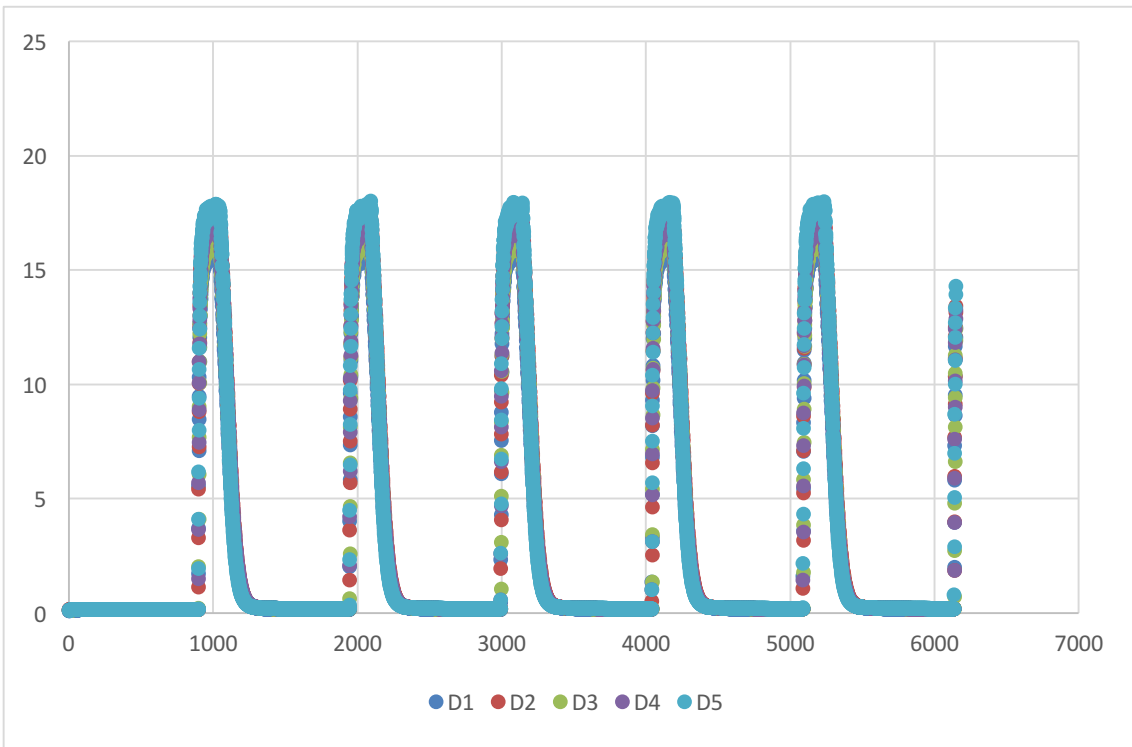
Sample A,  $t(\text{exp})=150 \text{ s}$ ,  $T=15 \text{ }^\circ\text{C}$ .



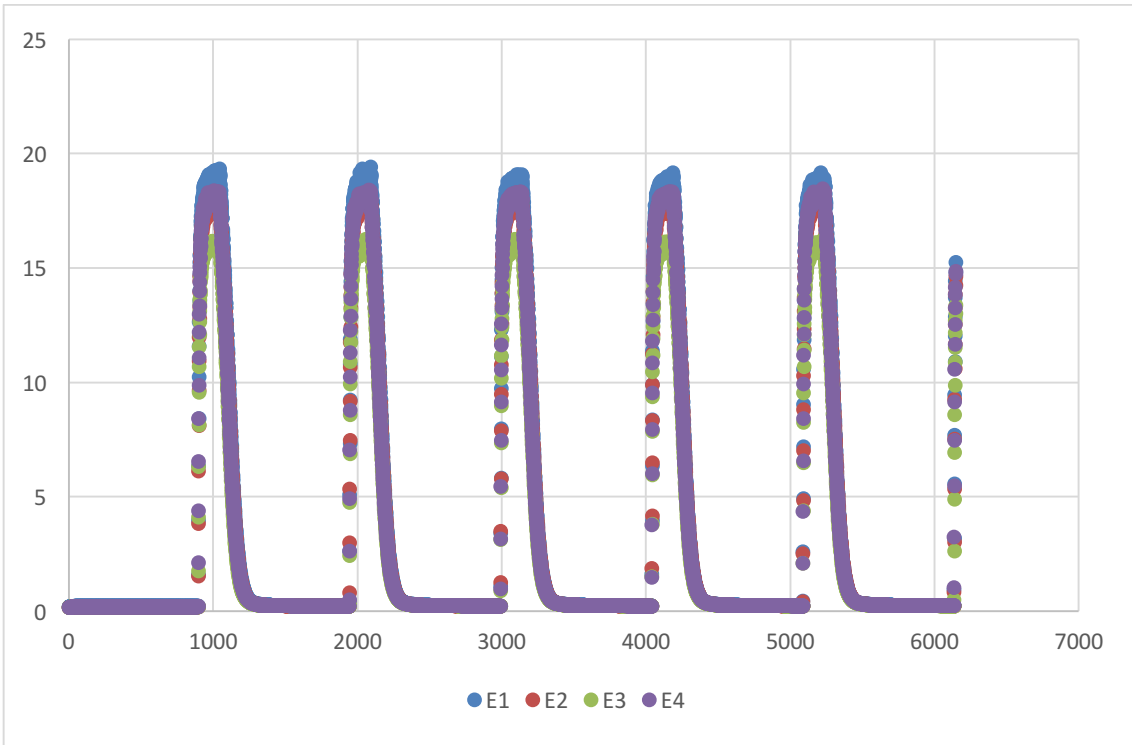
Sample B,  $t(\text{exp})=150 \text{ s}$ ,  $T=15 \text{ }^\circ\text{C}$ .



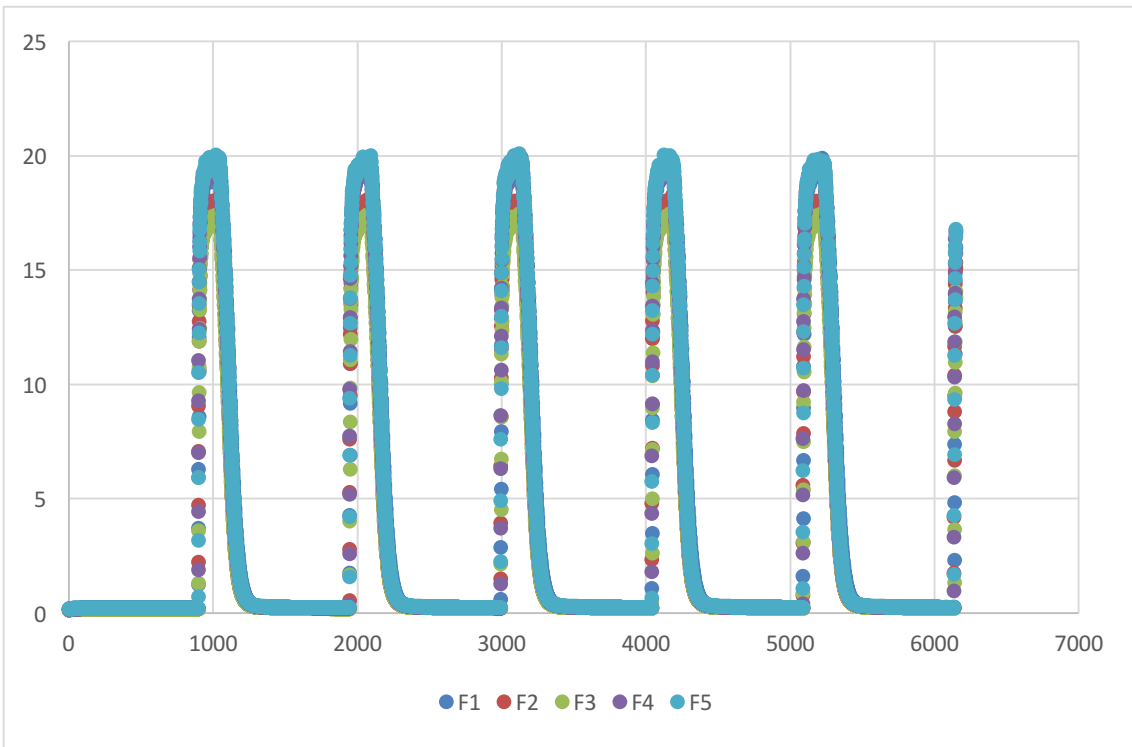
Sample C,  $t(\text{exp})=150 \text{ s}$ ,  $T=15 \text{ }^\circ\text{C}$ .



Sample D,  $t(\text{exp})=150 \text{ s}$ ,  $T=15 \text{ }^\circ\text{C}$ .

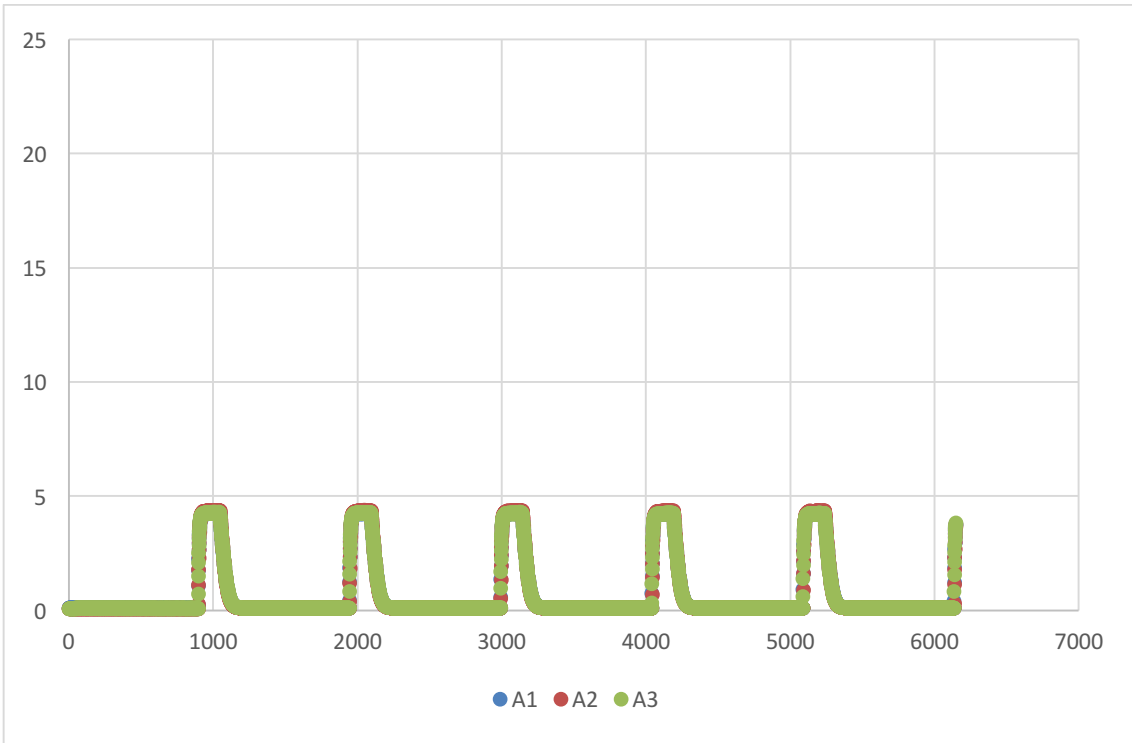


Sample E,  $t(\text{exp})=150 \text{ s}$ ,  $T=15 \text{ }^\circ\text{C}$ .

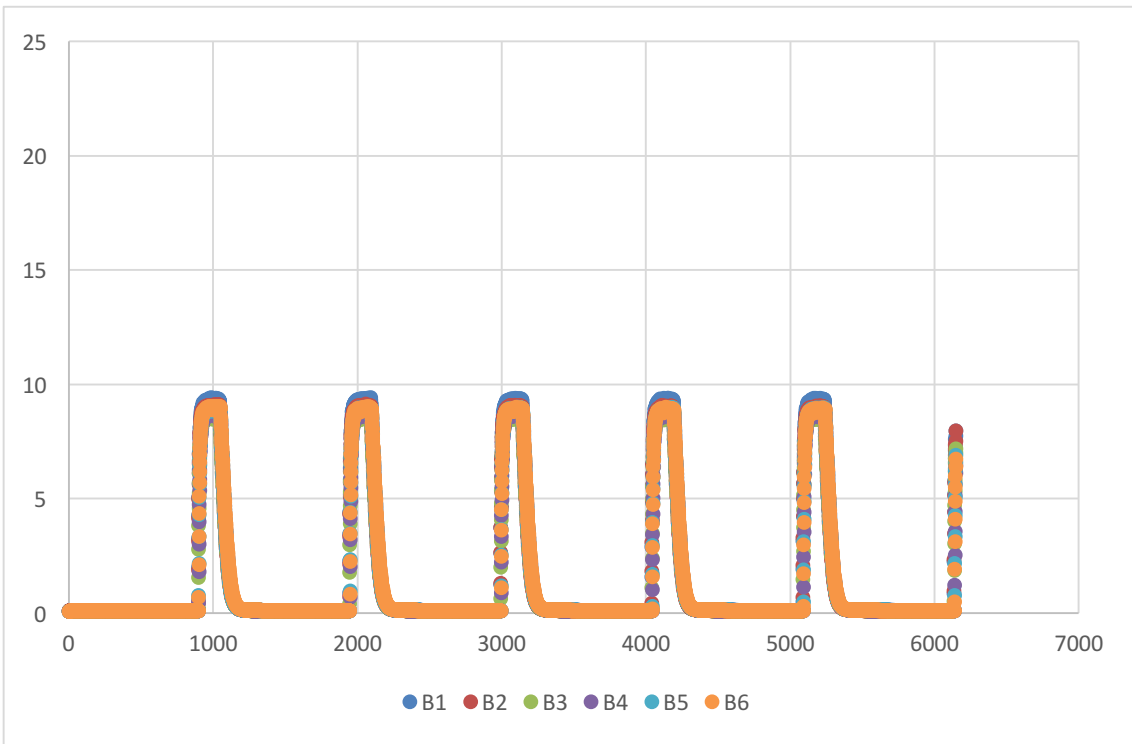


Sample F,  $t(\text{exp})=150 \text{ s}$ ,  $T=15 \text{ }^\circ\text{C}$ .

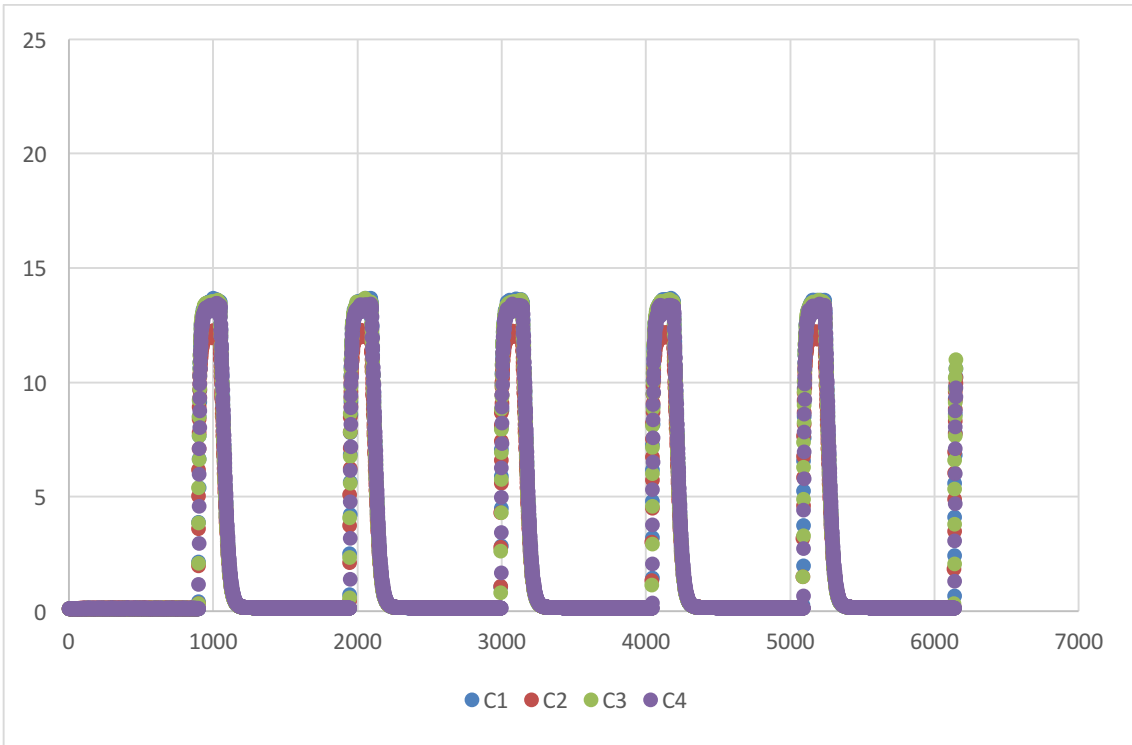




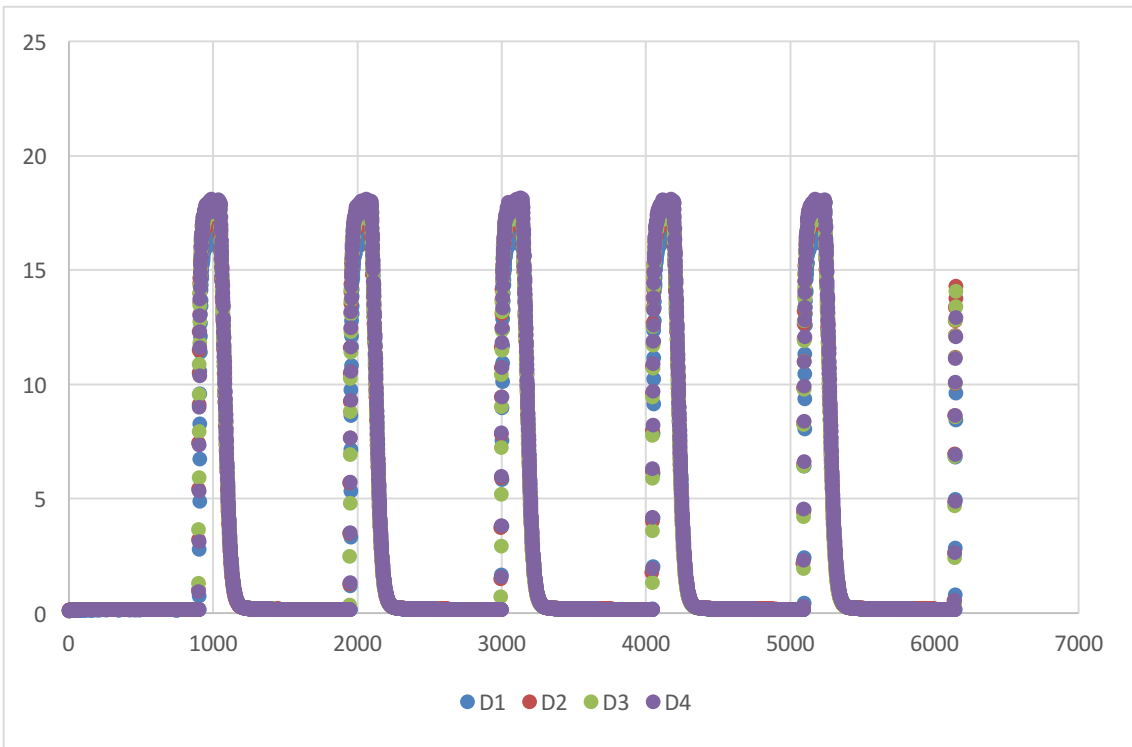
Sample A,  $t(\text{exp})=150$  s,  $T=20$  °C.



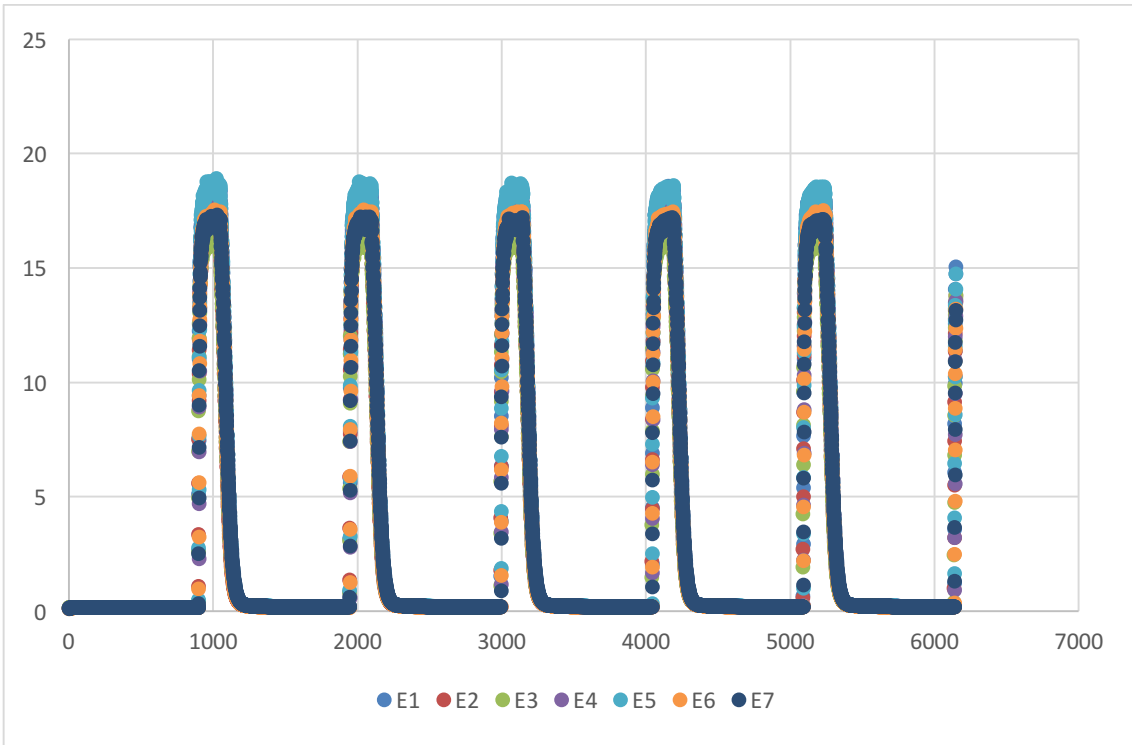
Sample B,  $t(\text{exp})=150$  s,  $T=20$  °C.



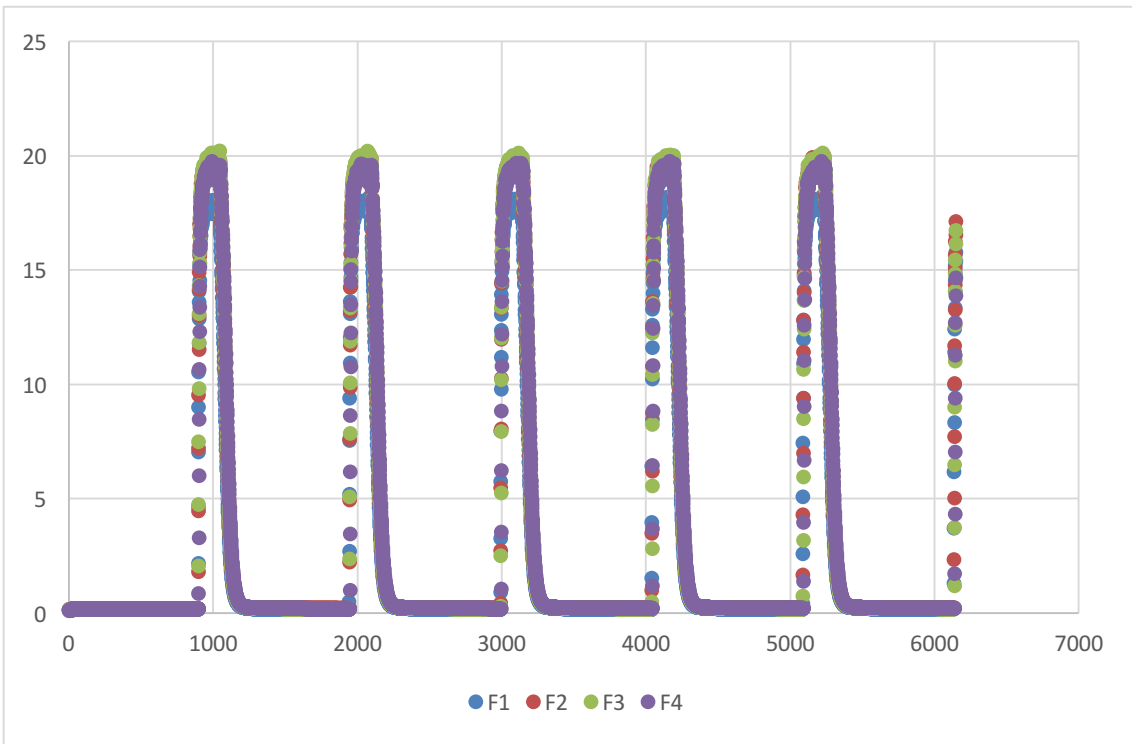
Sample C,  $t(\text{exp})=150$  s,  $T=20$  °C.



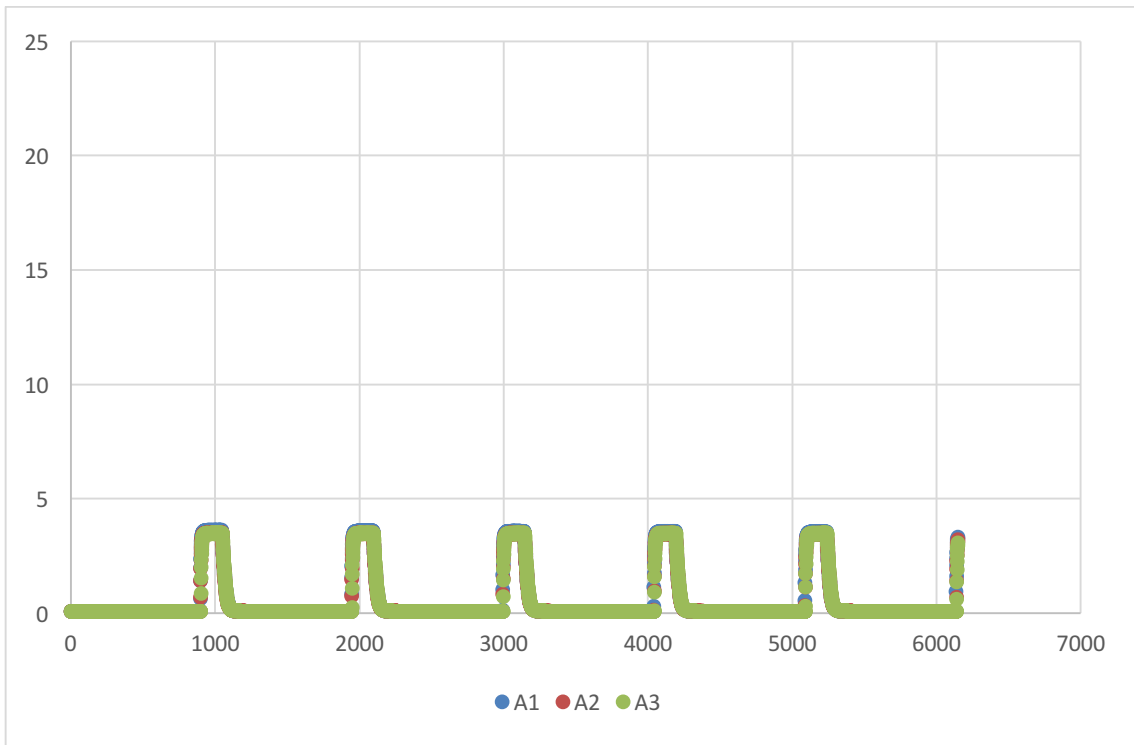
Sample D,  $t(\text{exp})=150$  s,  $T=20$  °C.



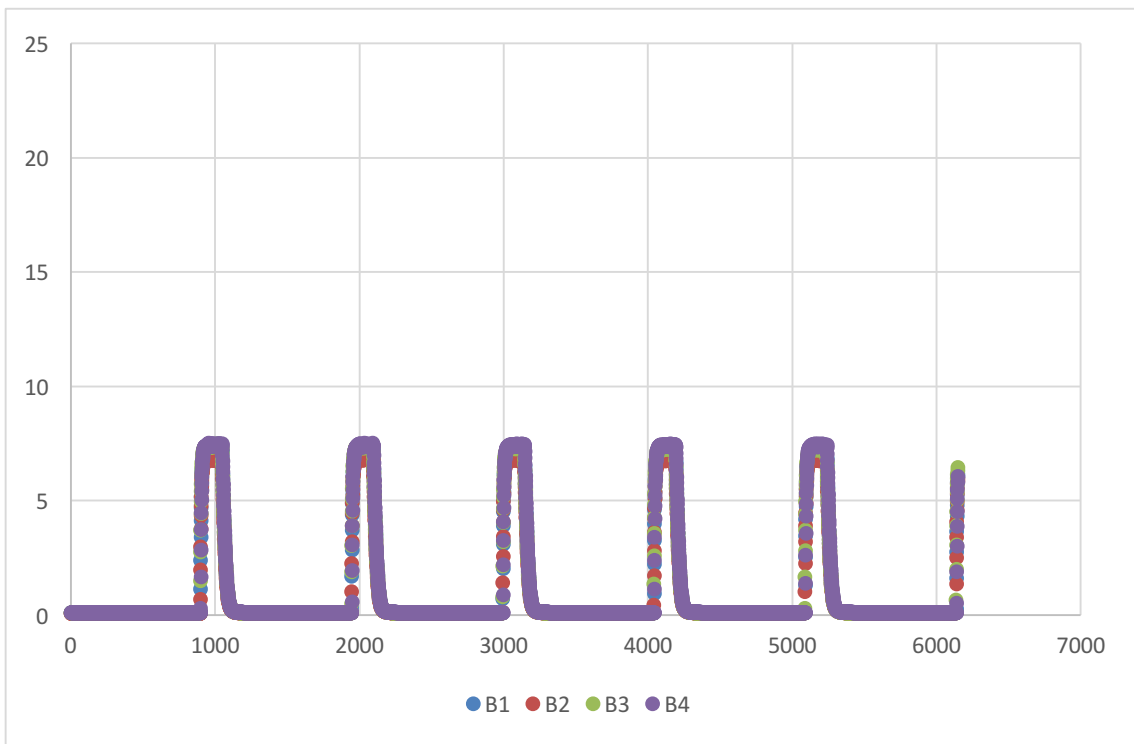
Sample E,  $t(\text{exp})=150 \text{ s}$ ,  $T=20 \text{ }^\circ\text{C}$ .



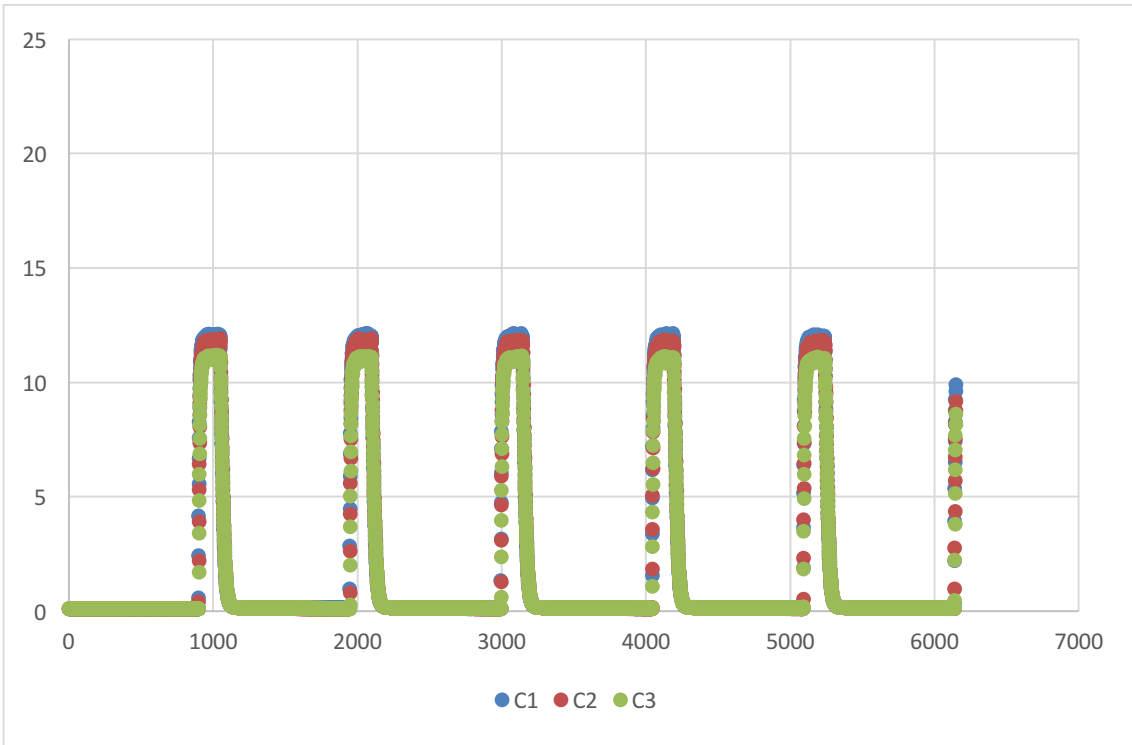
Sample F,  $t(\text{exp})=150 \text{ s}$ ,  $T=20 \text{ }^\circ\text{C}$ .



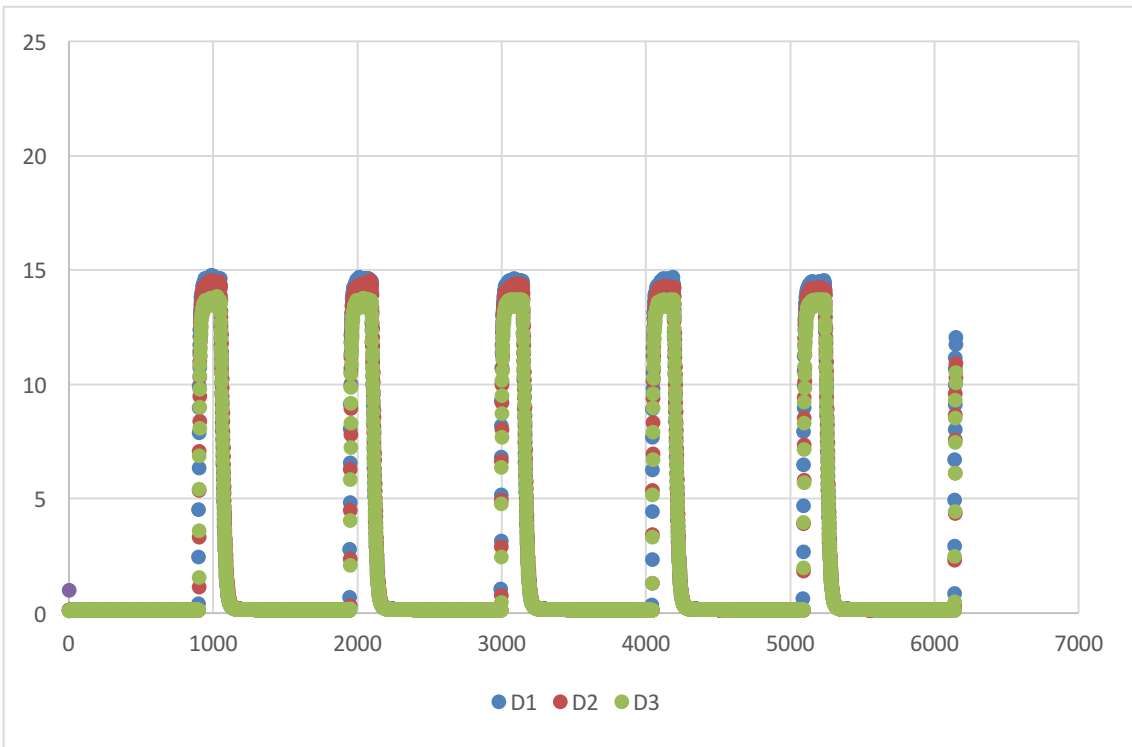
Sample A,  $t(\text{exp})=150 \text{ s}$ ,  $T=25 \text{ }^\circ\text{C}$ .



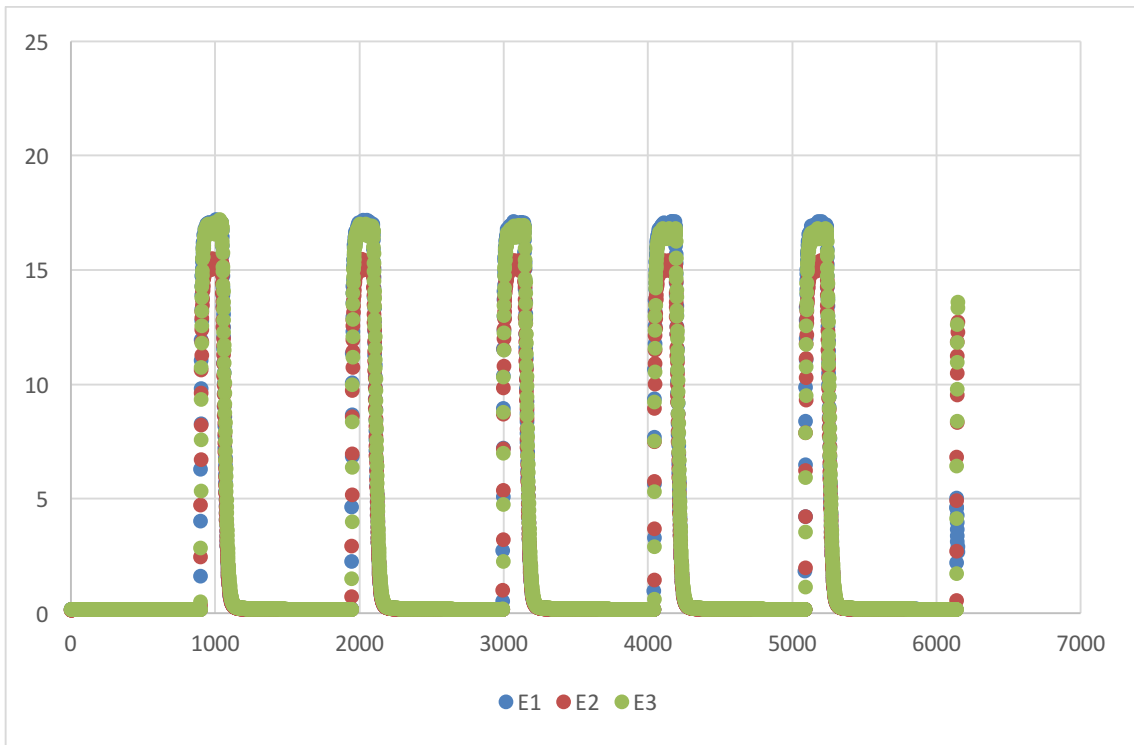
Sample B,  $t(\text{exp})=150 \text{ s}$ ,  $T=25 \text{ }^\circ\text{C}$ .



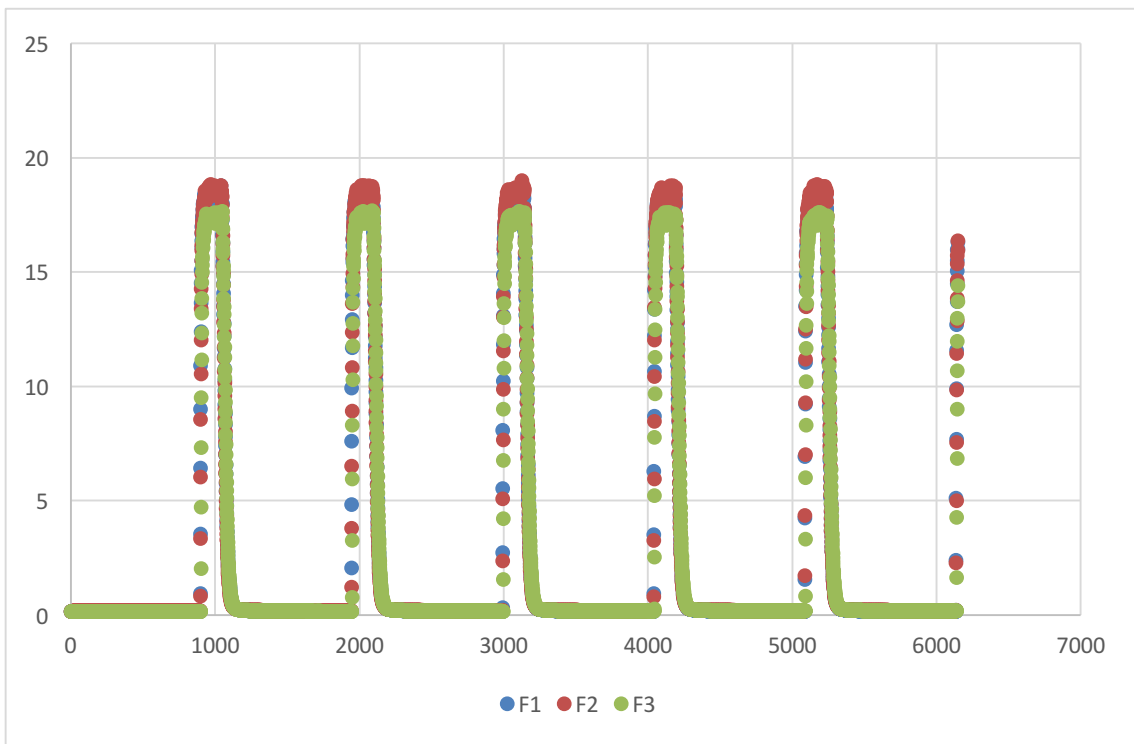
Sample C,  $t(\text{exp})=150$  s,  $T=25$  °C.



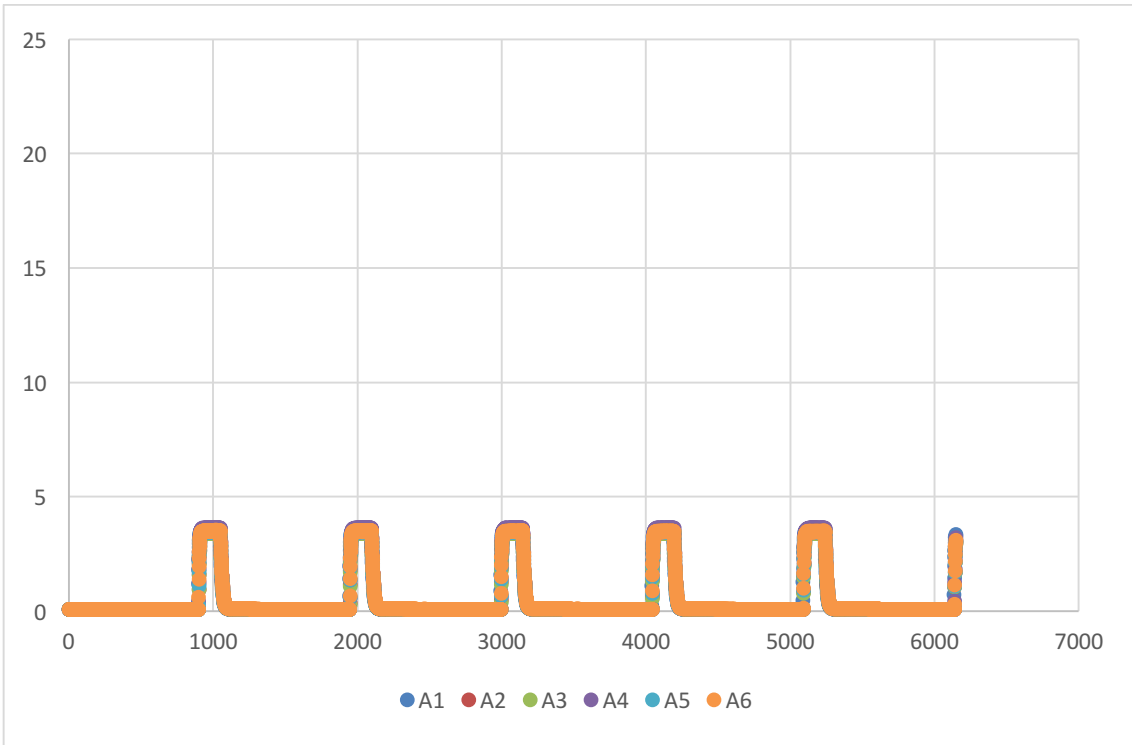
Sample D,  $t(\text{exp})=150$  s,  $T=25$  °C.



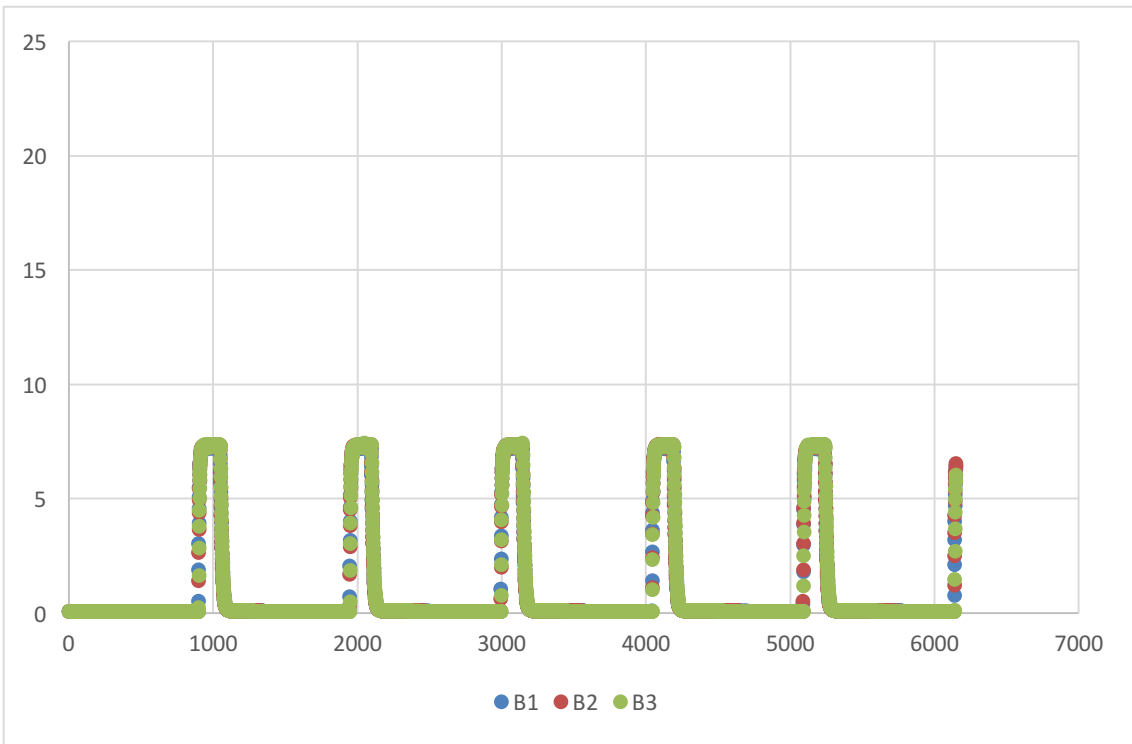
Sample E,  $t(\text{exp})=150$  s,  $T=25$  °C.



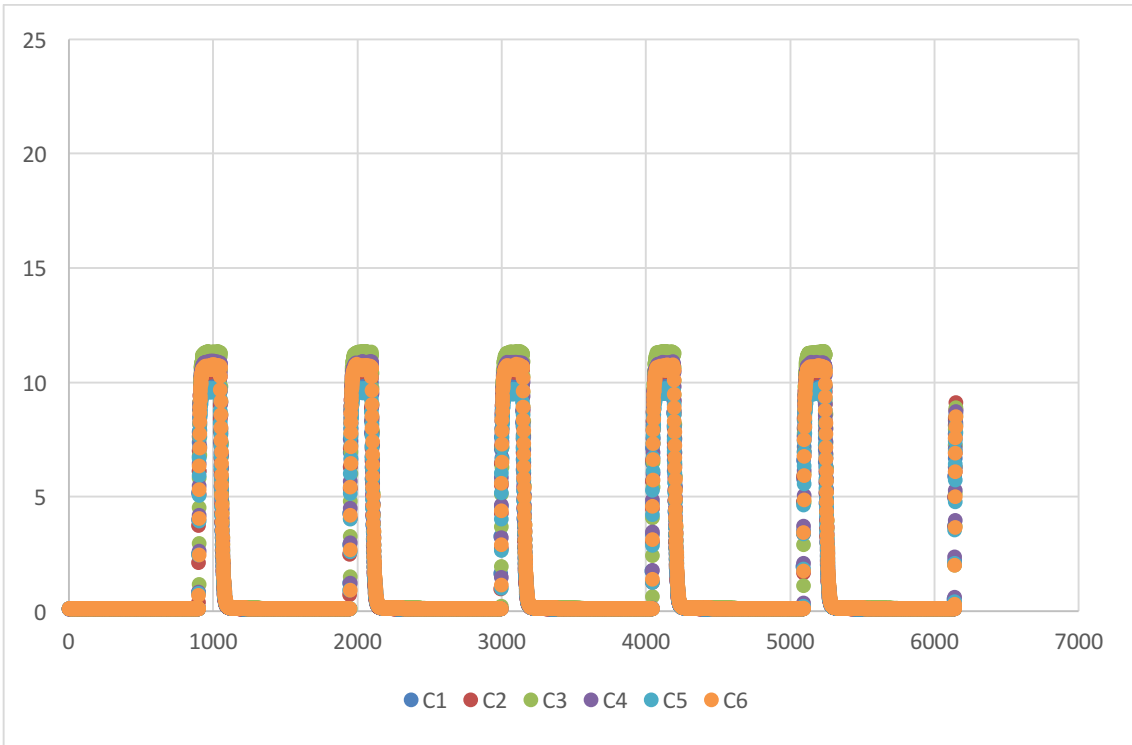
Sample F,  $t(\text{exp})=150$  s,  $T=25$  °C.



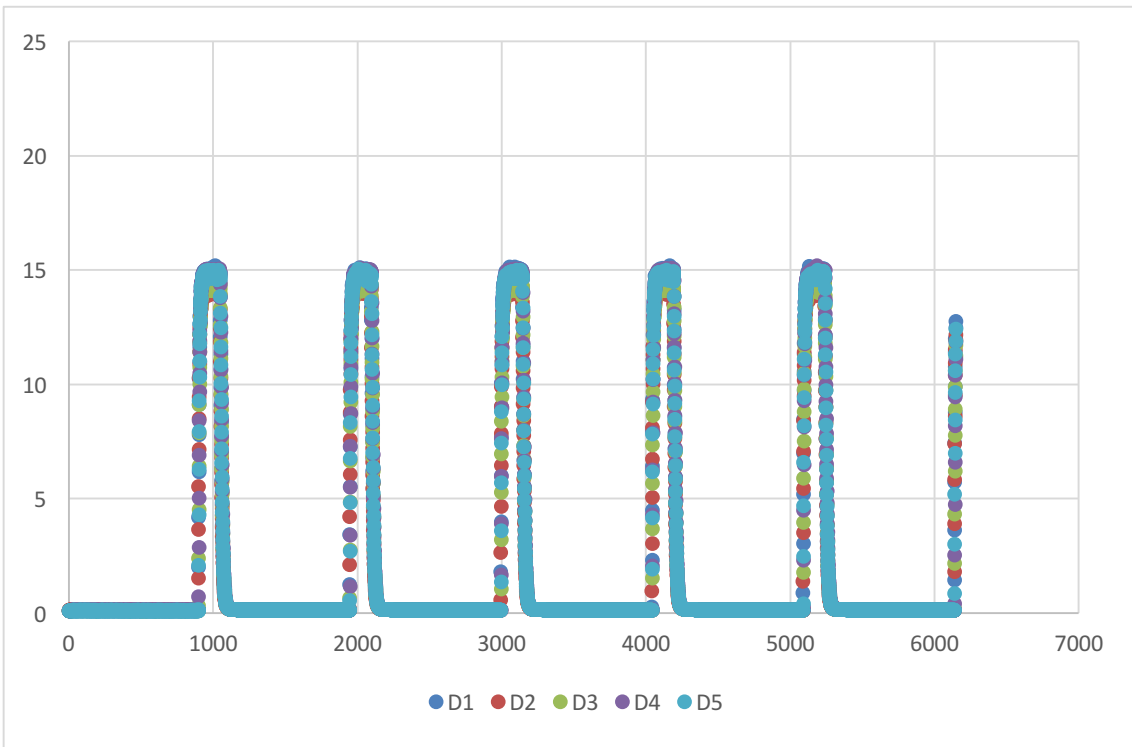
Sample A,  $t(\text{exp})=150 \text{ s}$ ,  $T=30 \text{ }^\circ\text{C}$ .



Sample B,  $t(\text{exp})=150 \text{ s}$ ,  $T=30 \text{ }^\circ\text{C}$ .

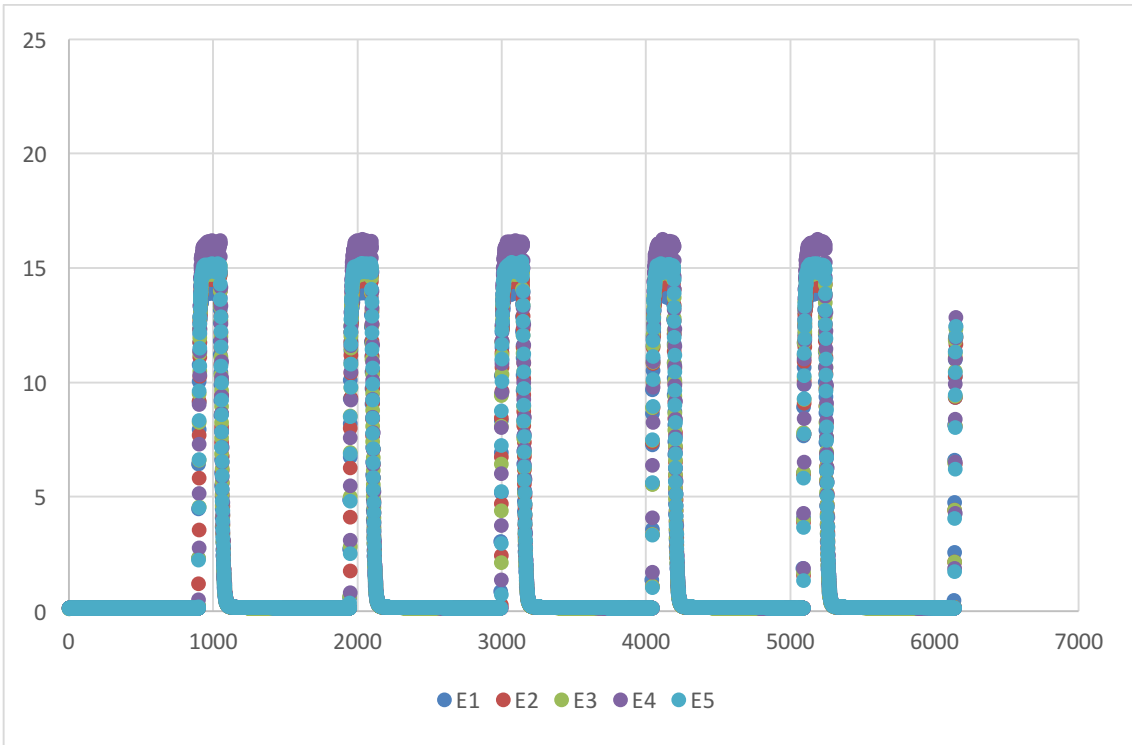


Sample C,  $t(\text{exp})=150 \text{ s}$ ,  $T=30 \text{ }^\circ\text{C}$ .

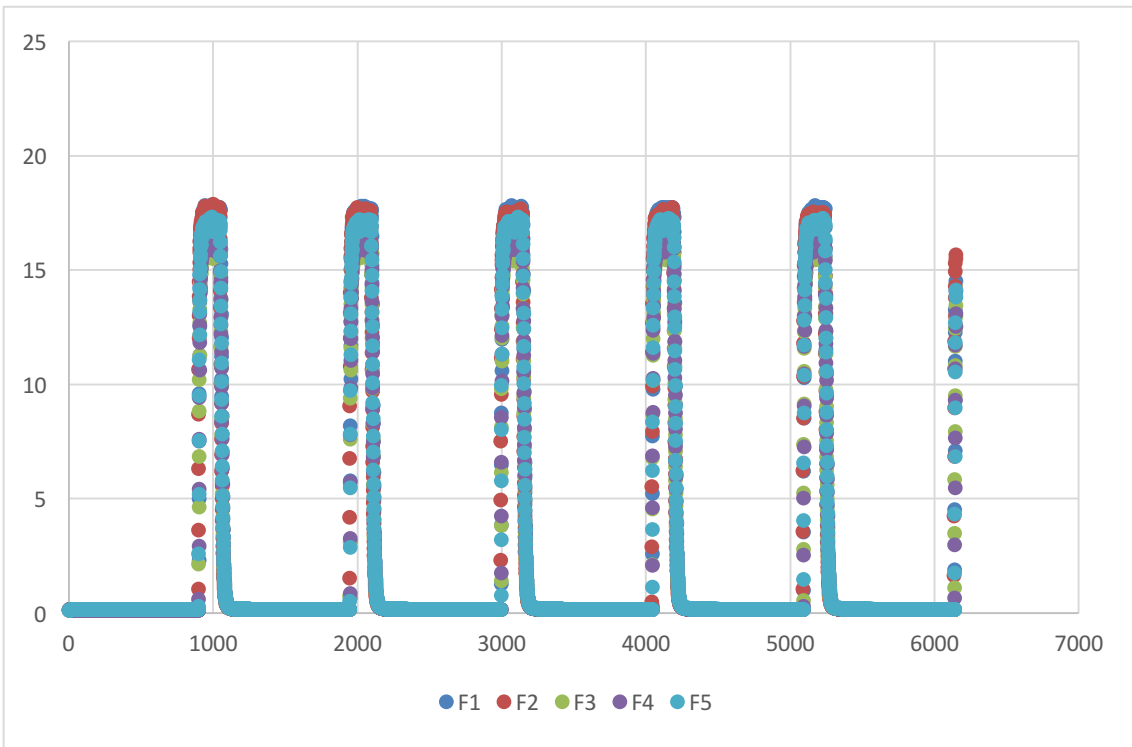


Sample D,  $t(\text{exp})=150 \text{ s}$ ,  $T=30 \text{ }^\circ\text{C}$ .

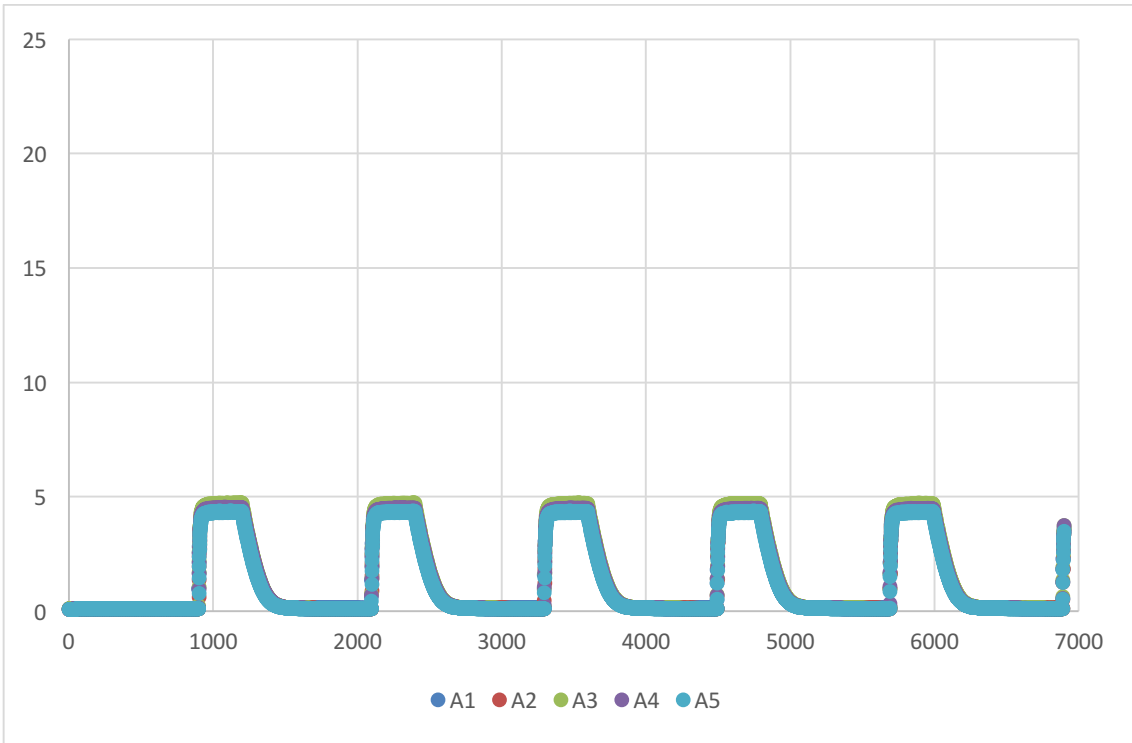




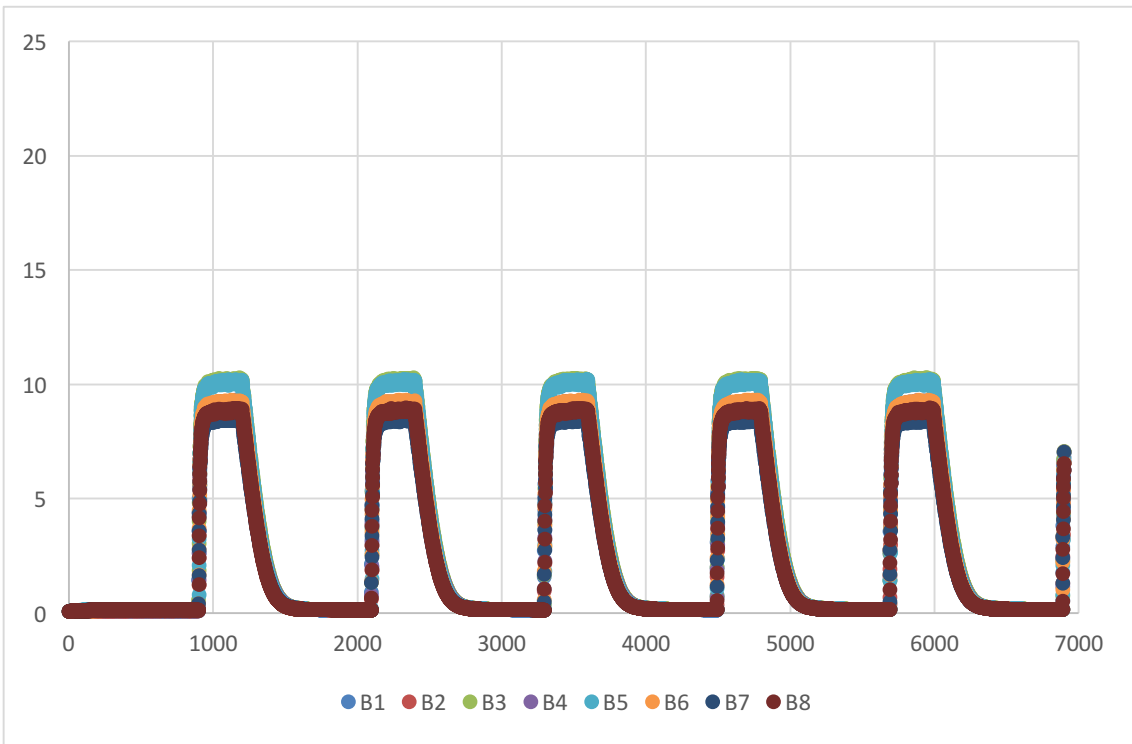
Sample E,  $t(\text{exp})=150 \text{ s}$ ,  $T=30 \text{ }^\circ\text{C}$ .



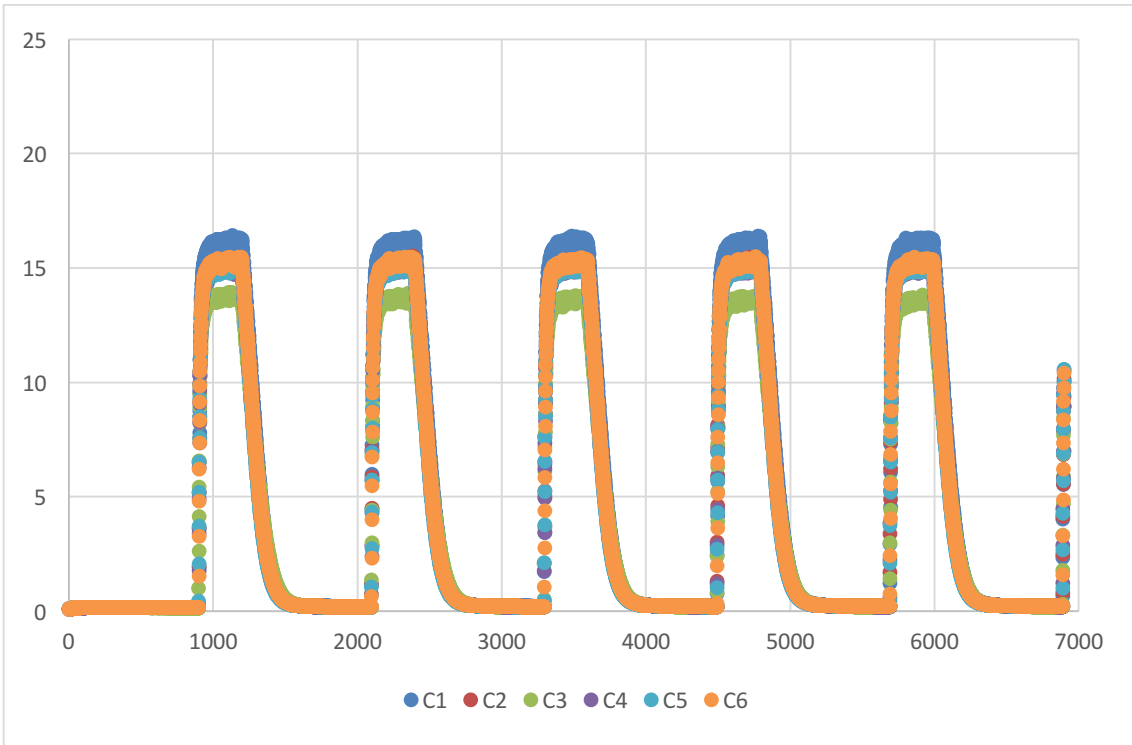
Sample F,  $t(\text{exp})=150 \text{ s}$ ,  $T=30 \text{ }^\circ\text{C}$ .



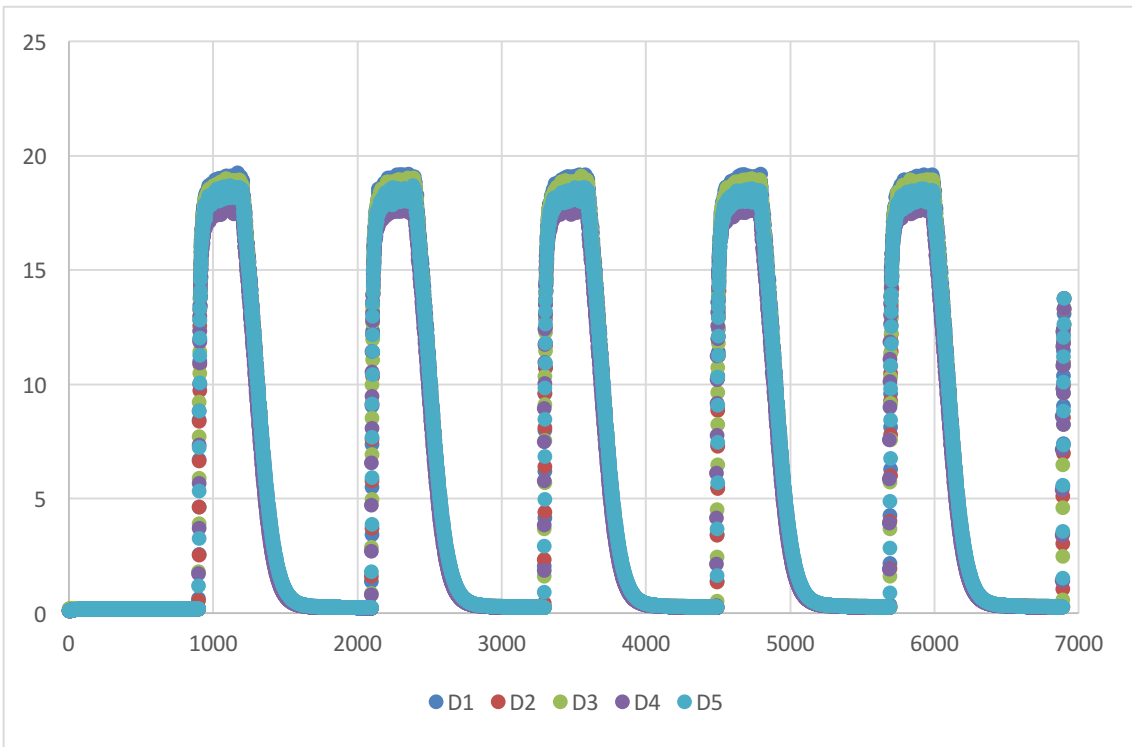
Sample A,  $t(\text{exp})=300$  s,  $T=10$  °C.



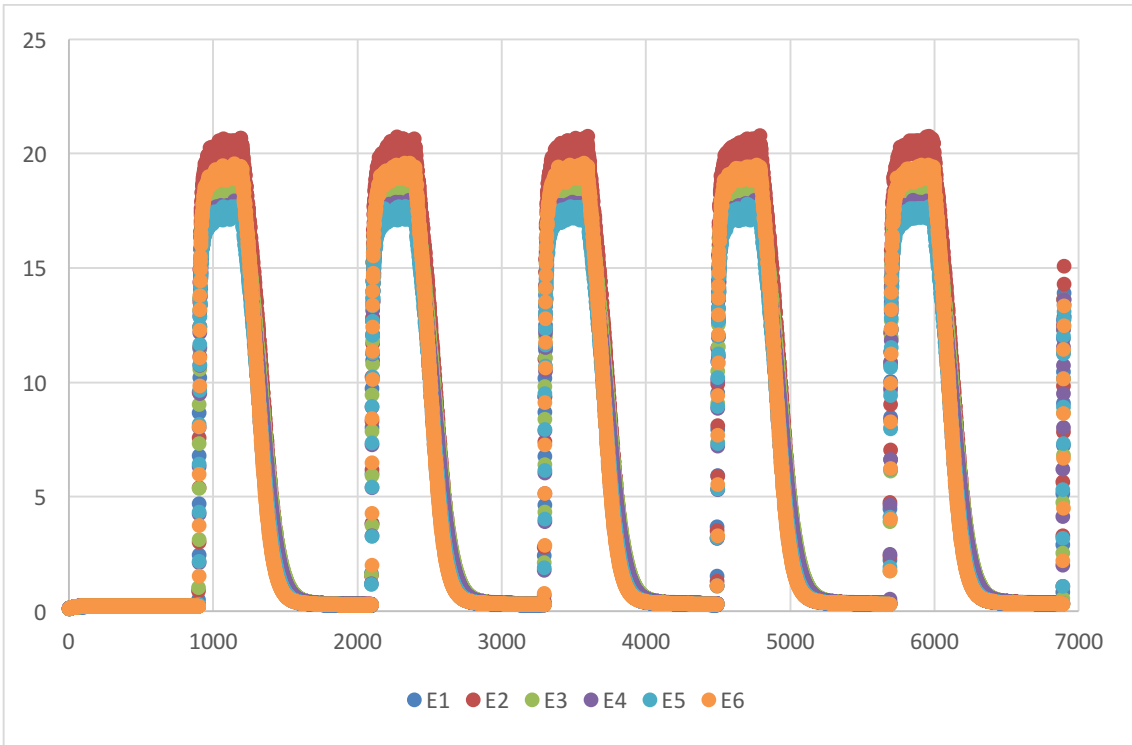
Sample B,  $t(\text{exp})=300$  s,  $T=10$  °C.



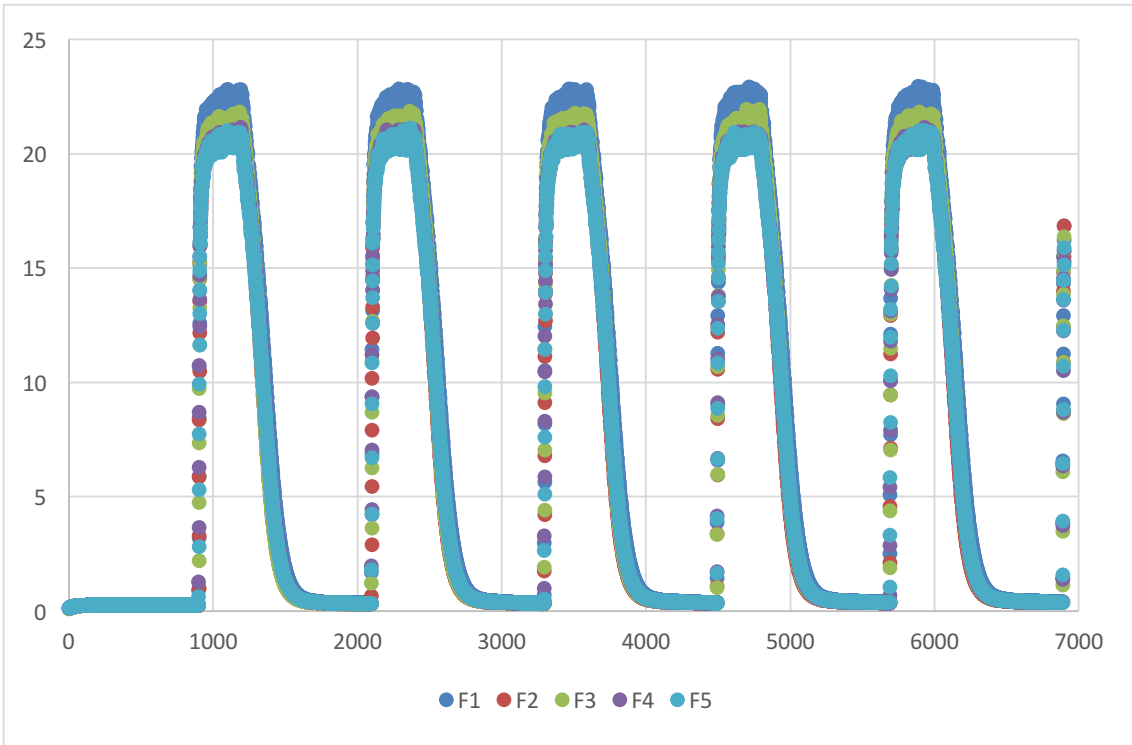
Sample C,  $t(\text{exp})=300$  s,  $T=10$  °C.



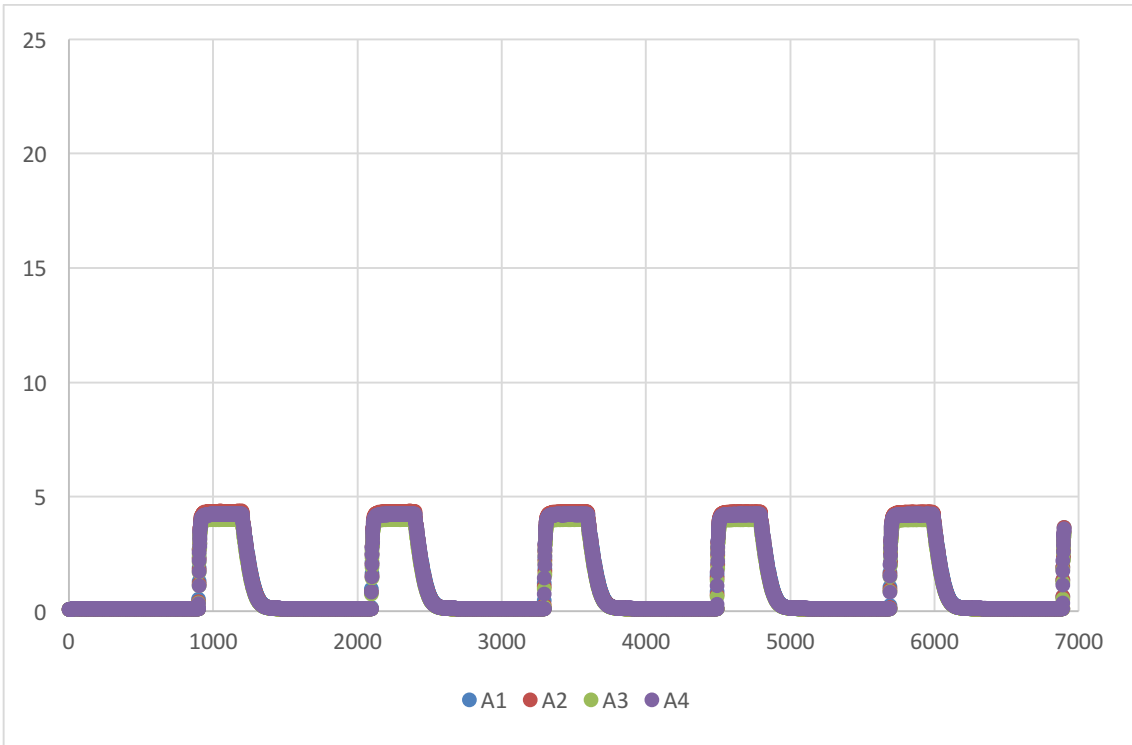
Sample D,  $t(\text{exp})=300$  s,  $T=10$  °C.



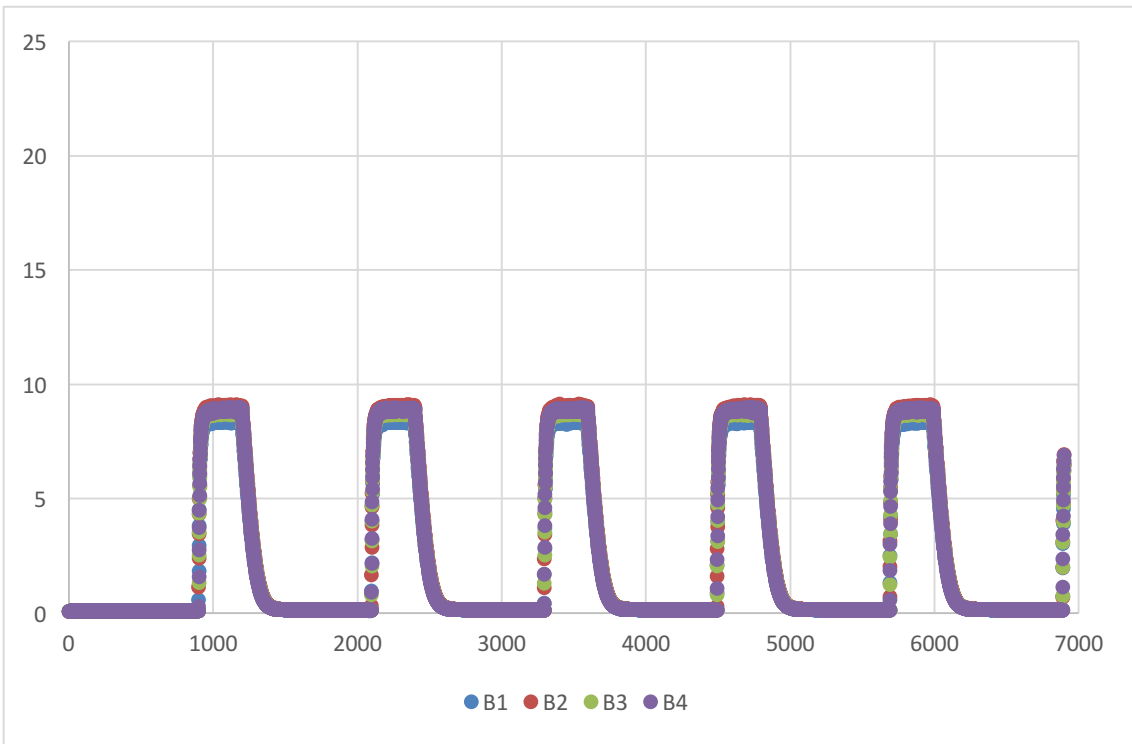
Sample E,  $t(\text{exp})=300 \text{ s}$ ,  $T=10 \text{ }^\circ\text{C}$ .



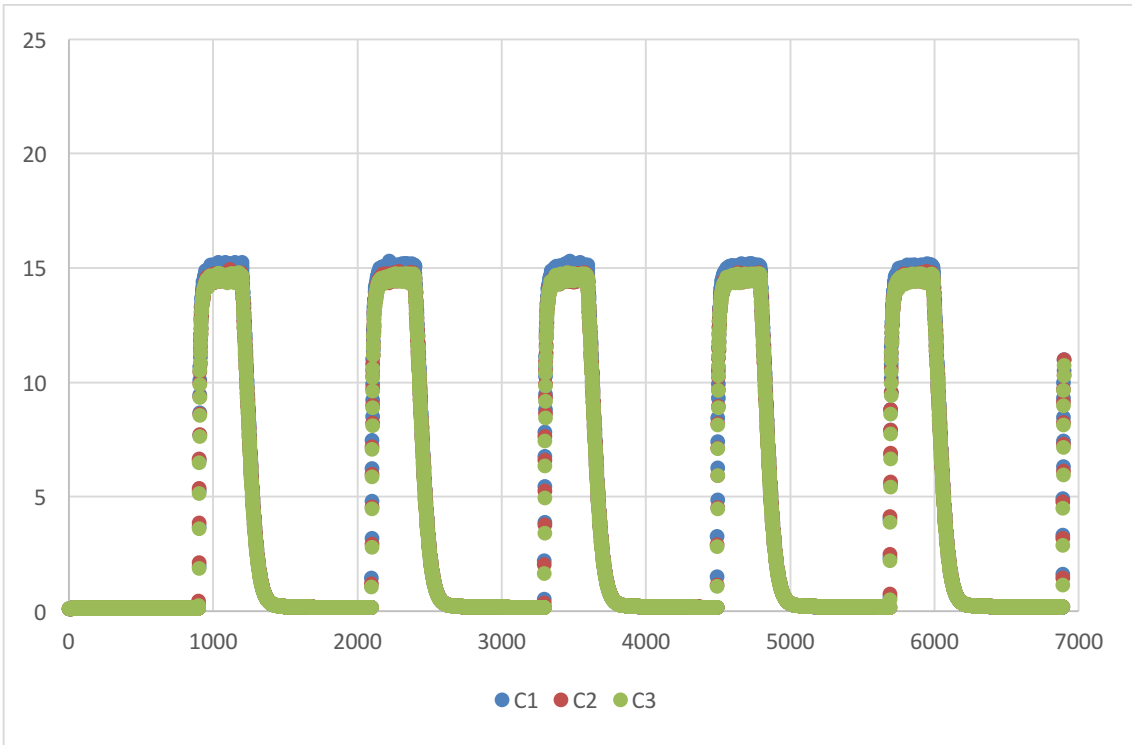
Sample F,  $t(\text{exp})=300 \text{ s}$ ,  $T=10 \text{ }^\circ\text{C}$ .



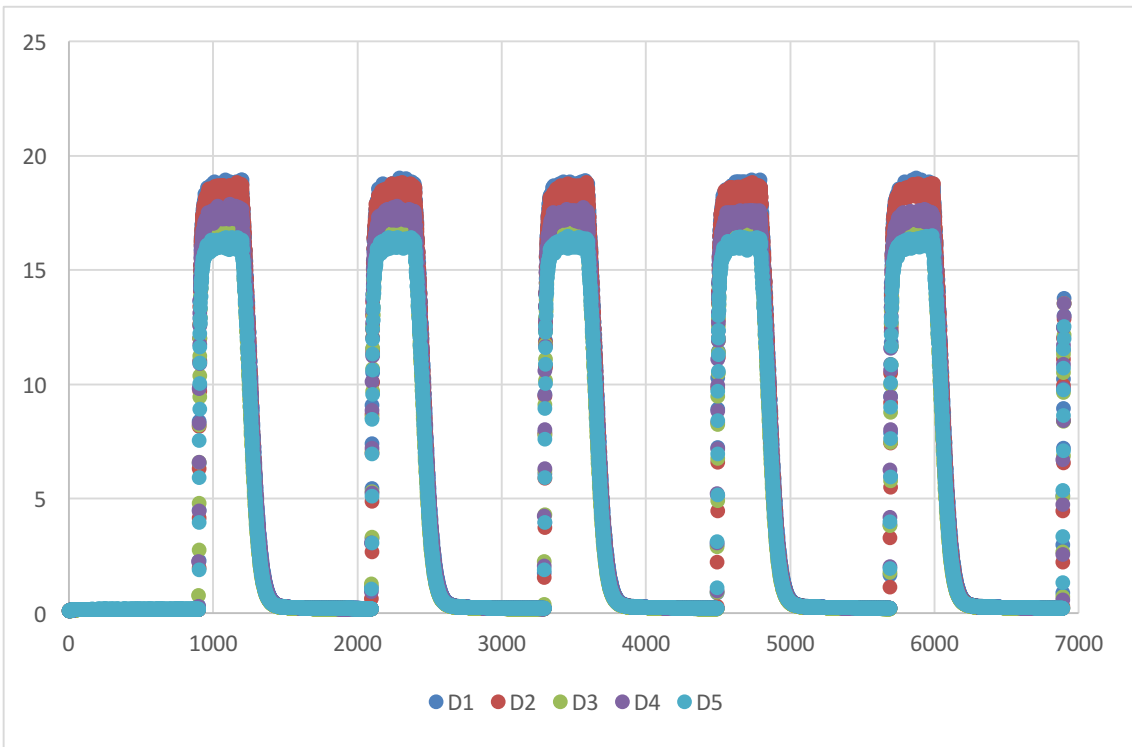
Sample A,  $t(\text{exp})=300$  s,  $T=15$  °C.



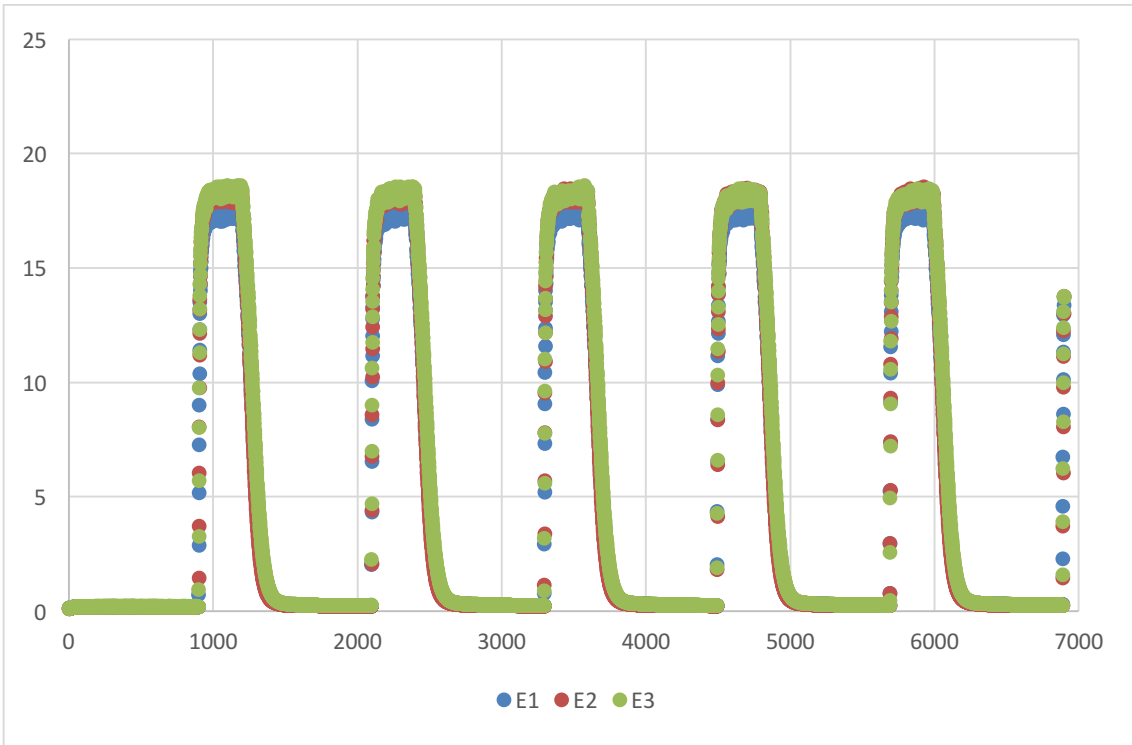
Sample B,  $t(\text{exp})=300$  s,  $T=15$  °C.



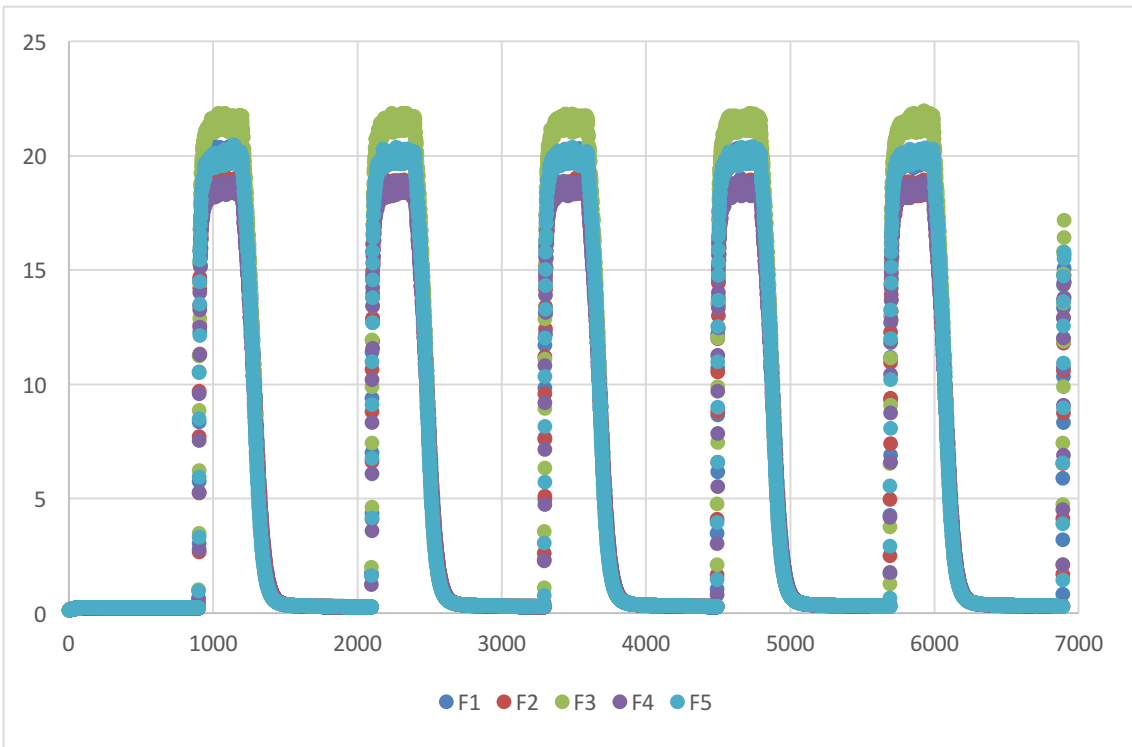
Sample C,  $t(\text{exp})=300$  s,  $T=15$  °C.



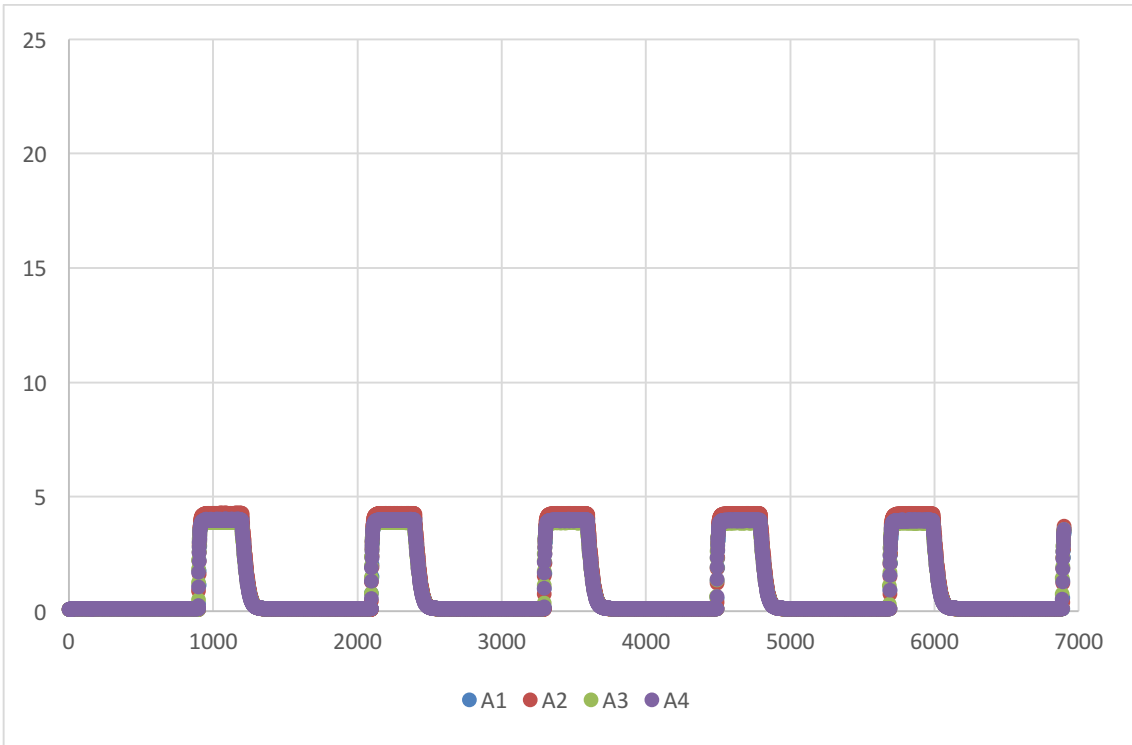
Sample D,  $t(\text{exp})=300$  s,  $T=15$  °C.



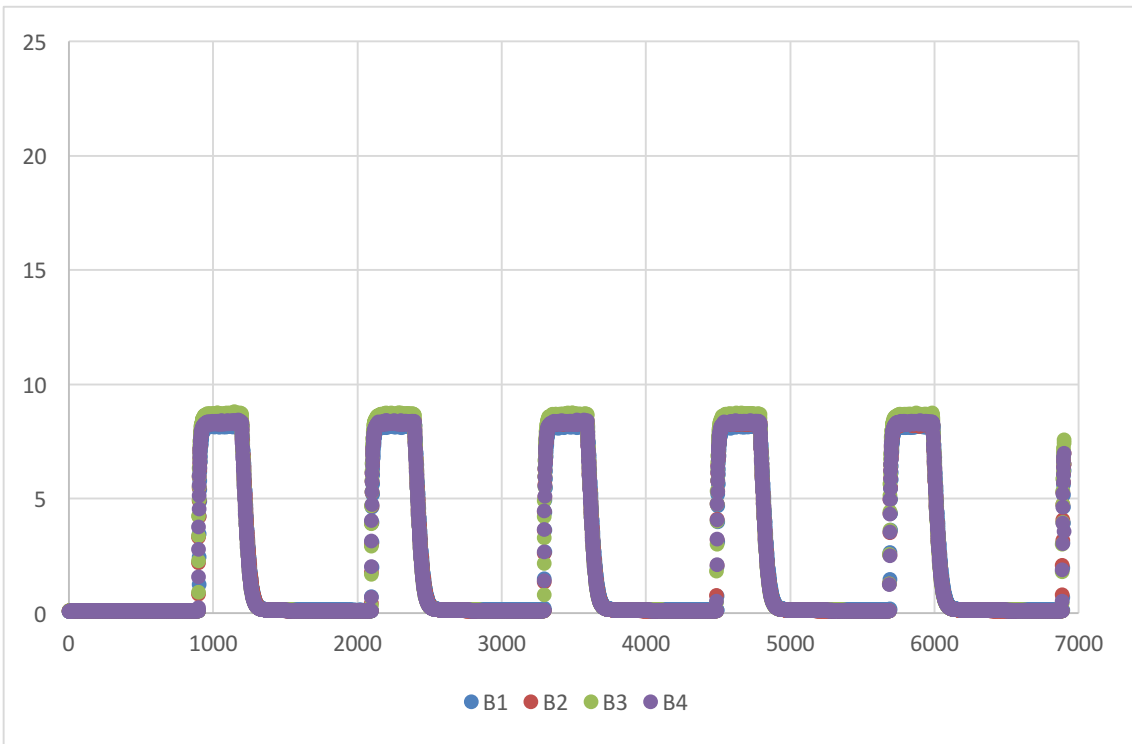
Sample E,  $t(\text{exp})=300$  s,  $T=15$  °C.



Sample F,  $t(\text{exp})=300$  s,  $T=15$  °C.

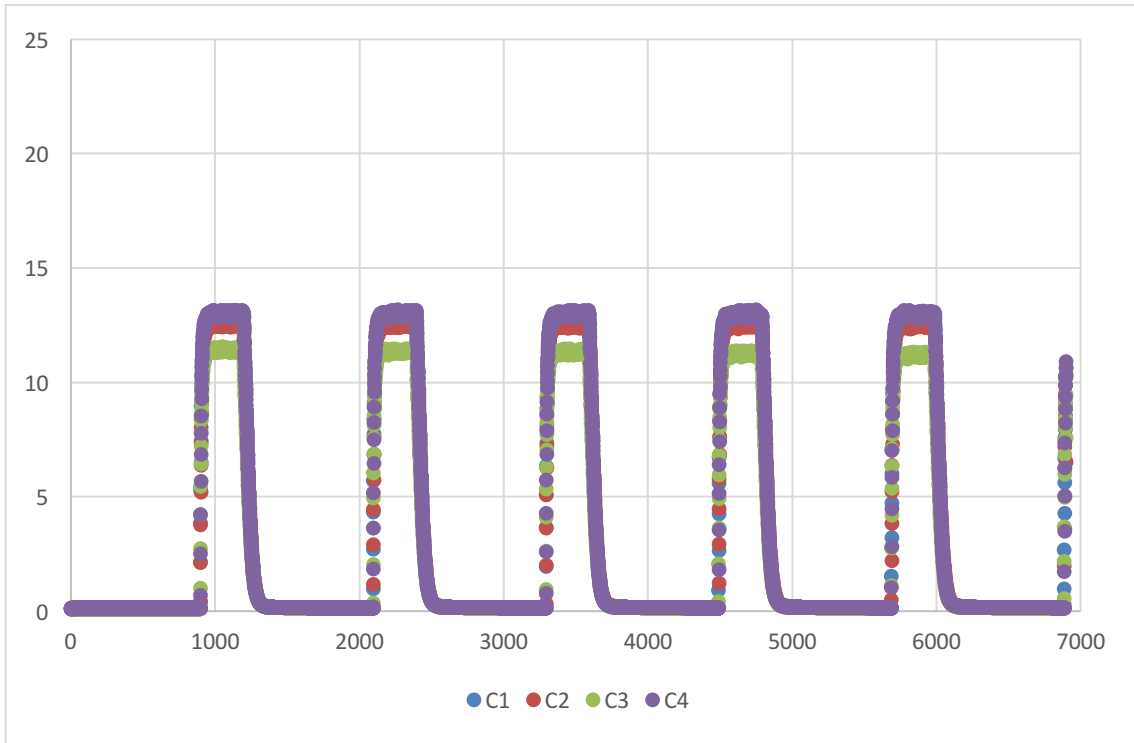


Sample A,  $t(\text{exp})=300$  s,  $T=20$  °C.

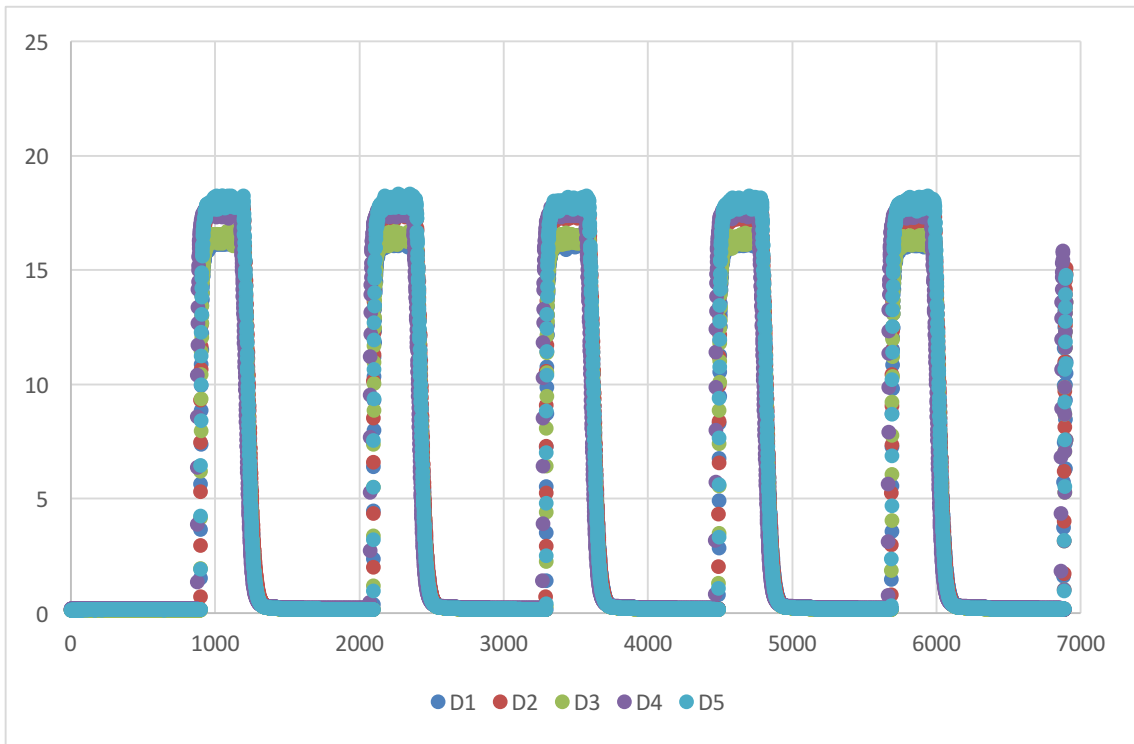


Sample B,  $t(\text{exp})=300$  s,  $T=20$  °C.

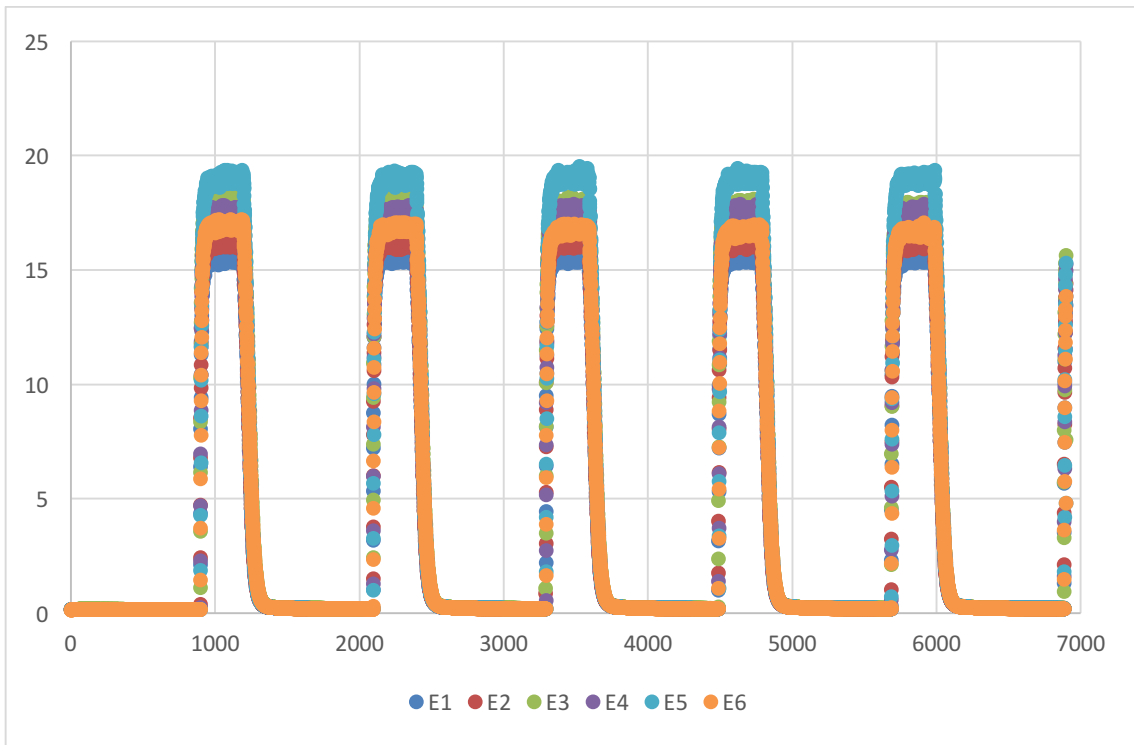




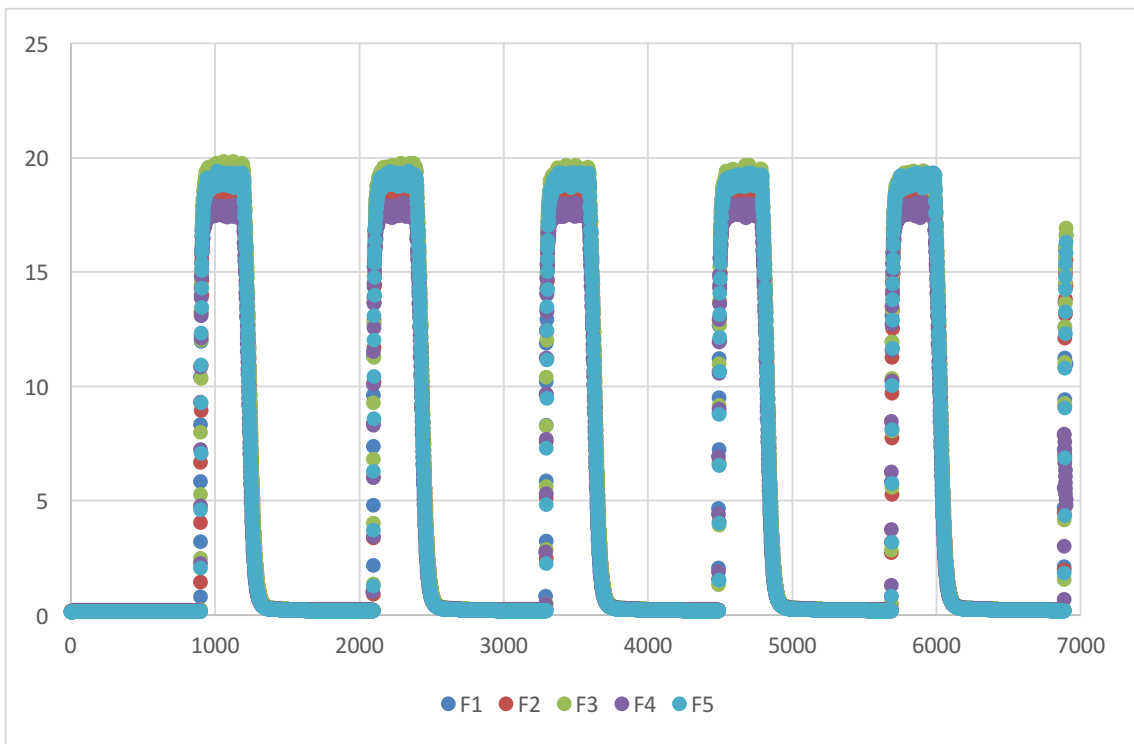
Sample C,  $t(\text{exp})=300$  s,  $T=20$  °C.



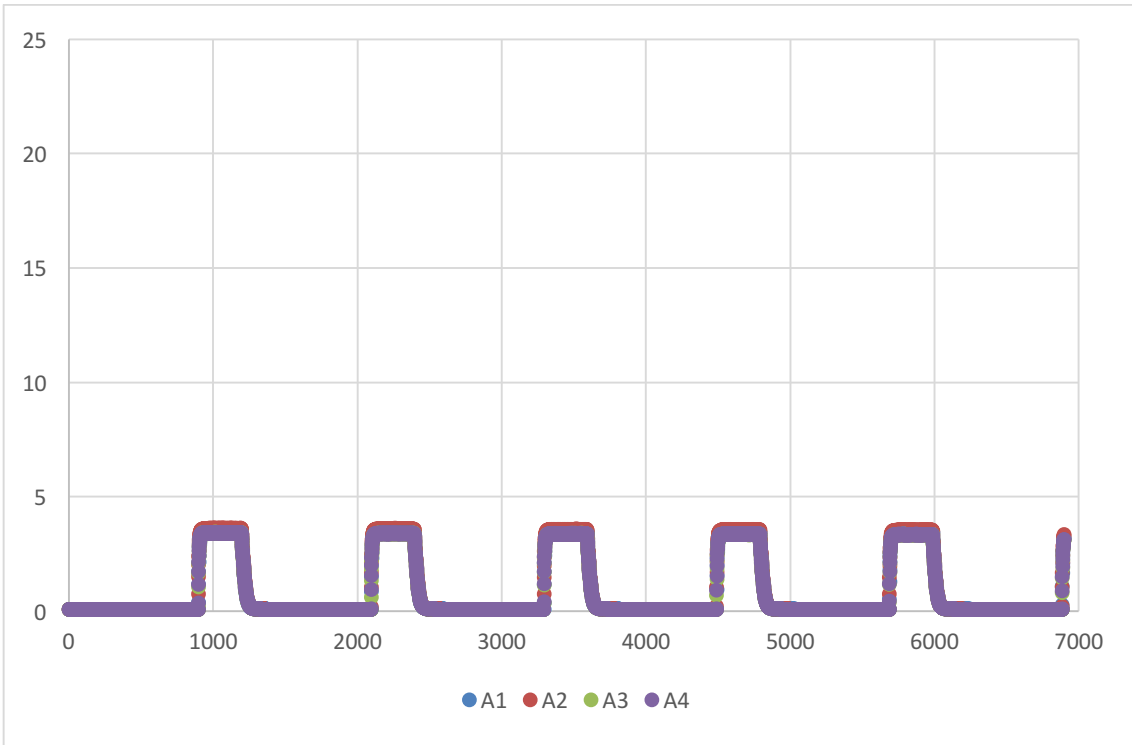
Sample D,  $t(\text{exp})=300$  s,  $T=20$  °C.



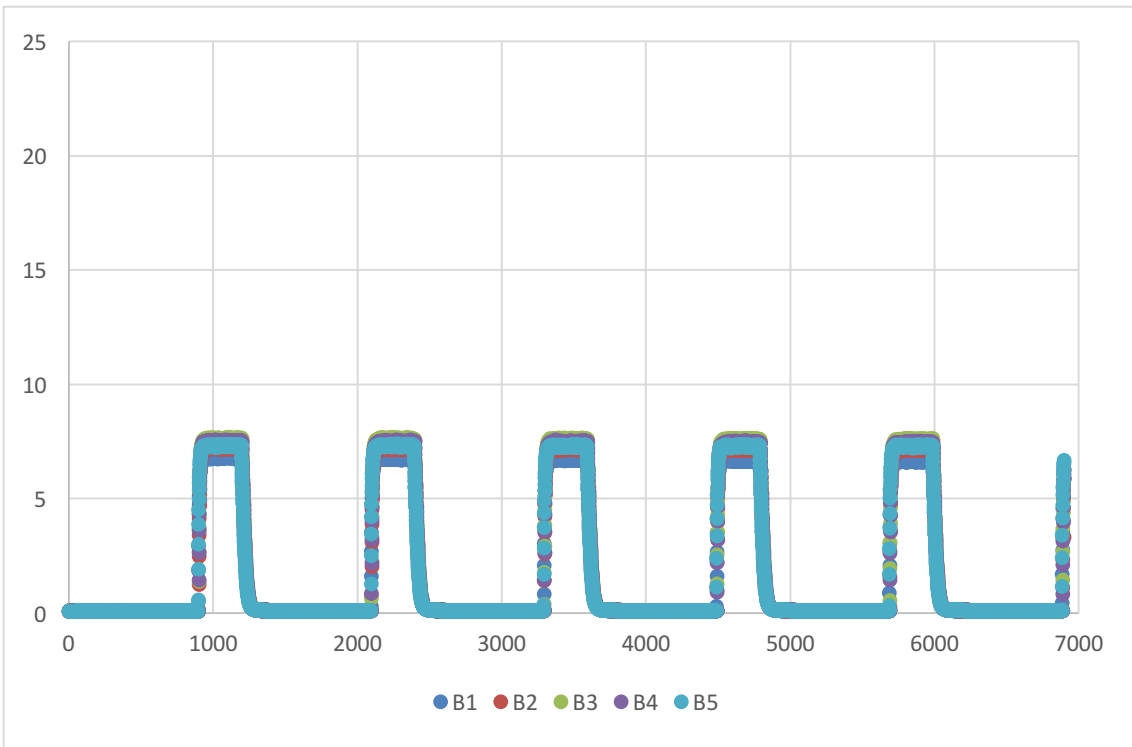
Sample E,  $t(\text{exp})=300$  s,  $T=20$  °C.



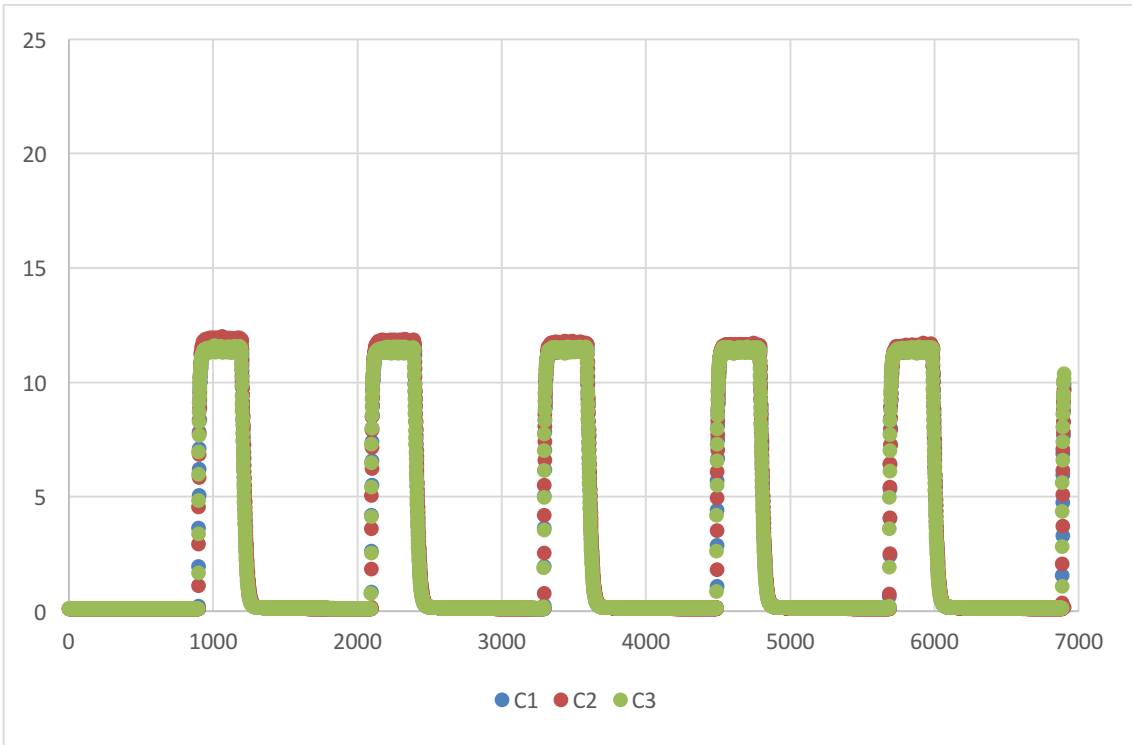
Sample F,  $t(\text{exp})=300$  s,  $T=20$  °C.



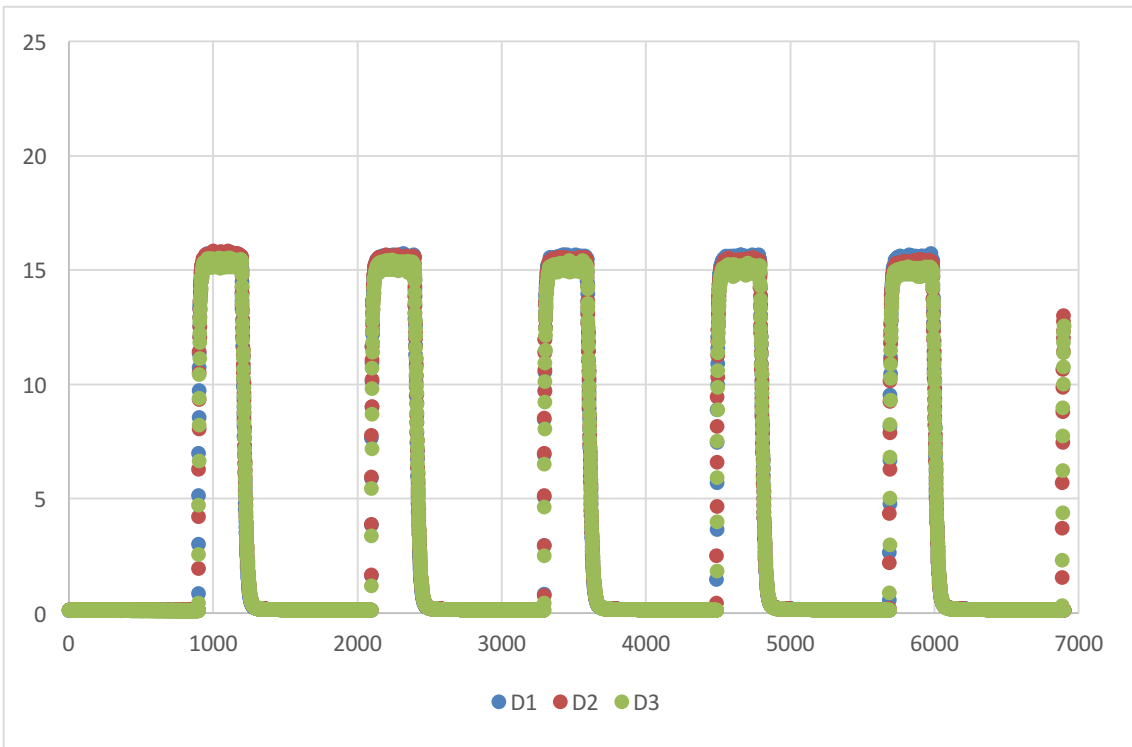
Sample A,  $t(\text{exp})=300$  s,  $T=25$  °C.



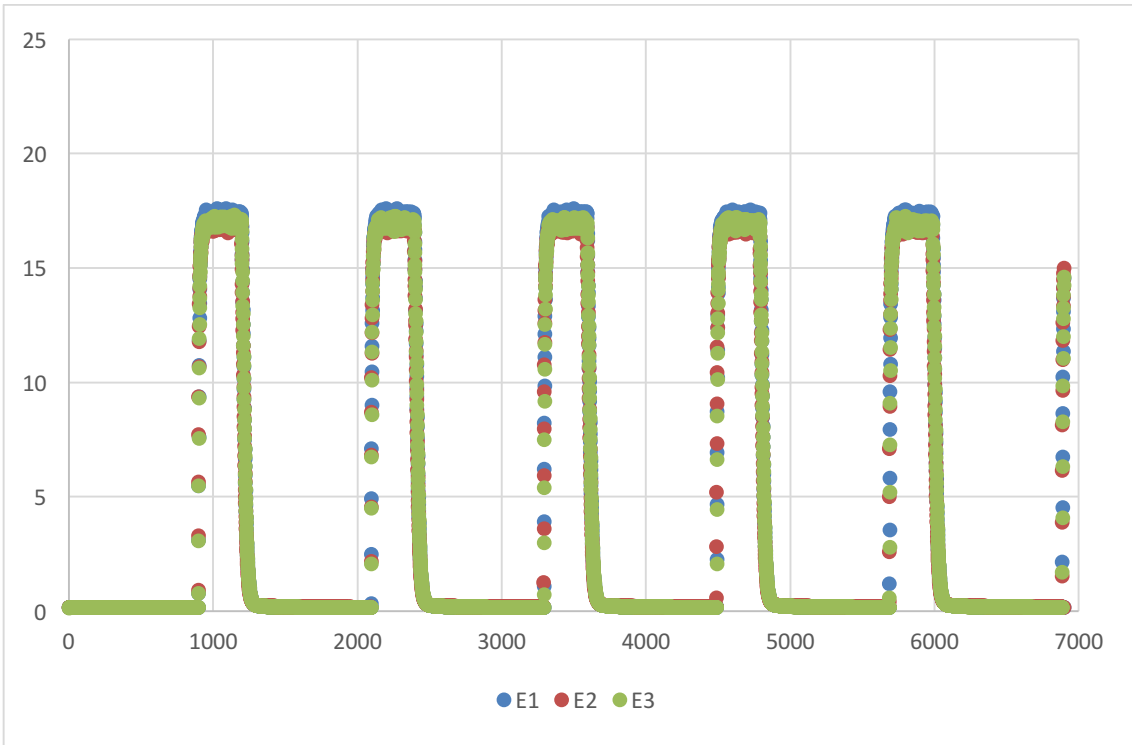
Sample B,  $t(\text{exp})=300$  s,  $T=25$  °C.



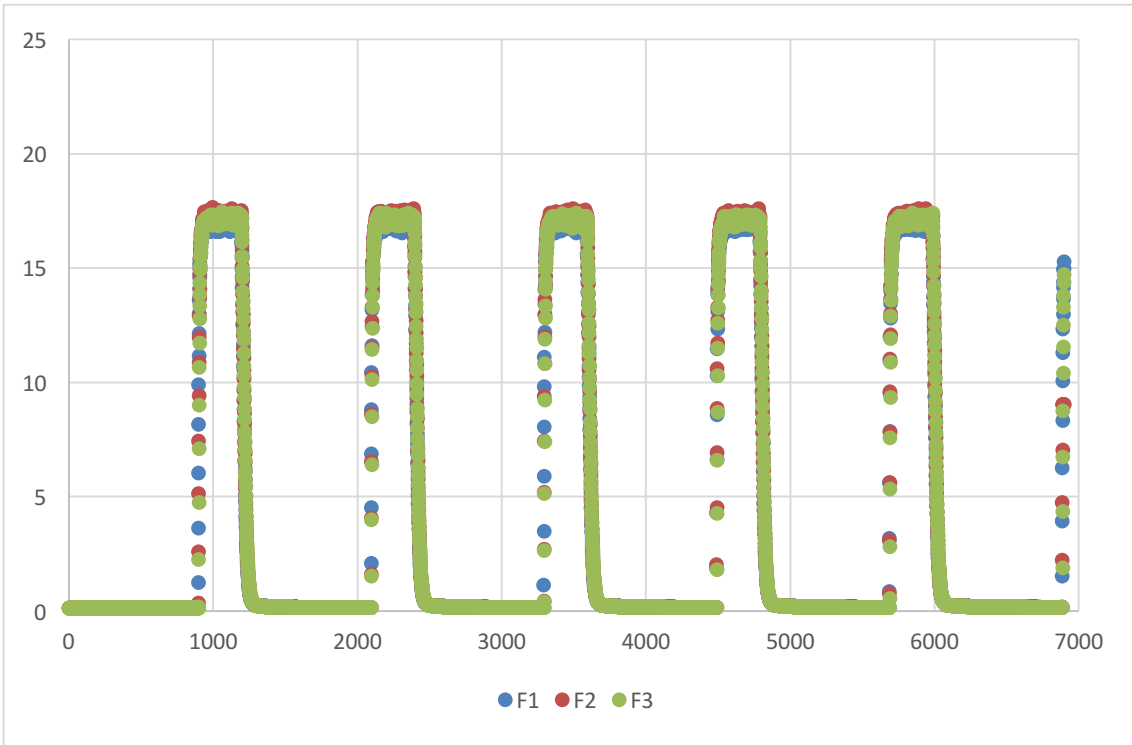
Sample C,  $t(\text{exp})=300$  s,  $T=25$  °C.



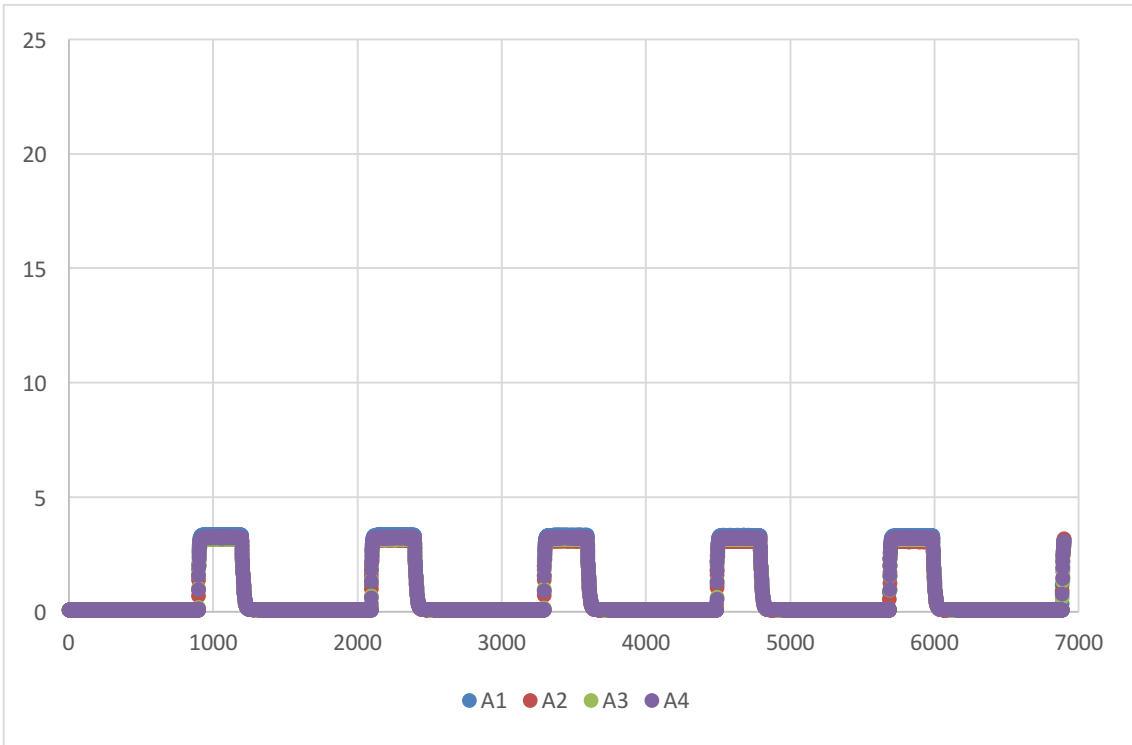
Sample D,  $t(\text{exp})=300$  s,  $T=25$  °C.



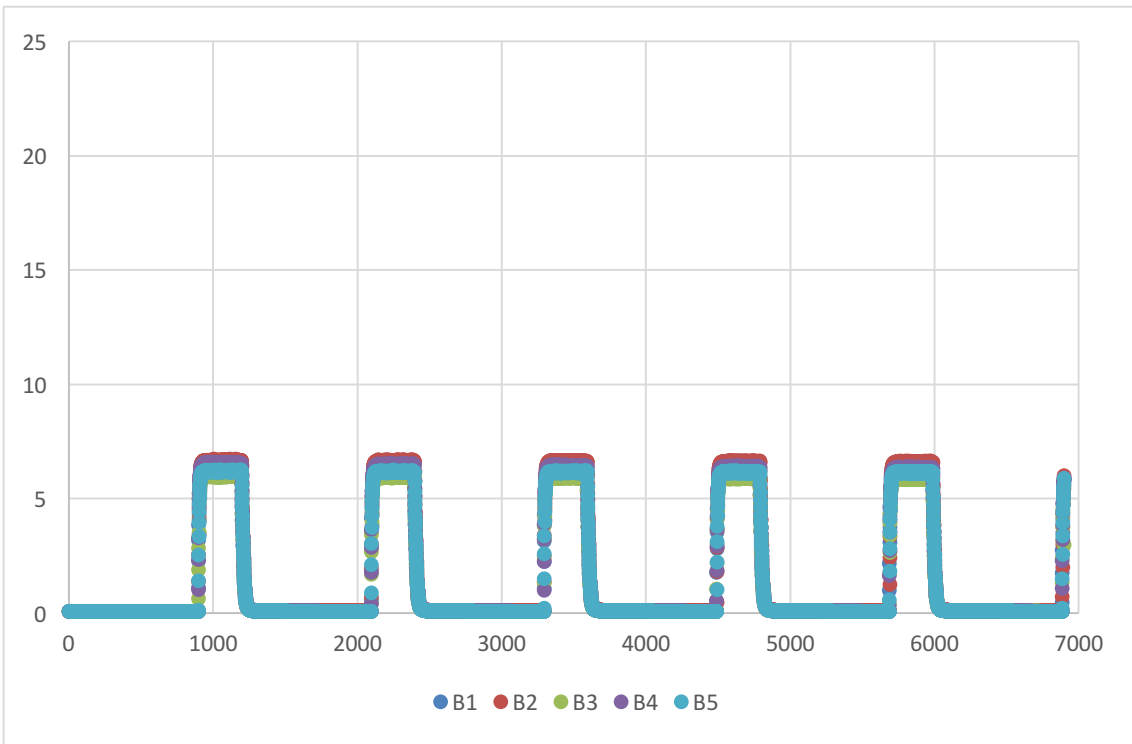
Sample E,  $t(\text{exp})=300$  s,  $T=25$  °C.



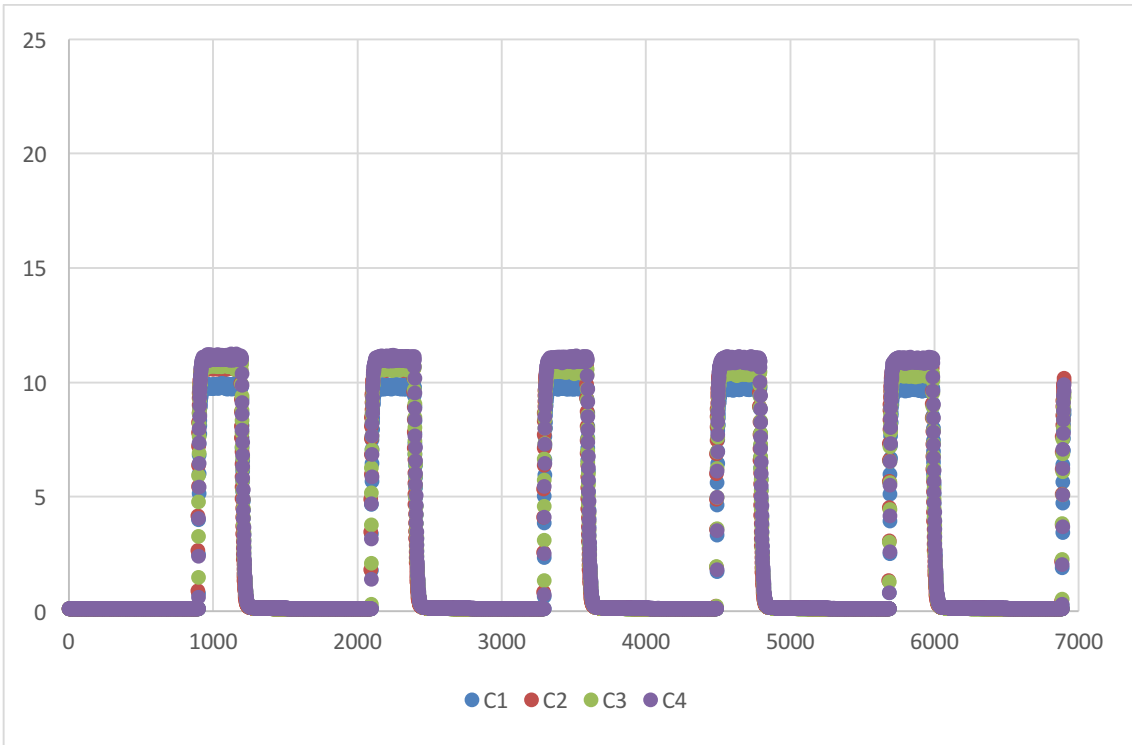
Sample F,  $t(\text{exp})=300$  s,  $T=25$  °C.



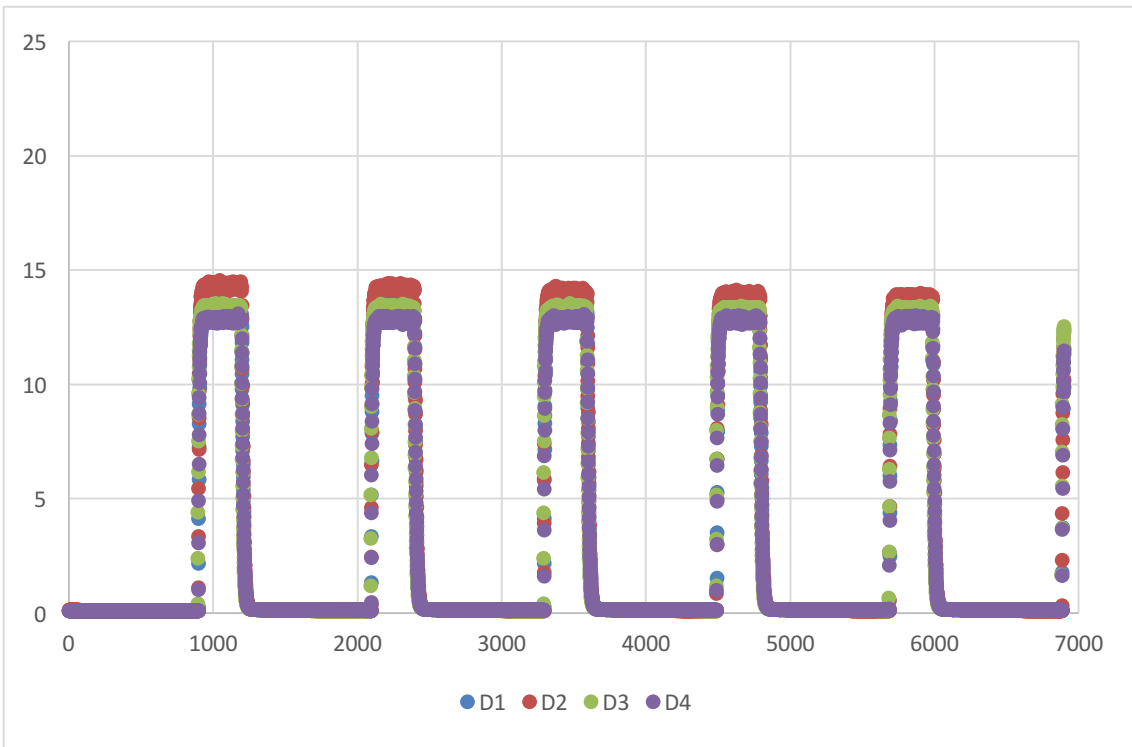
Sample A,  $t(\text{exp})=300$  s,  $T=30$  °C.



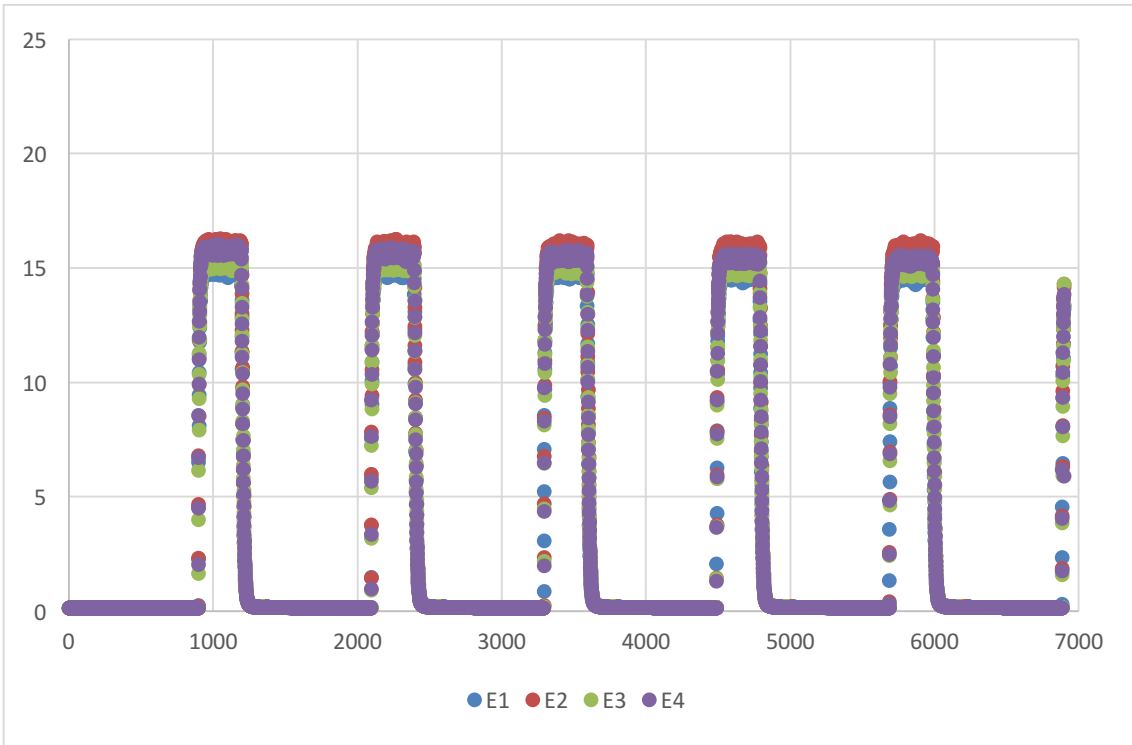
Sample B,  $t(\text{exp})=300$  s,  $T=30$  °C.



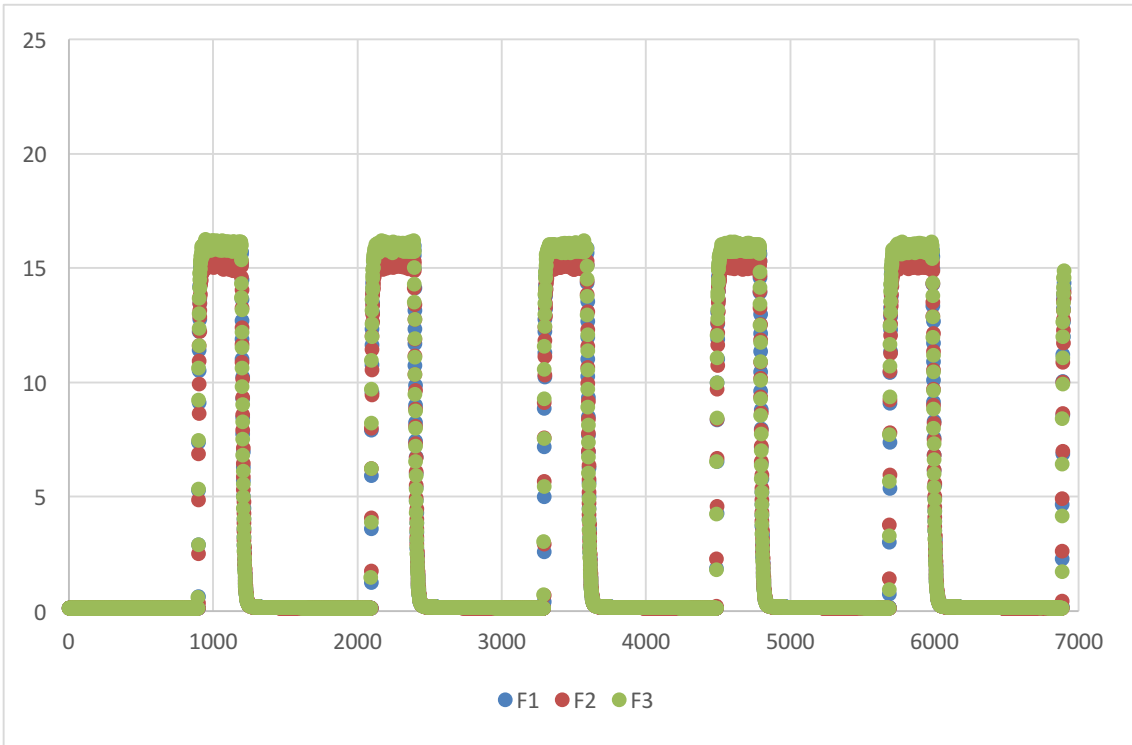
Sample C,  $t(\text{exp})=300$  s,  $T=30$  °C.



Sample D,  $t(\text{exp})=300$  s,  $T=30$  °C.



Sample E,  $t(\text{exp})=300 \text{ s}$ ,  $T=30 \text{ }^\circ\text{C}$ .



Sample F,  $t(\text{exp})=300 \text{ s}$ ,  $T=30 \text{ }^\circ\text{C}$ .